DIPLOMARBEIT

„Studies with selected antagonists of the N-methyl-D-aspartate receptor in an in-vitro blood-brain barrier model of ischemia"

verfasst von

Sebastian Membier

angestrebter akademischer Grad

Magister der Pharmazie (Mag.pharm.)

Wien, 2015

Studienkennzahl lt. Studienblatt:	A 449
Studienrichtung lt. Studienblatt:	Diplomstudium Pharmazie
Betreut von:	Ao. Univ.-Prof. Mag. Dr. Ernst Urban

Acknowledgement (german)

Zu Beginn möchte ich Hrn. Ao. Univ.-Prof. Mag. Dr. Ernst Urban danken, der mir die äußerst interessante Arbeit ermöglicht hat und mich weitestgehend unterstützt hat. Ein besonderer Dank gilt Hrn. Priv.-Doz. (habil. med) Dipl.-Ing. Dr.rer.nat. Winfried Neuhaus, der als mein Betreuer für die praktischen Arbeiten einen wesentlichen Teil zur Arbeit beigetragen hat und mir stets helfend zur Seite stand.

Weiters möchte ich Mag. Jakob Mayrhofer danken, der mir gewissenhaft einige Zellkulturmethoden beigebracht hat und mir auch in vielerlei anderer Hinsicht geholfen hat, die Diplomarbeit erfolgreich abzuschließen.

Der größte Dank gilt jedoch meiner Familie und meiner Partnerin, die mich in schwierigen Zeiten unterstützt haben und Geduld und Verständnis zeigten, um mich im Studium bestmöglich zu begleiten. Auch wenn es nicht leicht war, haben sie es immer wieder geschafft, mir Mut zuzureden und mich zu motivieren, wodurch ich schlussendlich mein Ziel erreichen konnte.

Table of contents

1.Introduction

1.1 The blood-brain barrier (BBB)

1.1.1 Structure of the blood-brain barrier

The blood-brain barrier (BBB) is necessary to maintain the chemical environment between brain capillaries and the central nervous system (CNS) [1].

It consists of several layers, listed from the inside to the outside of the capillary (see figure 1.1):

- capillary-endothelial cells with tight junctions between each other
- the basement membrane consisting of e.g. type IV collagen, fibronectin and laminin, surrounding endothelial cells as well as pericytes. It supports vessels in their structure and has some transport function.
- pericytes, which are embedded inside the basement membrane. They influence cell profileration of endothelial cells and can develop phagocytosic functions under pathophysiological conditions.
- astrocytes, which form end-feet that surround the basement membrane. They are essential for the barrier function and modulate other properties of the blood-brain barrier. Astrocytes regulate many BBB features leading to tighter tight junctions, the expression and localization of transporters, including P-glycoprotein and glucose-transporter 1 (GLUT1) [1, 2, 3].
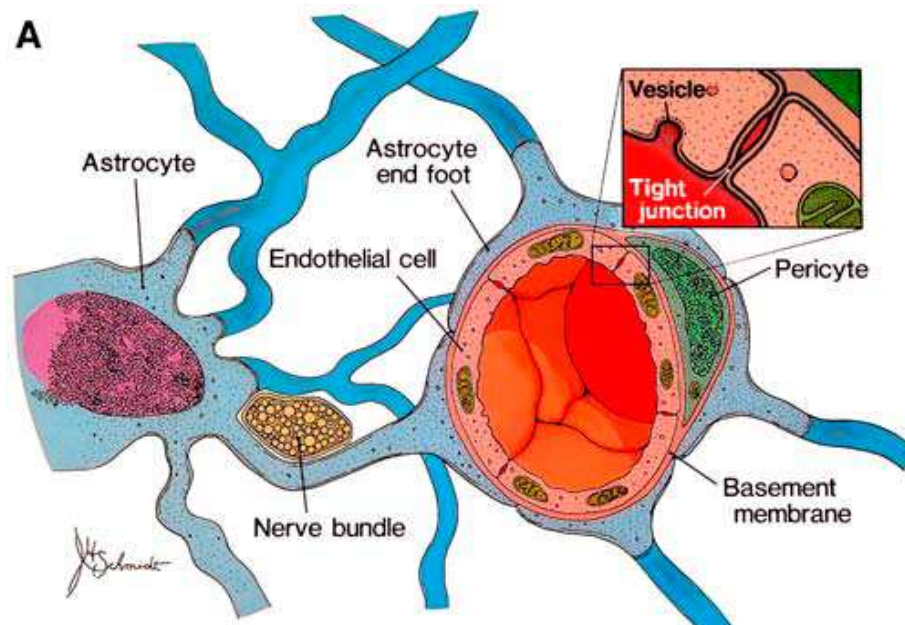
Figure 1.1 The blood-brain barrier is formed by several layers. Endothelial cells are surrounded together with pericytes by the basement membrane. Astrocytes are connected via end-feet to the basement membrane. Tight junctions are found between brain capillary endothelial cells. They restrict the paracellular transport [1, 3].
(Hawkins et al. (2006) Structure of the Blood–Brain Barrier and its role in the transport of amino acids. J Nutr,136 (1 Suppl):218S-26S)

Endothelial cells in the brain differ from other endothelial cells of the body in possessing less cytoplasmatic vesicles, more mitochondrias and much more tight junctions in-between, which are essential to build a tight barrier. There are brain regions such as pituitary gland, area postrema, pineal gland or the epithelium of choroids plexus with less blood-barrier, where tight junctions are discontinuous and more plasmalemmal vesicles are found [2].

Tight junctions prevent paracellular transport and play an important role in the integrity of the blood-brain barrier [1].

1.1.2 Transport-mechanisms at the blood-brain barrier

Membranes of endothelial cells are divided into two sides: luminal and abluminal. There are different systems which enable the transport between the blood and the CNS-side [4, 5].

Passive diffusion across the cellular membranes is the main transport through the blood-brain-barrier for lipophilic molecules [1, 2, 4].

Permeation of the essential (polar) D-glucose (carbon source) is mediated by selective transporters. One of them is GLUT-1, an insulin-independent transporter, which is widespread in brain capillaries. Glucose is the main energy source of the brain, but can be replaced by ketones in case of glucose-lack [1, 2, 4].

Most neurotransmitters can't enter the brain due to their low lipophilicity. Enzymes like the mono-amino-oxidase (MAO) are necessary to regulate the transport of neurotransmitters like dopamine or noradrenaline as it metabolizes these compounds. In that way, the enzyme can protect the brain from toxic substances by building its harmless metabolites [1, 2].

Another essential transport mechanism at the blood-brain barrier is transcytosis, which could be started with a receptor-mediated, adsorption-mediated, or bulk-phase endocytosis. All forms lead to formation of a vesicle. The formation starts after binding of a substrate at a receptor (receptor-mediated endocytosis), or is due to adsorptive, electrostatic interactions on the surface of the cell between cationic proteins and anionic sites on the membrane (adsorptive endocytosis) or the attachment of the protein clathrin, which leads to the formation of clathrin coated-pits and involves the uptake of substances that are solubilized in extracellular fluid (bulk-phase endocytosis) [6].

It is assumed that ions are transported across the blood-brain barrier mainly by passive diffusion [1].

In addition, several ion-transporter exist in the membrane, for example the Na^+/K^+-ATP-ase (abluminal), which is responsible for generating a high

concentration-gradient by effluxing Na^+, so that Na-dependent transport processes into the cells are possible [2].

Na^+ influx is neccessary to compensate the transport of other molecules. This allows selective transport of toxic or non – essential amino acids outside the extracellular fluid into the endothelial cell [1].

Glutamate is the amino acid with the highest concentration in the brain and has excitatory potential. The high intracellular concentration is due to the uptake of glutamate via Na-dependent transporters and the transformation of glutamine into glutamate via glutaminase. When the glutamate-concentration in the endothelial cell is higher than in blood, luminal transporters enable its efflux into the blood [1, 5].

Another important transport molecule is P-glycoprotein. It is physiologically expressed in endothelial-cells, astrocytes and microglia of the blood-brain barrier and epithelial barriers [6]. P-glycoprotein can lead to a "reduced permeability" by pumping the substance out of the endothelial cell of the blood-brain barrier [2, 7].

P-glycoproteins was explored initially due to their increased presence in neoplasmatic cells and because they lead to transport of antineoplasmatic-compounds out of the cell. It belongs to the family of transporters called ABC-transporters (ATP-binding cassette) [7, 8, 9].

ABC-transporters typically use biological energy that is gained via hydrolysis of ATP to transport molecules across a barrier against the concentration gradient in one direction [6].

They may also play an important role during stroke, when its expression is altered, which leads also to a differed transport [7]. In addition to P-glycoprotein, several other ABC-transporters such as breast cancer resistance protein (BCRP) or multidrug resistance protein (MRPs) are present and functionally active at the blood-brain barrier [10].

Another superfamily of transport-proteins that is essential for the transport of anionic and cationic small molecules as well as nucleosides and peptides across

the blood-brain barrier is summarized under the name solute carrier family (SLC). The transport is regulated by electrochemical – or concentration gradients [6].

1.1.3 Tight junctions at the blood-brain barrier

Tight junctions of brain endothelial cells differ from others in morphological and structural properties as well as in their higher sensitivity to microenvironmental changes. Well explored components of tight junctions are claudins, occludin, ZO-1(zonula occludins protein 1), ZO-2, ZO-3, cingulin and 7H6. Signalling pathways concerning tight junctions involve G-proteins, kinases, extra- and intracellular calcium levels, cAMP levels, proteases and cytokines [3, 11, 12].

Due to lack of ATP the paracellular transport barrier breaks down, which is accompanied by structural changes of the intracellular cytoskeleton [11].

Occludin: Occludin is an integral membrane tight junction protein and belongs with claudins and junctional adhesion molecules to the family of transmembrane linker proteins. Thus, they are necessary to form stable cointeractions with cytoplasmatic adapter proteins such as ZO-1, ZO-2, ZO-3 and 7H6 [13].

The phosphorylation of the cytoplasmatic domain of occludin correlates with density of tight junctions. Moreover, the transmembrane domain and the extracellular loops contribute to the regulation of paracellular permeability [11].

Claudin: Claudins are transmembrane-proteins consisting of four domains. The constitution of several claudin-subtypes influences the integrity of the tight junctions. Claudin-3, claudin-5 and claudin-12 are currently considered as the most important claudins at the blood-brain barrier [3, 11].

Adhesion molecules, for example junctional adhesion molecules (JAM) or endothelial (cell-) selective adhesion molecule (ESAM) are also found in tight junctions. JAMs belong to the immunglobuline superfamily and are important for homophilic and heterophilic interactions in the tight-junctional regions and regulate formation and maintenance of the tight junctions. JAMs also influence the integrity of cells without tight junctions [3, 11].

Astrocytes seem to have a regulatory function for tight junctions as they release for example humoral factors such as the glial-derived neurotrophic factor (GDNF) or transforming growth factor-β (TGF-β). Both influence the phenotype and the induction of the blood-brain barrier [3, 6, 11].

1.2 The N-methyl-D-aspartate-receptor (NMDAR)

1.2.1 Functionality and physiology of the NMDAR

NMDARs, as well as AMPAR (α-amino-3-hydroxy-5-methyl-4-isoxazolepropionic acid receptor) and kainate-receptors, belong to the so called ionotropic glutamate receptors. They are activated by glutamate, which is released presynaptically through several activating stimuli and cause an influx of ions after activation. NMDARs are not as important for the synaptic transmission as AMPAR but crucial for neuronal plasticity. Other binding sites for glutamate on the surface of the cell are metabotrope glutamate receptors, which lead to an activation of G-protein coupled pathways and act slower [6, 14, 15].

NMDARs are activated by glutamate and glycine and show high permeability for Ca^{2+}-ions. Whereas glycine has more of a modulatory role, glutamate can be described as the neurotransmitter, whose binding finally leads to an opening of the channel [15].

Glutamate is the amino acid that is most important for excitatory processes in the brain. On the other side glutamate evokes mechanisms that lead to cell death during ischemia, hemorrhage or traumatic brain injury [6, 14].

Permeability of NMDARs for Ca^{2+} plays an important role in physiology and pathology of concerned cells. NMDARs are widespread in the human brain and influence processes such as development of the brain, learning, memory or neuroplasticity. Furthermore, they occur as a significant factor in progress and formation of several diseases such as Morbus Huntington, Parkinson's and Alzheimer's disease as well as epilepsy, schizophrenia and neuropathic pain [16-20].

Besides the regulation by glutamate, the Ca^{2+}-influx is also controlled by a Mg^{2+}-ion, which is placed inside the channel of the receptor. Mg^{2+} is removed from the pore as the membrane is depolarized. Afterwards the Ca^{2+} influx begins. The Mg^{2+}-relieving depolarization can be induced in several ways. High frequent synaptic signals lead to a lasting depolarisation, called excitatory postsynaptic

potential (EPSPs), which is induced by activated AMPA-channels. This process is evoked by the long term potentiation (LTP), which is defined as a short burst of high frequent synaptic input (15 Hz for 15 sec or 100 Hz for 3 sec) that leads to reinforcement of synaptic transmission. LTP and its direct effects are influenced by NMDAR and AMPAR. Increase of synaptic transmission is achieved by phosphorylation of AMPARs, which results in higher opening-probability or by an enhanced installation of AMPA receptors in the postsynaptic membrane [15].

The opposite of the long term potentiation is the long term depression (LTD), which is induced by low frequent stimulation of excitatory synapses. The following effects are contrary to effects of LTP described above. LTP and LTD are controlled by NMDARs that show its importance for synaptic transmission as it is able to increase or decrease the concerned synaptic transmission [15].

Some studies confirm the presence of NMDA-receptors on the surface of brain-endothelial cells and their influence on its integrity [9, 12].

1.2.2 Structure of NMDARs

Typical NMDARs consist of four different subunits and build a heterotetramer that shows high permeability for Ca^{2+}-ions. The receptor most often contains two NR1 subunits representing the binding sites of glycine and the glutamate binding NR2 subunits. For NR1 eight splicing variants exist. In case of NR2 four different subtypes are known. The probably most important of these are NR2A, NR2B and NR2D which play different roles in cell function and viability due to their different location on the cell. NR2A are found in synaptic NMDARs, whereas NR2B subunits are more prominent at extrasynaptic sites. In special cases, one NR1 subunit could be replaced by a NR3 subunit. NR3 binds glycine and can be divided into 2 subunits: NR3A and NR3B. These domains form a pore, which has a high permeability for Ca^{2+}-ions (see figure 1.2) [15, 20].

One subunit itself possesses four different functional domains: an extracellular N-terminal domain, an intracellular C-terminal domain, a ligand binding domain and a pore forming transmembrane region. The hydrophobic segments M1 to M4 build the transmembrane-regions, whereas M2 forms the inner element (see figure 1.10). The ligand binding domains consist of the segments S1 and S2.

The extracellular amino terminus contains signal peptides, which is typical for all ion gated glutamate receptors and declares its localisation [15].
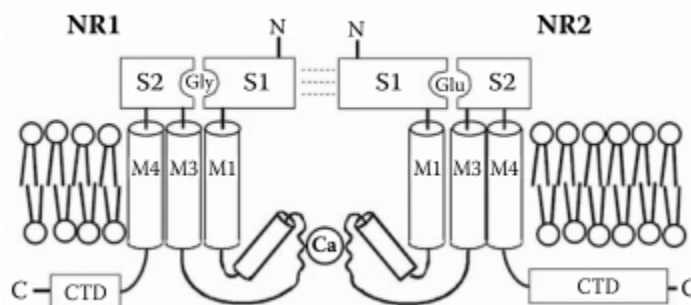
Figure 1.2 Structure of the NMDAR. NR1 builds the binding site of glycine, whereas NR2 subunit binds glutamate. Both binding domains consist of S1- and S2 segments and are sited extracellular. The transmembrane-domaine is represented by M-proteins. The amino terminus (N) is situated extracellular, whereas the carboxy-terminal domain (CTD) of the peptide is located inside the cell [15].
(Van Dongen, A. M. (Ed.). (2009). Biology of the NMDA Receptor. North Carolina: Duke University Medical Center)

1.2.3 The role of the localization of the NMDAR

An important function of NMDARs is the regulation of cell viability.

NMDARs are essential for neuronal survival as well as their death as they lead to cell degeneration and neuronal loss. For that, the localization of the receptor seems to be deciding. Synaptic NMDARs lead to an increase of cell-promoting genes as well as a down-regulation of genes that lead to cell death, whereas extrasynaptic NMDARs evoke the opposite. These different effects are justified by different receptor-activation on the one hand and by different localization of the receptors on the other hand. Thus, synaptic NMDA receptors indicate surviving cell-signals, whereas extrasynaptic channels don't influence this gene-regulation, but lead to a chlorid-dependent Ca^{2+}-influx and other effects, that could lead to cell death. These effects are triggered by signalling pathways such as activated MAP-ERK-kinases after increased Ca-influx or the intracellular calmodulin-kinase pathways [21, 22].

Receptors that are located in synapses are activated through low-frequency synaptic events. Extrasynaptic receptors, which are not activated by low frequency impulses, can be found for example on the cell body, the dendritic shaft or the neck of the dendritic spine of neurons [21].

Ca^{2+} influx through NMDAR is the main mechanism leading to neuronal cell death during cerebral ischemia, which is due to the excitotoxicty that is associated with high intracellular Ca^{2+}-concentrations [21].

1.2.3.1 Synaptic NMDARs

The two main targets of intracellular calcium after modulation of synaptic NMDAR are cAMP-responsive element binding proteines and the Ca^{2+}/calmodulin dependent protein kinase IV (CaMKIV) (see figure 1.3). CREB is a transcription factor which is important for neuronal survival, neurogenesis, addiction or synaptic plasticity for example [16, 21].

CREB-dependent gene expression leads to neuroprotectional, antiapoptotic effects and protection against excitotoxic insults in hippocampal neurons. In this way, nuclear Ca^{2+} signalling leads to increased transcription of several protective genes, summarised as activity-regulated inhibitors of death (AID). These include for example activating transcription factor 3 (Atf3), B-cell translocation gene 2 (Btg2), B-cell lymphoma 2 (Bcl2) and Bcl6, growth arrest and DNA damage induced gene 45 beta and gamma (GADD45beta/gamma) and Inhibin beta-A (Inhba). They act for example in increasing the mitochondria's resistance against cellular stress and toxic insults. Another factor that is regulated by Ca^{2+}/ CREB activation is the brain-derived neurotrophic factor (BDNF) which protects neurons from NMDAR blockade-induced cell-death [16, 21].

Activated ERK1/2 (extracellular-signal regulated kinase) and Ca^{2+}/calmodulin-dependent protein kinase pathway phosphorylate CREB-binding protein and thereby activate the co-factor of CREB [21]. (see figure 1.3)

Calcineurin dependent dephosphorylation leads to translocation of the transducer of regulated CREB activity (TORC) which is another essential step for CREB-activation. (see figure 1.3) [21].

Via the suppression of the Forkhead box (FOXO), p53 and the pro-apoptotic Bcl-2 homology domain3 (BH3)-only member gene *Puma*, FLASH (FLICE-associated huge protein) or Tia 1 synaptic NMDAR stimulation also inhibits pro-apoptotic cell-processes [16, 21, 23].

Akt is activated via PI3k (phosphoinositide 3 kinase) and phosphorylates FOXO which leads to its export from the core. (see figure 1.3)

Furthermore, activated signal-pathways lead to reduction of oxidative stress. Due to Ca^{2+}-induced gene expression there is an increase in thioredoxin activity and facilitation of the reduction of hyperoxidized peroxiredoxins, which are an important class of antioxidant enzymes [21].

1.2.3.2 Extrasynaptic NMDARs

After activation of extracellular NMDAR, the increasing Ca^{2+} concentration influences several signalling-pathways. It leads to dephosphorylation of CREB and to the blockade of the anti-aptoptotic effect of this transcription factor. CREB-phosphorylation seems to be dependent on Jacob (juxtasynaptic attractor of caldendrin on dendritic boutons protein) – a binding partner of the Ca^{2+} -binding protein caldendrin (see figure 1.3). Jacob has its binding site in the nucleus and there evokes a CBP (CREB-binding protein) dephosphorylation and thereby its deactivation. The delocalisation of Jacob inside the core is associated with extrasynaptic NMDAR activation, whereas it stays outside, when a synaptic NMDAR is modulated [21].

Another essential regulatory protein is ERK (1/2) which is dephosphorylated and therefore inactivated by extrasynaptic NMDAR stimulation. ERK would support CREB in its antiapoptotic effect [21].

Furthermore the activation of FOXO and other pro-aptoptotic proteins leads to NMDAR-induced neuronal death as pro-apoptotic genes are expressed such as Foxo1, Txnip (thioredoxin-interacting protein), Bim (Bcl2-interacting mediator of cell death) and Fasl (Fas-ligand) [21].
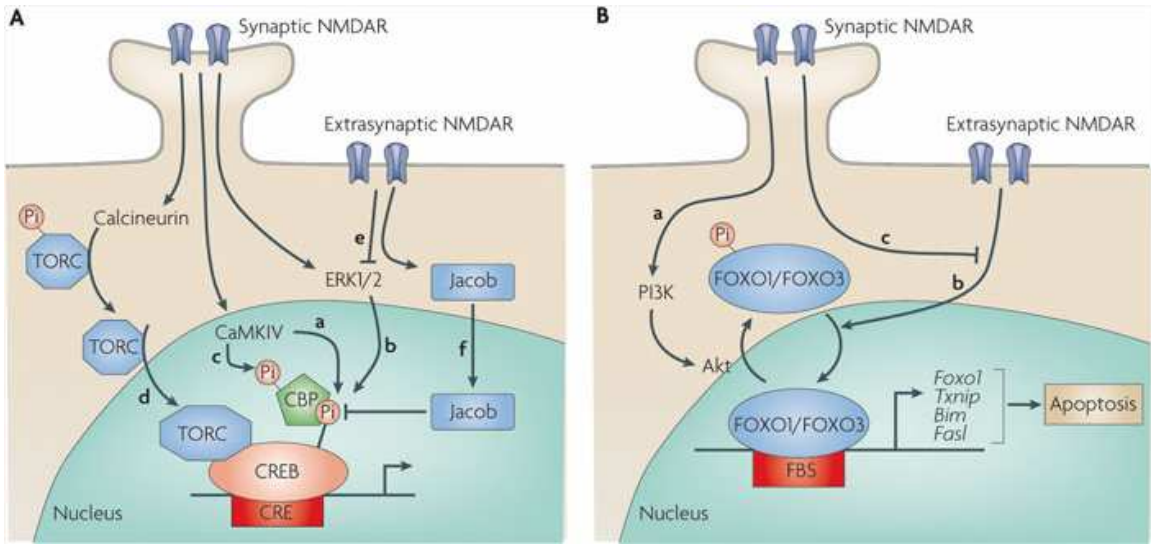
Figure 1.3: Opposing effects of synaptic NMDAR (A) and extrasynaptic NMDAR (B). Ca2+ influx via synaptic NMDAR leads to phosphorylation of CREB. This step is necessary to recruit its co-factor CREB binding-protein (CBP) and is mediated by the Ca^{2+}/calmodulin-dependent protein (CaM) kinase pathway and Ras–extracellular signal-regulated kinase 1/2 (ERK1/2). Another deciding step in CREB activation is the translocation of transducer of regulated CREB activity (TORC) which is accomplished after calcineurin dependent dephosphorylation.

Extrasynaptic NMDARs lead to CREB –pathway shutoff, as they inactivate the Ras–ERK1/2 pathway and the nuclear translocation of Jacob, which leads to CREB dephosphorylation. Translocation of FOXO (forkhead box protein O) into the core after activation of extrasynaptic NMDAR leads to expression of proapoptotic genes such as Foxo1, Txnip (thioredoxin-interacting protein), Bim (Bcl2-interacting mediator of cell death) and Fasl (Fas-ligand). Therefore, FOXO binds at FBS (FOXO binding site) and leads to transcription of these genes. Activation of synaptic NMDARs suppresses this effect by activation of Akt via PI3k (phosphoinositide 3 kinase). Akt phosphorylates FOXO and so leads to its export of the core [21].

(Hardingham GE, Bading H (2010) Synaptic versus extrasynaptic NMDA receptor signalling: implications for neurodegenerative disorders. Nat Rev Neurosci. (10):682-96. doi: 10.1038/nrn2911)

1.3 Excitotoxicity

Physiological cell death is associated with activation of apoptotic pathways and is a part of normal development of the brain as well as of several diseases. Excitotoxicity is a pathological process and its induced cell death is evoked by glutamate and its receptors. These operations seem to play a key role in stroke as well as in neurodegenerative diseases such as Huntington's disease, Alzheimer's disease, multiple sclerosis, Parkinson's disease and amyotrophic lateral sclerosis (ALS) [14, 24].

An elevated extracellular glutamate concentration in the CNS can be compensated under physiological conditions through uptake of the amino acid via sodium dependent active transporters in brain endothelial cells (see chapter 1.2.2) and subsequent efflux into the blood from the CNS. Lack of ATP during ischemia leads to an enhanced glutamate release and to a block of the reuptake mechanisms. The accumulated neurotransmitter leads to activation of several mediators in the CNS, which finally induce excitotoxicity. In addition, at the BBB lack of ATP leads to Na^+/K^+ -ATPase dysfunction which is later followed by decreased glutamate transport from the extracellular fluid into astrocytes and neurons [14].

High Ca^{2+} concentration after opening of the NMDAR leads to activation of NOS (nitric oxide synthase) and to mitochondrial toxicity. In case of ischemia neuronal NOS is translocated next to the NMDAR. The enzyme can then be activated via increased calcium influx, mediated by glutamate activated NMDARs and so forms NO. NO evokes formation of harmful metabolites causing protein nitration, protein oxidation, lipid peroxidation and direct DNA damage [14, 24].

Another consequence of the elevated Ca^{2+} level is the formation of reactive oxygen species (ROS). This is a result of the modulation of Na^+/Ca^{2+} transport in mitochondrias that leads to a decreased mitochondrial membrane potential followed by its dysfunction. ROS finally cause DNA-damage and protein degradation inducing neuronal death [14, 17].

1.4 The role of the NMDAR in pathology

1.4.1 Effects of NMDAR during ischemia

The activation of ionotropic receptors localised on pre-terminals such as GABA-gated Cl^- channels, presynaptic nicotinic acetylcholine receptors (nAChRs) and presynaptic glutamate receptors regulates the depolarization of the neuron. The Ca^{2+} concentration inside the cell can be enhanced by voltage-dependent Ca^{2+}-channels, by impaired activity of Na^+/Ca^{2+} transporters or by activation of NMDARs. The increased postsynaptic Ca-influx during ischemia leads to activation of nucleases, kinases and cytosolic proteases which induce neuronal death. During oxygen/glucose deprivation an elevated synaptic glutamate release occurs, which can't be compensated by an increased presynaptic uptake of glutamate like in physiological conditions [18].

After membranal depolarisation, Mg^{2+} is removed from the NMDAR-pore, which leads to the enhanced Ca-influx. Osmotic disbalance is also induced by the elevated Na^+ -concentration in the cell as a result of the long lasting depolarization. Cl^- ions follow passively, as well as water, which causes the swelling of the concerned cells. When the glucose and oxygen supply of the cell is impaired, the synaptic transmission is decreased. Only glutamate builds an exception due to its elevated liberation under these conditions and leads to cell death of the neuron [18].

1.4.2 The influence of NMDAR and Ca^{2+} release in Huntington's disease

Morbus Huntigton is a progressive neurodegenerative disease with typically increased CAG (cytosine-adenine-guanine) regions in the genome, which encode the amino acid glutamine, in the gene of Huntingtin, an ubiquitous protein. This results in an elongated stretch of glutamine at the N-terminus of this protein. Typical symptoms of Huntington's disease (HD) are abnormal movements, depressive mood or cognitive disturbances [25].

Neuronal loss during HD is mainly found in regions such as the striatum and cortex, but also in globus pallidus, thalamus, hypothalamus or substantia nigra.

Typically, there is an enhanced number of extrasynaptic NMDAR in HD. This contributes to increase of cell death and neuronal loss in Huntington's disease. Elevated induction of extrasynaptic NMDARs is induced by the mutant-form of Huntingtin, for example by inhibiting the presynaptic glutamate influx. Another factor influencing the progress of the disease is the increase of quinolinate, an endogenous agonist of the NMDAR (see figure 1.3). Moreover, mutant Huntingtin influences the pathway of metabotropic glutamate receptors, leading to Ca^{2+} increase inside the cell as well [25].

1.4.3 The influence of NMDAR and Ca^{2+} release in epilepsy

The enforced discharges during seizures start in a single region of the brain and can spread to neighboring regions. They are induced by high-frequency bursts of action potentials or hypersynchronisation of a group of neurons, which can be observed as a spike in the EEG. The long lasting depolarization of a single neuron leads to burst of action potentials in the neuron, so called paroxysmal depolarizing shift, followed by repolarization and hyperpolarisation. The sustained depolarization arises because of an elevated Ca^{2+}-uptake into the cell, followed by a Na$^+$-influx through voltage dependent channels [19].

Under physiological conditions, the propagation of a seizure can be suppressed by neighbored neurons. In epilepsy, the depolarizing shift can be spread to neighboring regions due to reduced activity of inhibitory neurons and sufficient hyperpolarization. These repetitive discharges induce activation of the NMDAR and an extended intracellular Ca^{2+}-level. Other consequences are the accumulation of Ca^{2+} in presynaptical terminals, followed by an elevated release of excitatory neurotransmitter (e.g. glutamate) and the enhancement of K^+, which promotes the depolarization of adjacent neurons [19].

In summary, NMDARs play an important role in pathophysiology of epilepsy as they promote the spreading of the discharge [19].
NMDAR-antagonists such as dizocilpine or ketamine succeeded in inhibiting seizures in animal models. They are still not used for therapy as they lead to severe undesired effects like reduced motor coordination, memory impairment and disorientation [26].

1.4.4 The influence of NMDAR and Ca^{2+} release in Morbus Alzheimer

Morbus Alzheimer is a neurodegenerative disease that is one of the main causes of dementia. It is accompanied by symptoms such as global cognitive dysfunction, especially memory loss, and behavior and personality changes. [11] Due to elevated activity of β- and γ-secretases, amyloid precursor protein is processed to accumulating amyloid-β peptide, which has several neurodegenerative effects. Further hallmarks are for example intracellular neurofibrillary tangles that consist of hyperphosporylated τ-protein, dystrophic neurites and amyloid angiopathy. These histopathologic changes influence CNS-regions such as hippocampus and cortex and affect memory and language. This neuronal disorder is mainly influenced by a changed Ca^{2+}-level, that could be mediated via enhanced activity of extrasynaptic NMDAR [17, 27].

Amyloid-β peptide leads to increased intracellular Ca^{2+} level as it activates the NMDAR. Furthermore, this pathologic protein causes Ca^{2+} overload also in mitochondria leading to decreased membrane potential. This mitochondrial dysfunction is one of the main factors that contribute to cell death [17].

Amyloid-β peptide influences the activity of several mitochondrial proteins, such as cyclophilin D that results in an increased formation of ROS. Furthermore, it promotes the release of Ca^{2+} from the endoplasmatic reticulum via the Inositol-triphosphate-receptor (IP_3-R), leading to depolarization of the mitochondrial membrane after Ca^{2+} influx through voltage-dependent channels into the mitochondria [17].

Long exposure with amyloid-β peptide leads to Ca^{2+} influx through NMDAR and AMPAR, mitochondrial dysfunction and building of ROS [17].

Memantine is one example for a NMDAR modulating compound that is used efficiently in the treatment of Alzheimer's disease [28].

1.5 NMDA-receptor agonists and antagonists

1.5.1 Agonists of the NR-2 subunit

The physiological agonist L-glutamate has the highest potency for NR2 subunits. Its affinity is dependent on several structures, like one positively charged center, represented by an ammonium-group and two negatively charged groups, represented by carboxylic-groups, which are localized in a certain distance on the NR-2 subunit of the NMDA-receptor [15].

N-methyl-D-aspartate has weaker agonistic activity than L-glutamate [15, 29].

By addition of a ring-system to the structure of potent agonists such as glutamate, new active compounds had been developed. These compounds imitate the active conformation of L-glutamate and include homoquinolinic acid (2S,1'R,2'S) 2-(carboxycyclopropyl)glycine (L-CCG-IV), (1R,3R) 1-aminocyclopentane-1,3-dicarboxylic acid (ACPD), and 1-aminocyclobutane-1,3-dicarboxylic acid (ACBD) [15, 29]. (see figure 1.4)
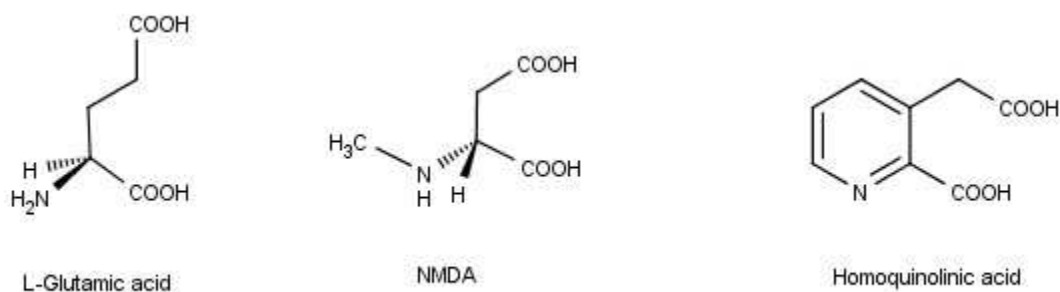
Figure 1.4 Selected agonists of the NR-2 subunit

1.5.2 Antagonists of the NR-2 subunit

The NR-2 subunit is generated by four distinct genes. The different products contribute individually to the structure and biochemistry of the receptor. Thus, selective antagonists influence the receptor in different ways. Antagonists can selectively bind on the NR2A-, or the NR2B subunit, whereas the subunit-composition of the receptor influences the affinity of the antagonists. Most glutamate antagonist show weaker activity so far, which is due to their low selectivity. Examples of structures, antagonizing the NR2 subunit are (*RS*)-*α*-aminoadipate, (*R*)-2-amino-5-phosphonopentanoate (D-AP5), 4-phosphonomethyl-2-piperidine carboxylic acid (CGS19755) and 4-(3-phosphonopropyl) piperazine-2-carboxylic acid (CPP) (see figure 1.5) [15].

D-AP5

CPP
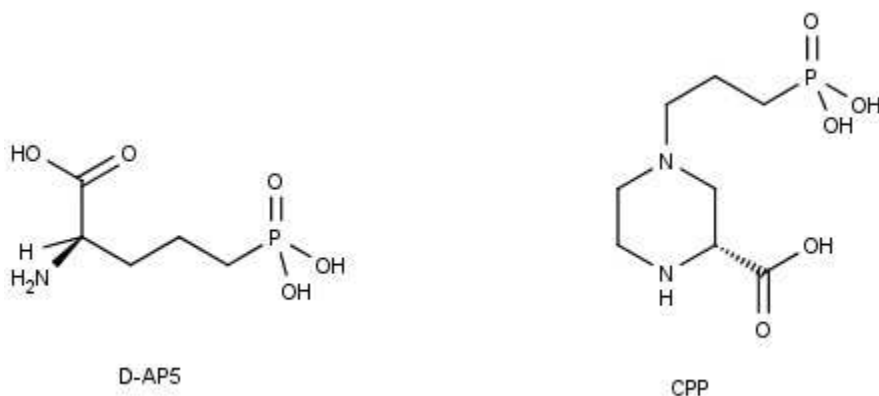
Figure 1.5: Selected antagonists of the NR-2 subunit of NMDAR

1.5.3 Agonists on the NR-1 subunit

Glycine, the agonist of the NR-1 subunit of the receptor, acts as a coactivator of the NMDAR, which means that both, glycine- and glutamate binding site, have to be occupied to activate the receptor. Other amino-acids, such as D-serine and D-alanine (see figure 1.6) show high affinity for this domain as well. ACPC, a cyclopropyl analogue and ACBC, a cyclobutane analogue of glycine show similar high affinity [15, 29, 30].
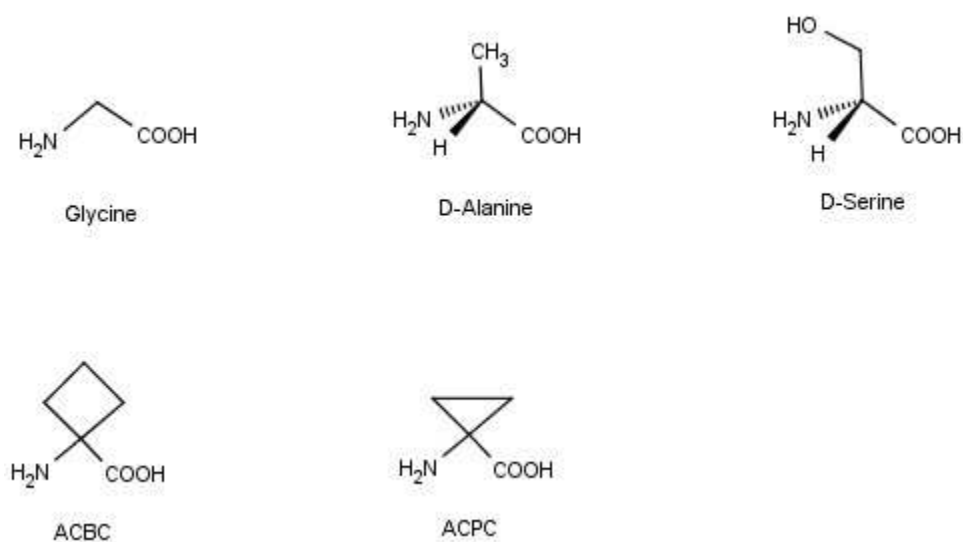
Figure 1.6 Selected agonists of the NR-1 subunit

1.5.4 Antagonists on the NR-1 subunit

The first identified compound antagonizing the NR-1 subunit was kynurenic acid (see figure 1.7). By development of structural modifications new potent glycine binding site antagonists were found, such as 5,7-dichlorokynurenic acid (5,7-DCKA), L-683,344, L-689,560 and L-701,324 (see figure 1.7) [15, 31].
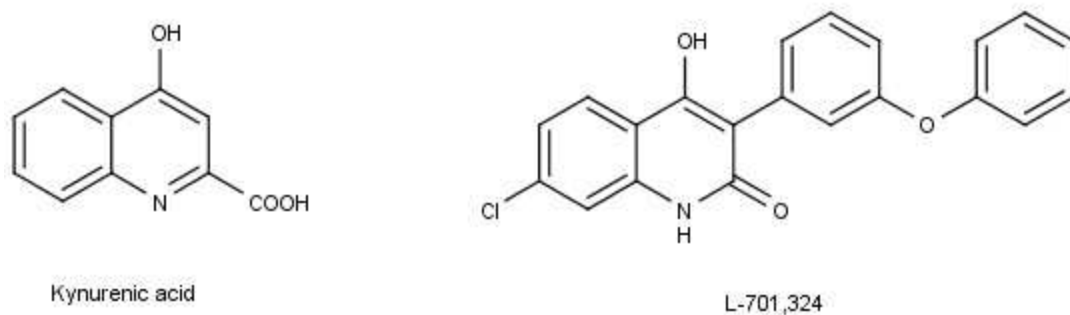
Figure 1.7 Selected antagonists of the NR-1 subunit

1.5.5 Allosteric modulators

Polyamines can modulate NMDAR's activity. First, they can increase the binding affinity for glycine, second, they induce glycine-independent activation by increase of the maximal amplitudes of NMDAR responses at saturating concentrations of glycine, and third, they block voltage-dependently. Several active compounds modulate the receptor in an allosteric way, the most popular of them is probably ifenprodile (see figure 1.8), which binds at the amino terminal domain. Williams K et al determined IC50 value of ifenprodile via voltage-clamp of Xenopus oocytes of 0,34µM for NR1A/NR2A and 146µM for NR1A/NR2B, respectively [32]. Also zinc acts as an non-competitive NMDAR-blocker [15]. (see figure 1.10)
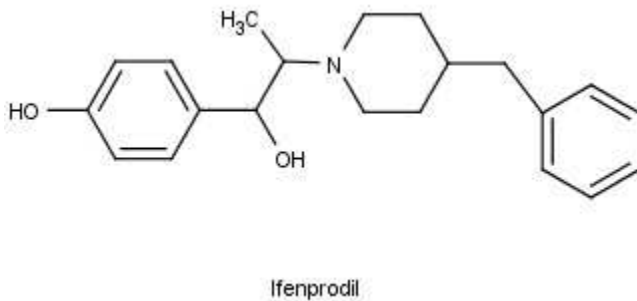
Ifenprodil

Figure 1.8 Ifenprodile as an example for allosteric modulators

1.5.6 Channel blockers

Blockers of the NMDAR-channel act as non-competitive antagonists. Physiologically, Mg^{2+} limits the activation of the NMDAR during resting membrane potential [15]. (see figure 1.10)

Several compounds block the channel in the same way, whereas their activity is dependent on the opening-state of the channel (=use-dependence). A glutamate-residue inside the pore which is placed on the M2-segment seems to be the essential structure for binding of the channel blockers. The dissociative anaesthetics ketamine and phencyclidine (see figure 1.9) act in this way. Furthermore, MK 801 (see figure 1.9), a compound which is used successfully as an experimental tool in models of ischemia, blocks the NMDA-channel [15, 28]. Memantine is well established for therapy of neurodegenerative diseases such as Alzheimer's disease, although it is only considered as a weak blocker of the channel [15, 28].
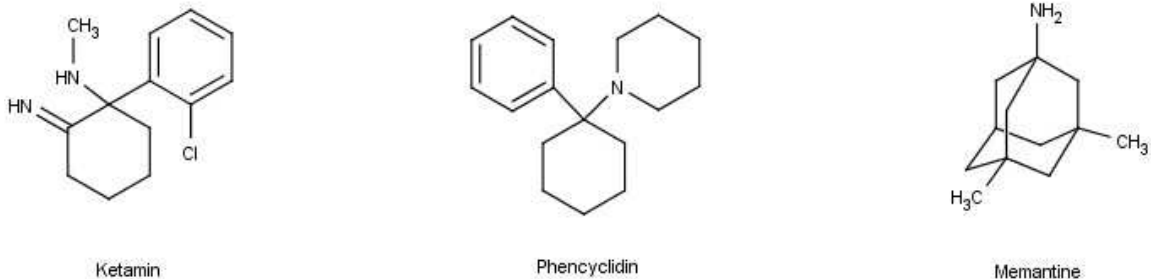
Figure 1.9: selected blockers of the NMDA-channel [33, 34, 35]
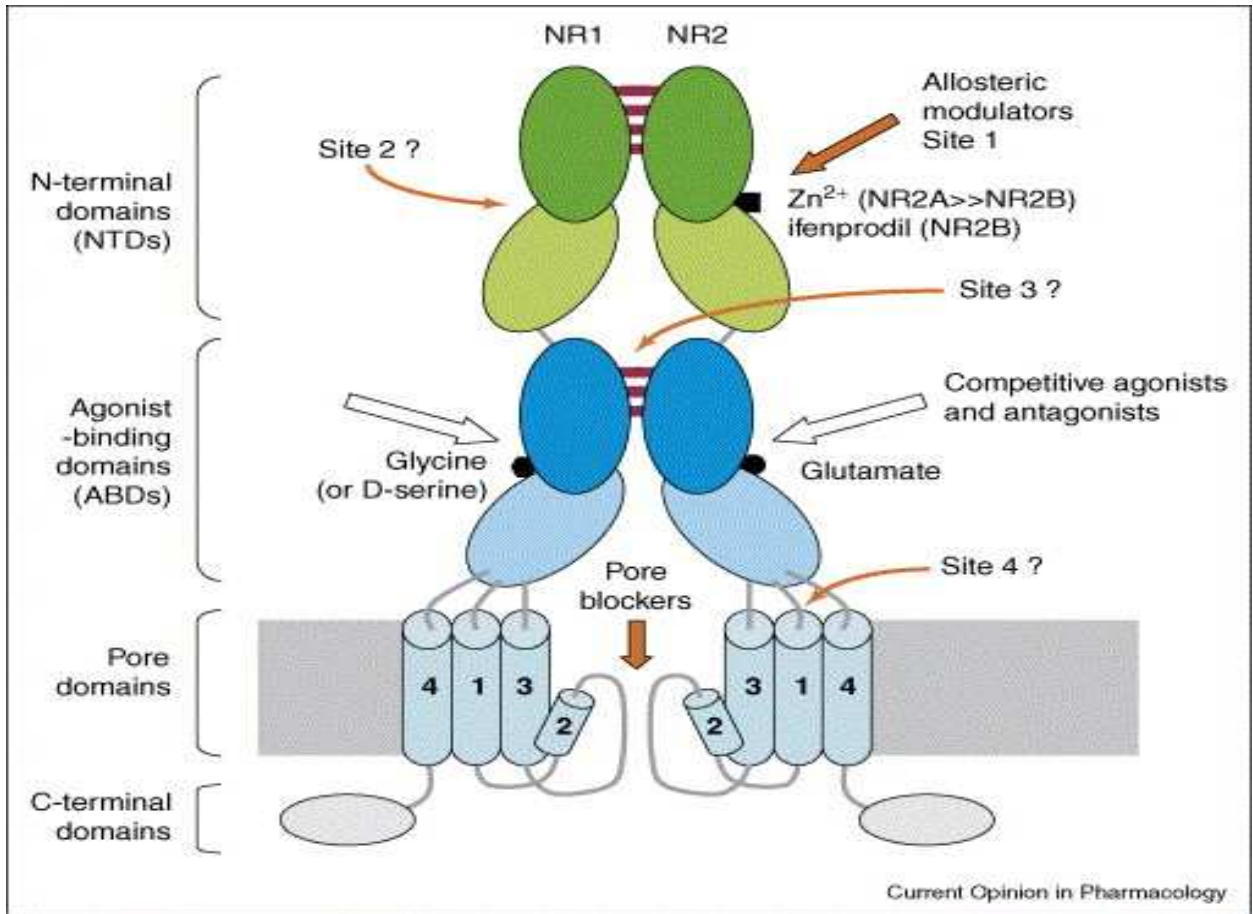
Figure 1.10: Binding sites of NMDAR modulators. One orange arrow shows the binding site of allosteric modulators like Zn^{2+} (which has higher affinity for NR2A- than NR2B-subunit) or ifenprodil at the N-terminal domain. The other orange arrow indicates the pore that is blocked by channel blockers like phencyclidine, ketamin or memantine. White arrows indicate the binding sites of competitive agonists and antagonists like glycine, L-glutamate or D-serine. The numbers 1-4 in the figure indicate the transmembrane-domains [32].
(Williams K (1993) Ifenprodil discriminates subtypes of the N-methyl-D-aspartate receptor: selectivity and mechanisms at recombinant heteromeric receptors. Mol Pharmacol. 44(4):851-859)

1.6 NMDAR at the blood-brain barrier

The investigation of the presence of NMDAR-subunits at the blood-brain barrier has not always been in agreement within the explorers, which worked on this topic. Some early studies by Morley et al. (1998) lacked of evidence of the expression of NMDAR-subunits at brain endothelial cells [36], whereas this presumption could be revised by studies by Giese et al. (1995) and König et al. (1992) [37, 38].

Up to now, NMDAR-subunits NR1, NR2A, NR2B and NR2C could be proved by real-time quantitative PCR (qPCR) to be sited and functionally active at the human blood-brain barrier [12, 39].

As the very potent NMDAR-blocker MK-801 was explored quite early, it could be used to prove NMDA-dependent effects in in-vitro and in-vivo assays [40, 41].

Giese et al (1995) examined the change of trans-endothelial electrical resistance and the change of permeability of paracellular transport in early studies in a co-culture of astrocytes and cerebral capillary endothelial cells after addition of NMDAR- modulators such as MK801 and ^{3}H-homochinolinic acid under normoxic as well as hypoxic conditions [73].

The further exploration of NMDAR-antagonists to reduce neurotoxicity that is caused via extracellular elevated glutamate appears as an interesting strategy to find possible drugs for therapy of ischemia-mediated brain damage. Nevertheless, many compounds failed in clinical trials, due to lack of efficacy and their strong side effects [15, 24, 42].

Actual research by Vivien et al (2015) shows the importance of the NR1 subunit in stroke. Ca^{2+}-dependent elevation of tissue plasminogen activator (t-PA) leads to worsening of the present process in stroke. This effect is mediated via binding of t-PA at the NR-1 subunit of NMDAR, which suggests that the blockade of this binding site serves as a potential strategy for preventing the progression of ischemic damage [43-46].

1.7 Aim of the work

Since the importance of blood-brain barrier regulation of physiological as well as pathophysiological processes has been explored, it represents an interesting target for drugs. Changes of blood-brain barrier functionality are associated with the progress of several neuronal diseases like Alzheimer's disease, Morbus Parkinson and stroke.

The N-methyl-D-aspartate receptor seems to mediate several effects and play an important role in the mentioned diseases. It is localized at neuronal synapses and is necessary for synaptic transmission and several physiological processes such as memory or learning [14]. Nevertheless, many compounds acting on the NMDA-receptor failed in clinical trials, due to lack of efficacy and side effects [15, 24, 42].

Recent studies showed that the NMDAR is expressed at the brain endothelium and functionally active during stroke [12]. The blockade of NR1 subunit at the BBB was able to reduce adverse stroke outcome [46].

The aim of this work was to test effects of chosen NR1 antagonists on several aspects of an in-vitro model of the blood-brain barrier consisting of mouse brain endothelial cell line cerebEND and rat glioma C6 cells.

The used NR1-antagonists were selected from a library of in house synthesized compounds which were previously tested for their NR1 blocking properties at the Department of Pharmaceutical Chemistry [47].

First, the influence of these substances on the cell viability of cerebEND and C6 cells should be tested under normoxic and oxygen/glucose deprivation conditions.

Then, transport studies with these compounds across cerebEND layers should be carried out, as well as the capability of the chosen NR1 antagonists should be tested to reduce barrier-damage in an in-vitro stroke model of the BBB.

Finally, experimental results should be compared with each other and their chemical structural properties in order to find the substances with highest potential for subsequent possible in-vivo studies.

2. Methods and materials

2.1 Materials

2.1.1 Chemicals and substances

Aqua purificata, 143AD-2029, Elisabeth Schubert GmbH

Ethanol, 1016AD-814, Elisabeth Schubert GmbH

Dimethylsulfoxide (DMSO), 41647, Sigma-Aldrich

Phosphoric acid, 015011006, Gatt-Koller GmbH&Co, Absam, Austria

Bu-082, Bu-090, Bu-099, Bu-108, Bu-113 (=Cs-294), Cs-182, Cs-191 (=Cs-241), Cs-199, Cs-224, Sie-20, provided by the Department of Pharmaceutical Chemistry Vienna, Austria (chemical structures follow in 2.1.1.1)

(+)-MK801 hydrogen maleate, 022M4616V, Sigma-Aldrich

L-701,324, 3B/88582, Tocris bioscience

2.1.1.1 Chemical structure and properties of the used substances

The structures of the used substances were gained from Buchstaller et al. and Owens et al. [48, 49].

L-701,324

ClogP=5.406

Figure 2.1.1
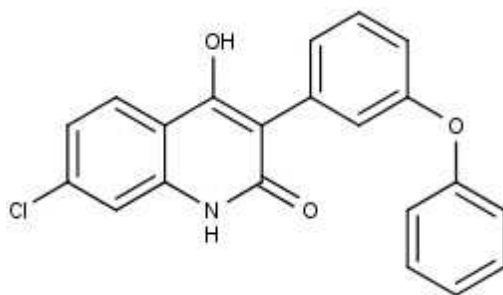
Bu-82 (17)

ClogP=5.024

Figure 2.1.2
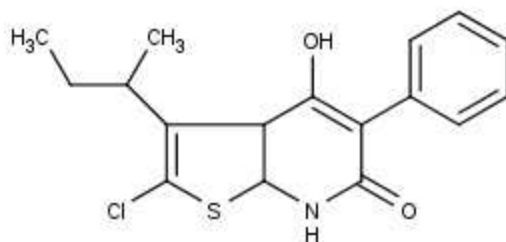
Bu-90 (23)

ClogP=3.308

Figure 2.1.3
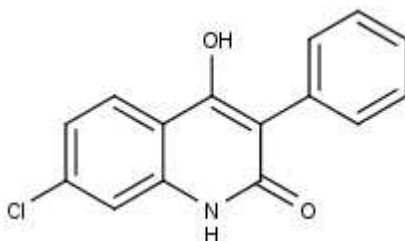
Bu-99 (15)

ClogP=4.495

Figure 2.1.4
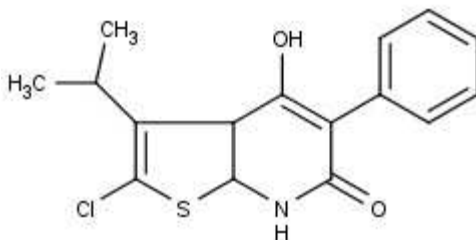
Bu-108 (11)

ClogP=4.096

Figure 2.1.5
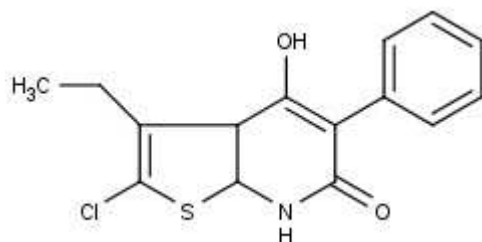
Bu-113 (34)

ClogP=7.122

Figure 2.1.6
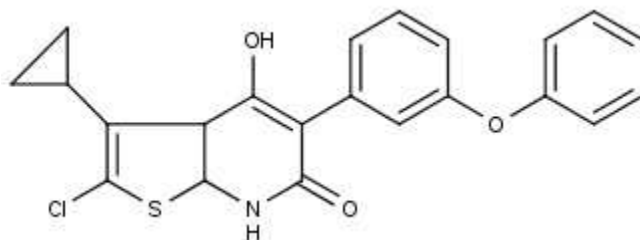
Cs-182 (40)

ClogP=6.723

Figure 2.1.7
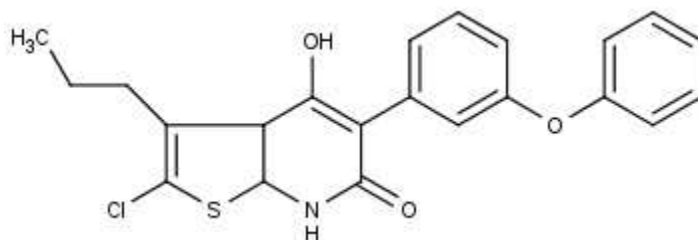
Cs-191 (41)

ClogP=6.593

Figure 2.1.8
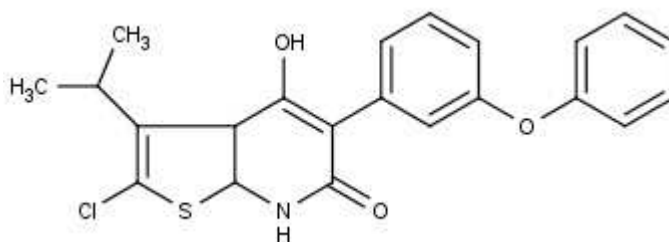
Cs-199 (42)

ClogP=6.992

Figure 2.1.9
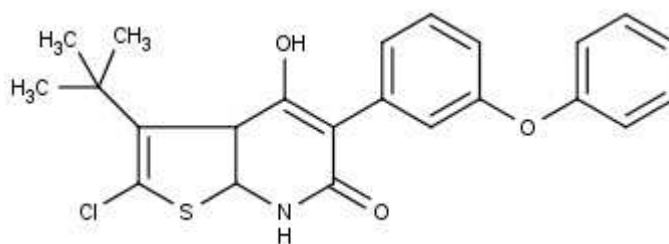
Cs-224 (45)

ClogP=4.964

Figure 2.1.10
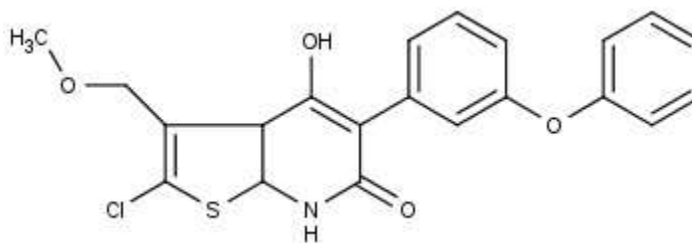
MK 801

ClogP=3,00

Figure 2.1.11
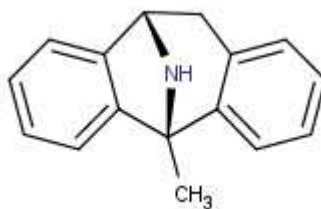
2.1.2 Devices and software

Laminar Air Flow Biosafe 3, Ehret GmbH & CoKG, Tulln, Austria

Light microscope, TMS, Nikon, Japan

Microplate-reader, Infinite M200Pro Tecan, Austria GmbH, Grödig, Austria

Waterbath, 355100, Müller-Scherr GmbH & CoKG, Linz, Austria

Thoma-chamber, Paul Marienfeld GmbH & CoKG, Lauda-Königshofen, Germany

Cover slip, 8000121, Hirschmann Laborgeräte GmbH & Co. KG, Eberstadt, Germany

Centrifuge, 5810R, Eppendorf AG, Hamburg, Germany

Fridge, 4°C, Liebherr GmbH, Kirchdorf, Germany

Freezer, -20°C, Liebherr GmbH, Kirchdorf, Germany

CO_2-incubator, $CO_2$6000, NAPCO, Ehret GmbH & CoKG, Tulln, Austria

Hypoxic chamber consisting of a two shelf C-chamber from Bio Spherix (Canada) controlled by a Pro Ox C21 System with 1% O_2 and 5% CO_2, placed in a $CO_2$6000 NAPCO, Ehret GmbH & CoKG, Tulln, Austria Vortex-mixer, IKA Vortex Genius 3, ROTH, Graz, Austria

Autoclave, CV-EL, Certoklav Sterilizer GmbH, Traun, Austria

Magnetic stirrer, MR 3001 K, Heidolph Instruments GmbH & Co.KG, Schwabach, Germany

pH-meter, model 250 A, Orion Research Inc, Boston, MA, USA

Ultrasonic-cleaner, Branson 3210, INULA, Instrumentelle Analytik, Wien Austria

Microsoft Excel 97™

HPLC-device with Auto-Sampler, SI2-20A/20AC Prominence, Shimadzu corporation Kyoto, JPN

HPLC-software, Solvent Delivery Module, LC-20AD Prominence, Shimadzu corporation Kyoto, JPN

Marvin-sketch®, by chem.-axon downloaded from the homepage of the Department of Pharmaceutical Chemistry in Vienna

http://merian.pch.univie.ac.at/pch

2.1.3 Cell culture material

Trypsin/EDTA-solution, 0,05%/0,02% (w/v), L 2143, Biochrom AG, Berlin, Germany

Fetal calf serum (FCS), A15-151, 56℃ heat-inactiva ted, # 10720-106, PAA laboratories GmbH, Pasching, Austria

Phosphate buffered saline (PBS), sterile, 14190-094, Invitrogen life technologies, Gibco™, Carlsbad, CA, USA

Hanks balanced salt solution, H6648, Sigma Aldrich Chemie GmbH, Steinheim, Germany

Dulbecco's modified eagle medium (DMEM), D5796, Sigma Aldrich Chemie GmbH, Steinheim, Germany

Dulbecco's modified eagle medium (DMEM), W/O-Glucose 11966-035, Gibco™, Baisley, UK

Cell culture flasks, surface 75 cm², 658175, Greiner Bio-One GmbH, Frickenhausen, Germany

Cell culture flasks, surface 25 cm², 690175, Greiner Bio-One GmbH, Frickenhausen, Germany

96 well microplates, clear, Cellstar®, 655180, Greiner Bio-One GmbH, Frickenhausen, Germany

24 well plates, 353226, Becton Dickinson and Company, Franklin Lakes, NJ, USA

12 well plates, 353503, Becton Dickinson and Company, Franklin Lakes, NJ, USA

24 well inserts, 0.4μM pore size, 353095, Becton Dickinson and Company, Franklin Lakes, NJ, USA

12 well inserts, 1μM pore size, 35103, Becton Dickinson and Company, Franklin Lakes, NJ, USA

Multi channel pipettes, 100 μl, 300 μl, Eppendorf AG, Hamburg, Germany

Pipettes, 10 μl, 100 μl, 1000 μl, Eppendorf AG, Hamburg, Germany

Pipette tips, 0.1-10 µl, 1-200 µl, 5-300 µl, 100-1000 µl, 1-061-96-0, 1-110-96-1, 1-104-96-0, 1-200-96-2, AHN Biotechnologie GmbH, Nordhausen, Germany

Tubes, 15 ml, 50 ml, 188271, 227261, Cellstar®, Greiner Bio-One GmbH, Frickenhausen, Germany

Sterile pipettes, 5 ml, 10 ml, 25 ml, 86.1253.001, 86.1254.001, 86.1685.001, Sarstedt AG, Nürnbrecht, Germany

Syringe filters, Rotilabo®syringe filters, P666.1, PVDF, 0.22 µm, sterile, Carl Roth GmbH & CoKG, Karlsruhe, Germany

Needles, 100 Sterican®, 4665791, Braun Melsungen AG, Melsungen, Germany

Syringe 10 ml 57B-9140, BD Laagstraat, Temse, Belgium

Petri dishes, 101VR203V, 90 mm, Sterilin Ltd., Newport, UK

Reagent-reservoirs, 89094-662, VWR, USA

Cell culture assay:

EZ4U, BI-5000, Biomedica GmbH & CoKG, Vienna, Austria

2.1.4 Cell lines

2.1.4.1 Cell line C6

C6 is a glioma cell line which enables in-vivo and in-vitro exploration of fast-growing brain cells. Hence the induced tumor of glial cells contains oligodendrocytes, microglia cells and astrocytes. The latter are most important for the blood-brain barrier in-vitro cell culture model, due to their contribution to the maintenance of the chemical environment and the structure of the blood-brain barrier [7, 50].

C6 cells were generated from rat glioma cells. The tumor was induced after incubation with methyl-nitroso-urea over a period of 8 months by Benda et al. and Schmidek et al. in Sweet's laboratory at the Massachusetts General Hospital. As the animals showed first symptoms they were euthanized. One of the cell lines was numbered as "# 6", and when it was cloned it was called "C6" [50].

Glioma cell line C6 was obtained from ATCC initially gathered from rattus norvegicus.

2.1.4.2 cerebENDs

CerebEND (Mouse Cerebellar Capillary Endothelial Cell Line) is a brain microvascular endothelial cell line which is generated for exploration of the physiological and pathological functionality of the in-vitro blood-brain barrier model. Cells were gained and provided from cerebellum of neonatal mice by Silwedel and Förster (2006).

CerebENDs show very similar morphology to primary brain endothelial cells of mice. Typically they build monolayers of tightly packed, elongated cells. As they show confluence, they stop spreading and growing due to contact-inhibition [53].

2.2 Methods

2.2.1 Cell-culture

2.2.1.1 Coating of tissue flasks, well plates and transwell inserts

To enable a better adherence of the according cell line, flasks and well plates were coated with a 0,5% gelatin solution. (Solution volume: 2ml/T25; 6ml/T75; 50µl/96-well; 200µl/24-well)

Transwell inserts were coated with collagen IV for 2h at 37˚C according to Neuhaus et al. [7].

2.2.1.2 Medium exchange

To supply the cell line sufficiently with medium, the exchange was accomplished every 2-3 days. Therefore, prewarmed DMEM containing 10% FCS and penicillin/streptomycin was added, after the used medium was removed.

Volume of medium in according materials:

75 ml tissue flasks: 15ml

25ml tissue flasks: 5ml

96-well plates: 0,2ml per well

24-well plates: 0,9ml per well

12-well plates: 1,5ml per well

24-well inserts: 0,3ml per insert

12-well inserts: 0,5ml per insert

During specific assays, it was necessary to use different media, e.g. lacking glucose and/or FCS and antibiotics. Medium was added in the same volume as mentioned above.

2.2.1.3 Subcultivation

To subcultivate the actual cell line and reduce its number after they have grown nearly confluent (surface is fully covered with cells so that each cell is completely surrounded by neighbouring cells), cells needed to be splitted.

Following these rules, cerebENDs were always splitted in ratio 1:3, whereas C6 cells were splitted in a ratio of 1:20, to gain 90-95% confluency of the present cells after cultivation of a week according to Neuhaus et al. [7].

2.2.1.4 C6

C6 cells were cultured in T75 or T25 tissue flasks or wellplates, when they were seeded for several tests like EZ4U-assays.

Exchange of media was accomplished each 2-3 days.

Due to the fast growth of glioma cells, they had to be splitted in ratio 1:20 each seven days.

For EZ4U-assays, 200µl of a cell suspension in DMEM (containing FCS and antibiotics) were seeded in 96-well plates with a concentration of 20000 cells/cm² according 34000 cells/ml. Every 2-3 days medium had to be exchanged by removing the old medium and adding 200µl of the new DMEM (containing glucose, FCS and antibiotics) per well.

For the generation of a co-culture between C6 cells and cerebEND cells, C6 were seeded in 24 well plates with a density of 20000 cells/cm² according to Neuhaus et al. [7].

2.2.1.5 cerebENDs

Due to slower growth and contact inhibition this cell line had to be splitted in a ratio of 1:3 once a week. This was accomplished by trypsination (10% trypsin solution in PBS).

Medium had to be exchanged each 2-3 days.

For EZ4U-assays, 200 µl of a cell-suspension had to be seeded out in 96-well plates. The cell concentration had to be about 40000 cells/cm² according 68000 cells/ml. Medium had to be exchanged every 2-3 days by hovering the used medium and adding 200µl of new medium (DMEM, containing glucose, FCS and antibiotics).

2.2.2 Cell viability test (EZ4U)

2.2.2.1 General procedure

EZ4U-assay was used as a pre-test in order to investigate the cytotoxicity of the used substances and was necessary to find out in which concentrations the compounds don't act toxic for further transport studies.

The assay was accomplished according to the manufacturer's instruction on day 6 after cell seeding.

EZ4U-test substrate (tetrazolium salt) was dissolved in 2.5 ml activator solution (PMS), which lead to a yellow colored solution. 10µl of the solution were added to 100µl assay solution after according incubation time in each well. [18, 19]

The absorption was measured at 470 nm and a reference wavelength at 620 nm [51, 52].

The resulted coloring was measured with Tecan® multi-plate reader, after 15, 30, 60 and 120 minutes of incubation

2.2.2.2 Assay design

For the assays 96-well plates were used. The first row was prepared only with gelatin and medium (DMEM with glucose and without serum or antibiotics), which represented the blank value. The second row with cells was for vehicle treated cells. The last row contained cells with DMEM with serum and antibiotics to see if there is a difference in cell viability concerning different constitutions of media. The rest of the microtiter-plate was transferred with cells in DMEM without additives and the substances in a concentration of 100µM.

In later approaches the experimental arrangement with lower concentrations was varied with still one blank row and one vehicle treated control row.

		Bu-082	Bu-090	Bu-099	Bu-108	Bu-113	Cs-182	Cs-191	Cs-199	Cs-224	
Blank	Control	100µM	100µM	100µM	100µM	100µM	100µM	100µM	100µM	100µM	Control
Blank	Control	100µM	100µM	100µM	100µM	100µM	100µM	100µM	100µM	100µM	Control
Blank	Control	100µM	100µM	100µM	100µM	100µM	100µM	100µM	100µM	100µM	Control
Blank	Control	100µM	100µM	100µM	100µM	100µM	100µM	100µM	100µM	100µM	Control
Blank	Control	100µM	100µM	100µM	100µM	100µM	100µM	100µM	100µM	100µM	Control
Blank	Control	100µM	100µM	100µM	100µM	100µM	100µM	100µM	100µM	100µM	Control
Blank	Control	100µM	100µM	100µM	100µM	100µM	100µM	100µM	100µM	100µM	Control
Blank	Control	100µM	100µM	100µM	100µM	100µM	100µM	100µM	100µM	100µM	Control

Figure 2.2.1: Scheme of a prepared 96 well-plate:

2.2.2.3 Preparation of the substance solutions

Stock-solutions were prepared in DMSO dilution series starting from 100mM stock solutions. To obtain the needed concentration, the stock-solution was diluted in an according ratio (1:100) in DMEM (dependent on the performed assay with or without glucose, but in all assays without FCS).

2.2.3 Transport assay

2.2.3.1 Preparation of the cells

Cells were cultivated in 12-well-inserts.

Inserts had to be coated with collagen IV for 2h at 37ºC.

After coating, inserts were washed with PBS three times. Cells were seeded 13 days before the assay with a concentration of 40000 cells/cm^2 according to Neuhaus et al. [7]. Per substance, two inserts with cells, and two inserts, only coated with collagen (which served as blanks in the later assay) were used for each independent experiment.

Medium exchange and addition of medium supplements were accomplished according to Neuhaus et al. [7].

The transport assay protocol was according to Novakova et al. [54]. In brief, basolateral volume was 1500µl DMEM supplemented with 0,1% DMSO, filled wells were prewarmed with DMEM and DMSO for 30 minutes at 37˚C.

Compound solutions in DMEM were prepared by adding 1:1000 from 10mM stock solutions in DMSO to reach final concentrations of 10µM. These 10µM compound solutions were prewarmed at 37˚C for 30 minutes.

As internal standard 10µM diazepam were added additionally. Before starting the transport assay, cell layers in inserts were washed with prewarmed HBSS twice and DMEM was added. After 30 minutes at room temperature, TEER was measured to ensure integrity according to Neuhaus et al. [7].

Then well plates with inserts were put in the incubator. After temperature equilibration of approximately 30 min, cell-inserts were placed in the first prepared well-plates. Afterwards, 500µl of the substance solutions were added.

Inserts were then transferred after 10, 30, 60 and 120 minutes in new wells filled with prewarmed DMEM + 0,1% DMSO. At the end of the transport experiment, supernatants, samples and stock solution were collected and prepared for HPLC.

2.2.3.2 HPLC analysis

Mobile phases were composed of acetonitrile and 10mM potassium-phosphate buffer (pH=3) in according ratio (See table 2.1). For sufficient separation of the compounds, an 18C-reversed phase (Clarity Oligo-RP column, 5µM; 240*4,6 mm (Phenomenex)) with according pre-column was used.
Instructions were followed as recommended in [55].

Table 2.1: Compositions of the mobile phases and the running time of the tested components (used eluent-constitutions are marked grey)

Substances	55%ACN	60% ACN	65% ACN	75% ACN
L-701,324		8.0-8.6	6.3-6.9	
Cs-182			13.1-14.3	7.5-8.5
Cs-191			12.2-13.3	7.3-8.0
Cs-199			15.5-17.0	8.9-9.6
Cs-244			8.3-9.0	
Bu-82			7.7-8.3	
Bu-90	9.3-9.9		3.9-4.4	
Bu-99	9.3-9.9		6.3-6.9	
Bu-108		6.2-6.8	5.4-5.8	
Bu113			15.5-16.7	8.6-9.5
Diazepam	*8.3-8.9*	*6.7-7.3*	*5.8-6.3*	*4.5-5.1*

Samples of transport assays were precipitated 1:2 in acetonitrile at 4°C for 30min. After centrifugation at 14000 rpm for 5min, supernatants were subjected to HPLC analysis.

Results were presented as clearance/time-curves and permeability coefficients were calculated according to Novakova et al. [54]. In order to account for cell layer variabilities permeability coefficients of internal standard diazepam (see

figure 2.5) were calculated and were used to normalise permeability coefficients of the test compounds. The resulting ratio factor F was used to rank the permeability of the compounds.
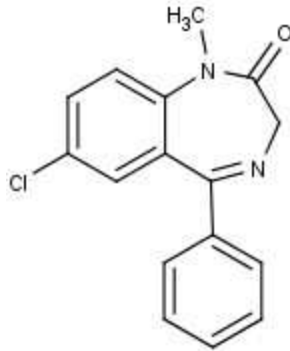
Figure 2.5: Diazepam [56]

The factor was calculated for the values of 0-10 min time of transport as well as for 10-120min. The values of 0-10min transport-time are often imprecise, as the cells that are exposed to the substance need some time for equilibration.

Furthermore, the recovery of the tested substances and diazepam was calculated to describe possible interactions between the (lipophilic) compounds and the cells or the cell-culture material, especially the insert membranes. Substances with a low recovery value probably got stuck in the cell or the insert.

2.2.4 Oxygen/glucose deprivation barrier experiments

With this assay the change of transendothelial electrical resistance (TEER) under OGD-conditions was measured. Thereby, the difference between the OGD-effect with and without substances was observed to see, if the applied compounds are able to reduce breakdown of the in-vitro blood-brain barrier.

This was followed by a transport study accomplished with carboxyfluorescein, which is a marker of the paracellular transport, also describing the tightness of the barrier [57].

A co-culture consisting of cerebEND- and C6 cells is necessary as the C6 cells contribute to the tightness of the layer of the endothelial cells as well as to the damage during OGD-conditions [7].

Protocols and assay conduction was according to Neuhaus et al [7].

The substances dissolved in DMSO in concentrations of 0.1-30 mM, were diluted in a 1:1000 ratio in DMEM without glucose to gain concentrations of 0.1-30µM. 10ml of each substance solution were needed. For the control DMEM with glucose was supplemented with 0,1% DMSO.

For normoxic controls DMEM was supplemented also with 0,1% DMSO.

In order to apply OGD, co-cultures were incubated in a hypoxic chamber situated in an incubator from Napco at 37˚C for 4,5-5 hours. The hypoxic chamber consisted of a two shelf C-chamber from Bio Spherix (Canada) controlled by a Pro Ox C21 System with 1% O_2 and 5% CO_2.

Normoxic control monoculture, co-culture and blank inserts were incubated in an incubator with 5% CO_2 and saturated humidity atmosphere at 37˚C.

TEER-values before and after incubation were gained by measuring with chopstick-electrodes from Millipore to gain the change of the TEER in %. Values that were obtained in context of the assay were referred to the cerebEND cells under normoxia-conditions, whose values were so set on 100%. Then the values of the assay were normalized to the averaged TEER in % of co-cultured cells to see the difference between the TEER with and without substances under OGD-conditions and afterwards again referred to values normalized on normoxia cerebEND-cell values. These final results allow the comparison of the changed TEER in % to normalized co-culture OGD values.

After OGD-treatment and second TEER measurment, 10µM carboxyfluorescein were added in the apical compartiment and a transport study was carried out at 37˚C under normoxic conditions for 1 hour. In that way, reoxygenation was simulated, which also takes place in case of stroke-therapy.

This additional supply with oxygen may prevent the cells from death, nevertheless an elevated amount of oxygen also induces the formation of reactive oxygen species, which means that an over-supplementation with oxygen can also lead to cell-death [58, 59].

Samples were measured by using Tecan plate reader and result calculation of carboxyfluorescein transport was according to Neuhaus et al. [7].
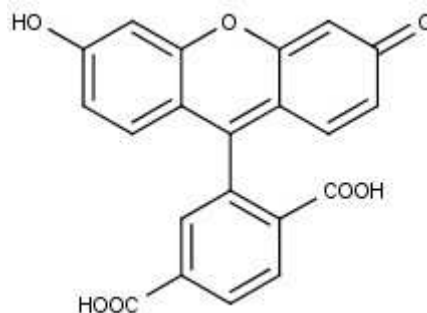
Figure 2.6: 6-Carboxyfluorescein [57]

In detail, 1mg/ml carboxyfluorescein-solution was added to the substance stock solutions, whereas 3,76 µl per ml stock solution of the medium where transferred in the residual medium to achieve 10µM. Apical medium was aspirated and 300µl of the carboxyfluorescein solution in DMEM±glucose were added.

After 1 h of incubation in normoxia incubator with normal O_2, 5% CO_2, 37˚C and saturated humidity atmosphere, the basolateral samples as well as the residual volume of the stock-solutions were collected. Therefore, 100µl triplicates were tansferred in black 96 well-plates and measured with a fluorescence microplate reader (Infinite Pro Tecan Reader) at 485nm/520nm.

2.3 Ranking by Spearman's rank-correlation-coefficient

The coefficient (r_s) enables to prove the correlation between two parameters. The calculation was accomplished as proposed in [60].

$$r_s = 1-(6*\sum D^2(n*(n^2-1))$$

Equation 2.1: Calculation of the Spearman's rank-correlation-coefficient (r_s): D² equals the square of the difference of one pair and n equals the number of pairs.

To correlate two parameters, they were ranked considering their value. After the rankpairs were determined, the difference of each pair was calculated, squared and afterwards all results were summed up ($\sum D^2$). By placing the number of rankpairs in the formula (n) the rank-correlation-coefficient could be determined. Te resulting rs value was compared to the cutoff (r) at the probability values (p) of 0,05 and 0,01 within the table received from the website www.york.ac.uk/depts/maths/tables/spearman.pdf [61]. As far as rs > r, the null hypothesis was rejected, according p-value <0,05 or <0,01, which means that there is no correlation between the according parameters. Instructions were followed as recommended in [62].

3. Results

3.1 Effects of glycine antagonists on cell viability

The first aim was to determine cell toxicity of glycine antagonists at a concentration of 100µM in order to be able to find out whether following OGD experiments could be accomplished at these concentrations in glioma cell line C6 and cerebellar endothelial cell line cerebEND.

3.1.1 CerebEND cells under normoxic conditions

Toxicity of the substances on cerebEND cell line was tested to adapt used concentrations in later assays (especially transport assays).

Figure 3.1.1 shows the influence of the 9 glycine antagonists on cerebEND cells. Absorption values were between 0,004 and 0,39 (see figure 3.1.1A) after 120 minutes EZ4U-reagens incubation.

Bu-113, Cs-182 and Cs-224 harm the cells, as it can be seen at the reduced cell viability. The viability decreased to 3,0 ± 0,9% by Bu-113, 29,5 ± 7,1% by Cs-182 and 0,9 ± 0,5% by Cs-199. All other substances didn't cause reduced cell viability at 100µM (see figure 3.1.1B).

Also Bu-82 showed weak but significant reduction of cell viability to 93,0 ± 9,3%.

A
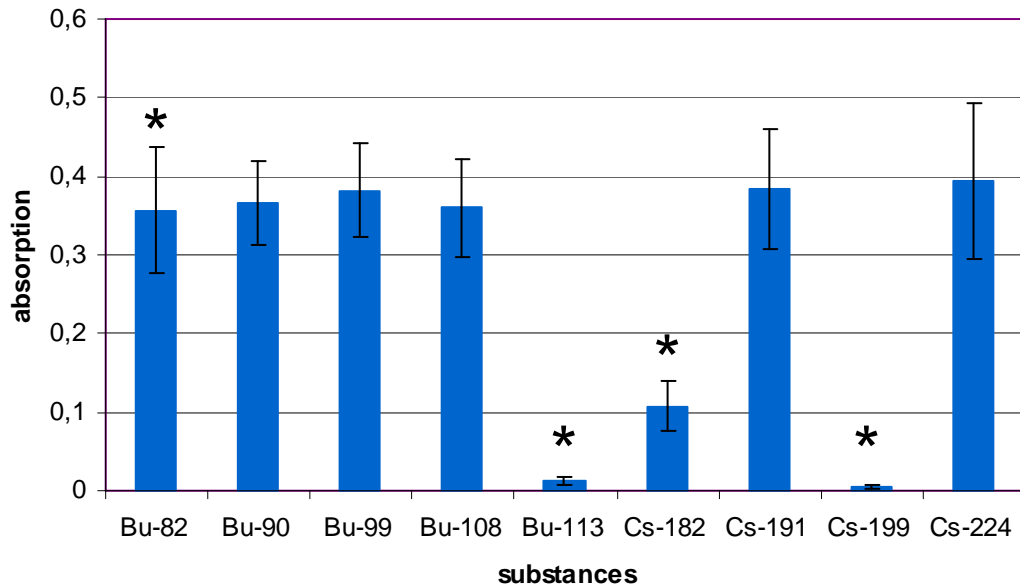
B
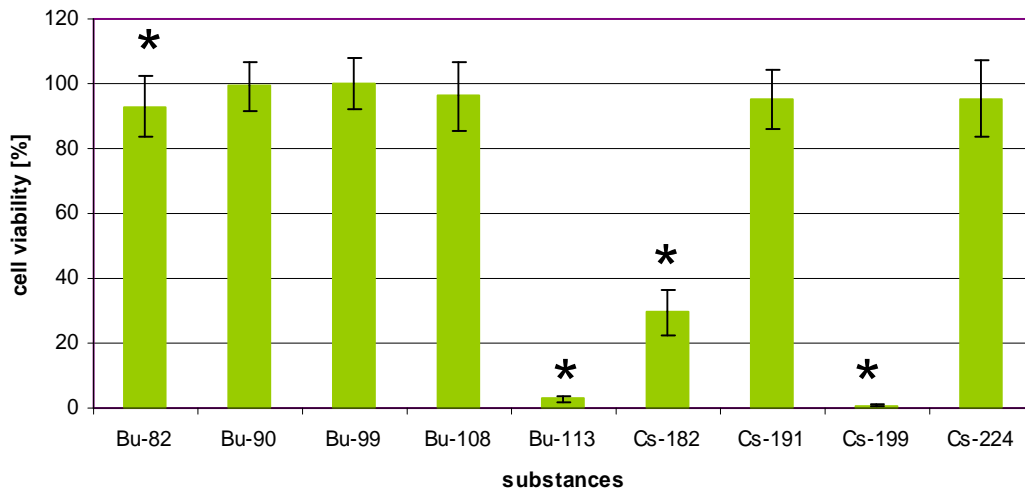
Figure 3.1.1: Absorption of the formed XTT-derivate after addition of glycine antagonists on cerebEND cell viability at 100µM under normoxia conditions using EZ4U-assay (4h incubation) (A) and 120min measuring time, effects of glycine antagonists on cerebEND cell viability at 100µM under normoxia conditions using EZ4U-assay (4h incubation) in [%] (B), data are presented as mean ± standard deviation (SD) (n=32) from 2 experiments.
*: statistically significant vs. control, p<0,05, double sided t-test with the same variance

To find out in which concentration the toxic substances don't harm the cells any more during 4h incubation the according substances were added in concentrations of 1µM, 3µM, 10µM, 30µM and 100µM.

A
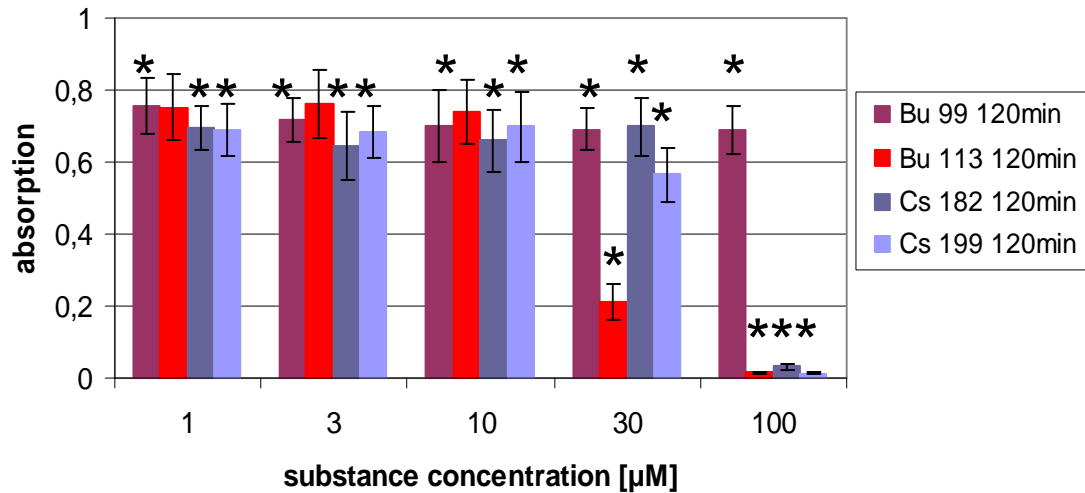
B

Figure 3.1.2: Absorption of the formed XTT-derivate after addition of Bu-99, Bu-113, Cs-182 and Cs-199 (1µM, 3µM, 10µM, 30µM and 100µM) on cerebEND cell viability under normoxia conditions using EZ4U-assay (4h incubation) and 120min measuring time (A), effects of Bu-99, Bu-113, Cs-182 and Cs-199 (1µM, 3µM, 10µM, 30µM and 100µM) on cerebEND cells under normoxic conditions on cell viability (4h incubation) in [%] (B), data are presented as mean ± standard deviation (SD) (n=16) from 2 experiments.
*: statistically significant vs. control, p<0,05, double sided t-test with the same variance

Absorption values in figure 3.2 were between 0,01 and 0,76.

Bu-99 as a non-toxic compound was used as a control-value. The cell viability didn't change much. However the values were still significant. Gained values were 93,6 ± 8,3% (1µM), 90,0 ± 10,0% (3µM), 87,0 ± 8,9% (10µM), 86,0 ± 7,1% (30µM) and 85,9 ± 0,2% (100µM).

Bu-113 damaged the cells at 30µM (26,7 ± 5,3% cell viability) as well as at 100µM (2,1 ± 0,4% cell viability), which demonstrated the elevated sensitivity of cerebENDs to the substance compared to C6 cell line (see figure 3.6A).

Cs-182 reduced the cell viablity at 100µM to 4,0 ± 1,0%, lower concentrations didn't affect the cells in such an extent, although the values were still significant. Cell viability was reduced to 86,6 ± 7,2% at 1µM, 80,1 ± 8,4 at 3µM, 81,8 ± 7,6% at 10µM and 86,8 ± 7,6% at 30µM Cs-182.

Also Cs-199 decreased cell viability to 72,1 ± 5,1% at 30µM and 1,6 ± 0,6% at 100µM. Lower concentrations showed significant reduction of cell viability to 88,1 ± 6,8% (1µM), 87,5 ± 8,6% (3µM) and 89,0 ± 8,0% (10µM) (see figure 3.2b).

The same assay was accomplished with a shortened time of incubation (1h instead of 4h). These conditions simulated the reduced duration of exposition of each substance during the transport experiments.

A

B
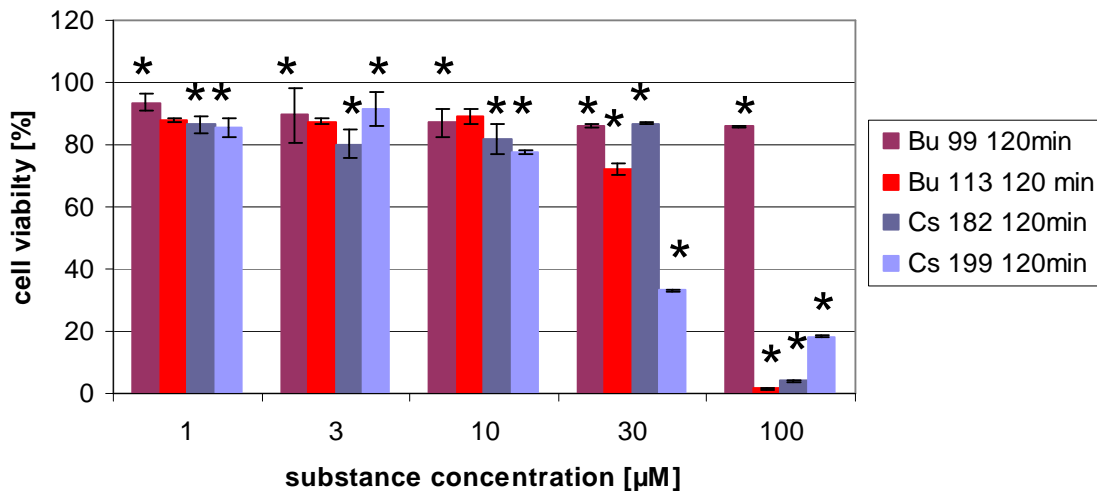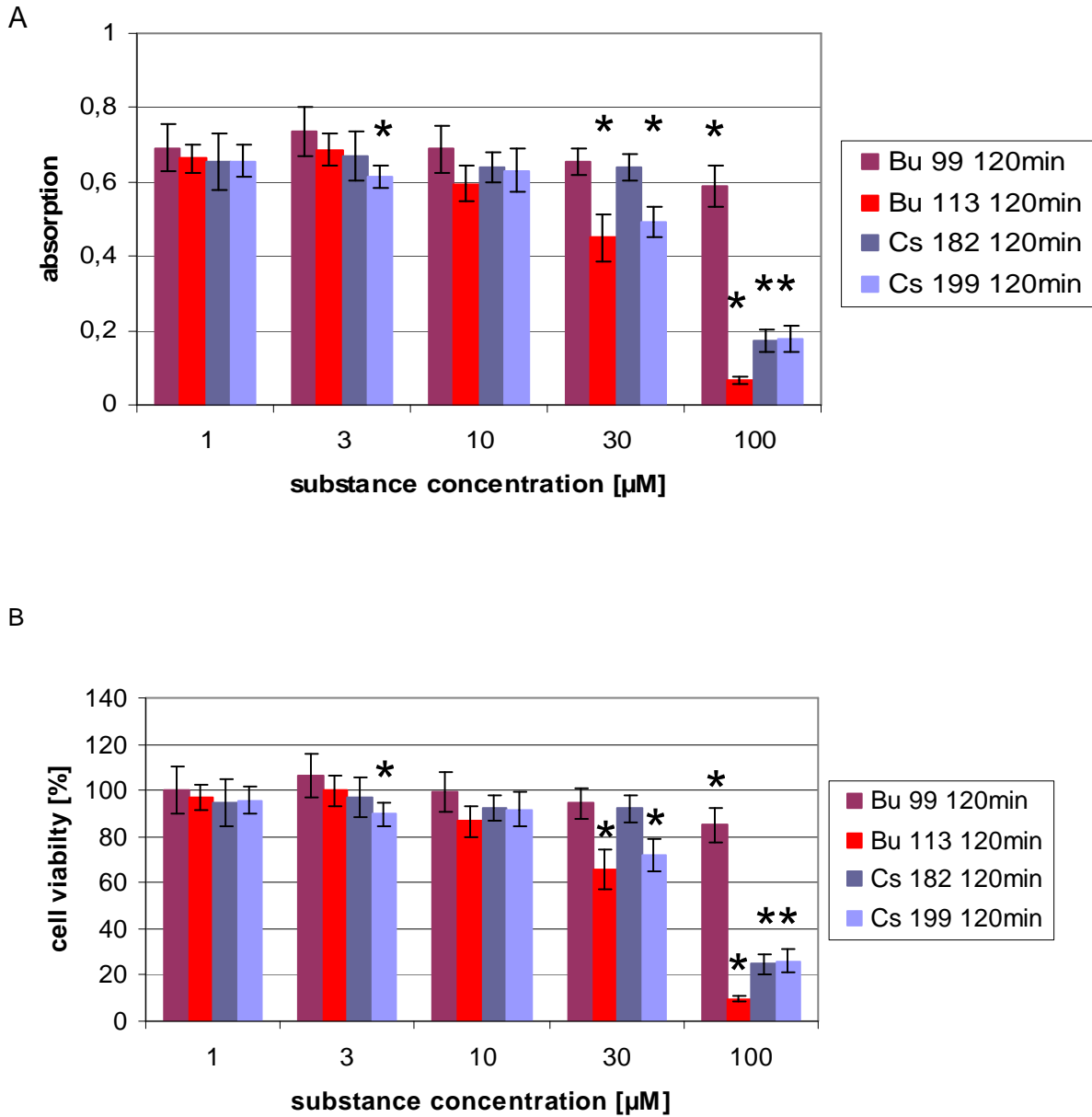

Figure 3.1.3: Absorption of the formed XTT-derivate after addition of Bu-99, Bu-113, Cs-182 and Cs-199 (1µM, 3µM, 10µM, 30µM and 100µM) to cerebEND cells under normoxic conditions (1h incubation) and 120 min measuring time (A), effects of Bu-99, Bu-113, Cs-182 and Cs-199 (1µM, 3µM, 10µM, 30µM and 100µM) on cerebEND cells under normoxic conditions on cell viability (1h incubation) in [%] (B), data are presented as mean ± SD (16) from one experiment.
*: statistically significant vs. control, p<0,05, double sided t-test with the same variance

The range of absorption values was between 0,07 and 0,73 (see figure 3.1.3A).

Bu-99 didn't show many remarkable effects. It reduced cell viability at 100µM to 85,13 ± 7,6% in a significant manner.

Cs-182 reduced cell viability to 24,9 ± 4,2% at 100µM, compared to 4,0% in the same concentration with 4 hours of incubation.

Viability of cells treated with Bu-113 was decreased to 65,6 ± 8,7% (30µM) and 9,8 ± 1,5% (100µM), whereas longer incubation of 4 hours led to values of 26,7% cell viability (30µM) and 2,1% cell viability (100µM) (Figure 3.1.3B). Cs-199 reduced cell-viabilities to 71,9 ± 7,1% (30µM) and 26,1 ± 5,3% (100µM), which were also higher than in previous assays with increased incubation-duration of 4h: 72,1% at 30 µM and 1,6% at 100µM (see figure 3.1.3B).

This assay proved that cell viability reduction depends on the duration of the incubation of each substance. Shorter incubation of 1h led to less damage, whereas long incubation of 4h with toxic substances harmed the used cell line even more. Non-toxic compounds didn't show different results in dependence on the incubation time.

3.1.2 CerebEND cells under oxygen/glucose deprivation (OGD)

3.1.2.1 Concentration of 100µM

A
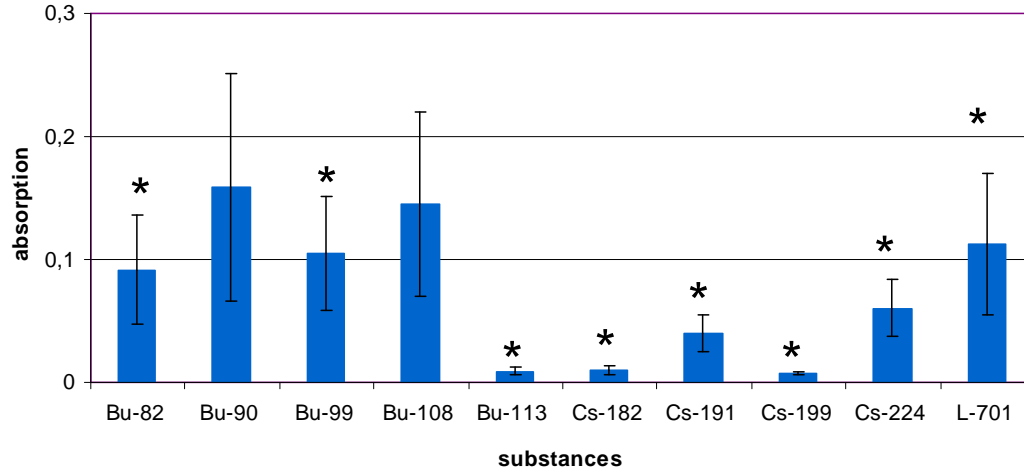
B

Figure 3.1.4: Absorption of the formed XTT-derivate after addition of glycine antagonists on cerebEND cell viability at 100µM under OGD conditions using EZ4U-assay (4h incubation) and 120 min measuring time (A), effects of glycine antagonists on cerebEND cell viability at 100µM under OGD conditions using EZ4U-assay (4h incubation) in [%] (B), data are presented as mean ± standard deviation (SD) (n=16) from one experiment.
*: statistically significant vs. control, p<0,05, double sided t-test with the same variance

Absorption values were between 0,05 and 0,17 (see figure 3.1.4A)

Bu-82 reduced cell viability to 50,9 ± 23,8%. Bu-90 as well as Bu-108 didn't show any significant changes. Bu-99 yielded to a value of 58,7 ± 25,5%. Bu-113 showed decreased cell viability of 5,2 ± 1,7%. Cs-182 induced cell damage to 5,7 ± 2,1%. Cs-191 reduced cell viability to 22,7 ± 9,1%. Cells that were treated with Cs-199 showed a viability of 4,4 ± 0,9%. The exposition with Cs-224 reduced cell viability to 34,0 ± 13,0% (100µM). L-701,324 treatment revealed a value of 63,7 ± 33,7% (100µM).

3.1.2.2 Concentration of 10µM

A

B
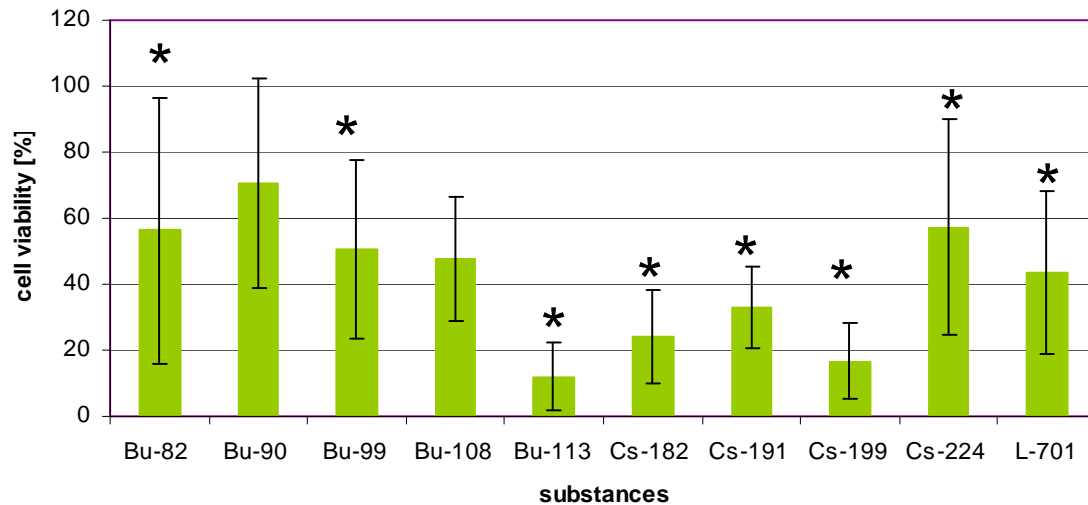
Figure 3.1.5: Absorption of the formed XTT-derivate after addition of glycine antagonists on cerebEND cell viability at 100µM under OGD conditions using EZ4U-assay (4h incubation) and 120 min measuring time (A), effects of glycine antagonists on cerebEND cell viability at 100µM under OGD conditions using EZ4U-assay (4h incubation) in [%] (B), data are presented as mean ± standard deviation (SD) (n=16) from 2 experiments.

*: statistically significant vs. control, p<0,05, double sided t-test with the same variance

The absorption was generally lowered due to oxygen/glucose deprivation conditions, especially the glucose free medium (values between 0,03 and 0,17) (see figure 3.1.5A).

Bu-082 decreased cell viability to 56,2 ± 40,3%. Bu-90, as well as Bu-108 didn't harm the cells significantly. Bu-99 reduced to 50,5 ± 27,1%, Bu-113 to 12,0 ± 10,3%. Cs-182, which was already toxic under normoxic conditions, showed elevated cell damage as it decreased cell viability to 24,2 ±14,0%. Cs-191 reduced cell viability to 33,1 ± 12,3%. Cells that were treated with Cs-199 showed a viability of 16,8 ± 11,3% compared to vehicle treated cells. The exposition with Cs-224 reduced cell viability to 57,2 ± 32,7%. L-701,324 showed values of 43,5 ± 24,9% (see figure 3.1.5B).

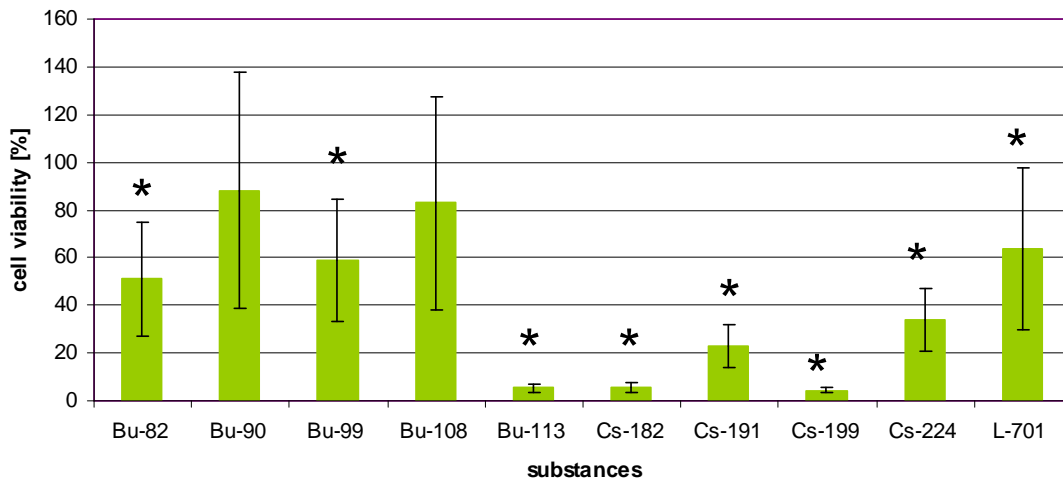## 3.1.3 Glioma cell line C6 under normoxic conditions

A
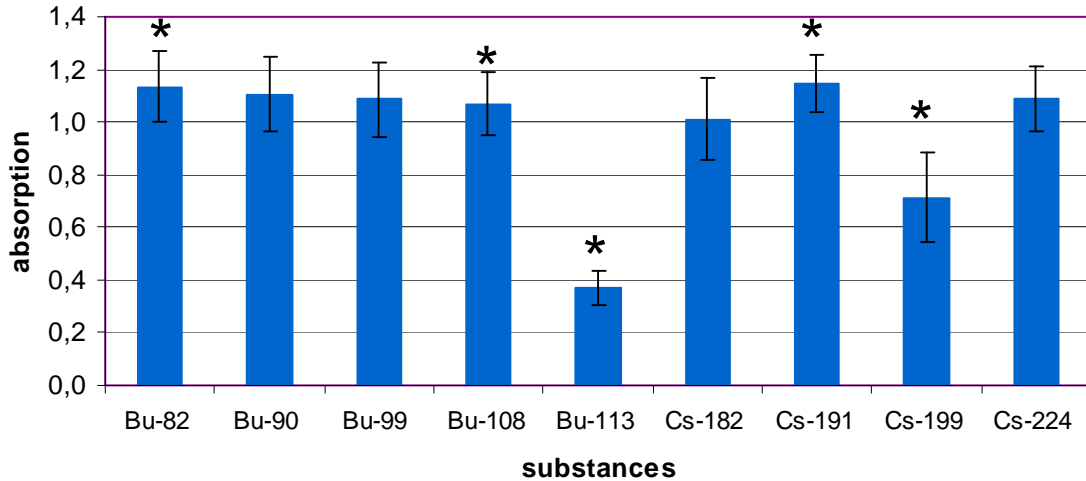
B
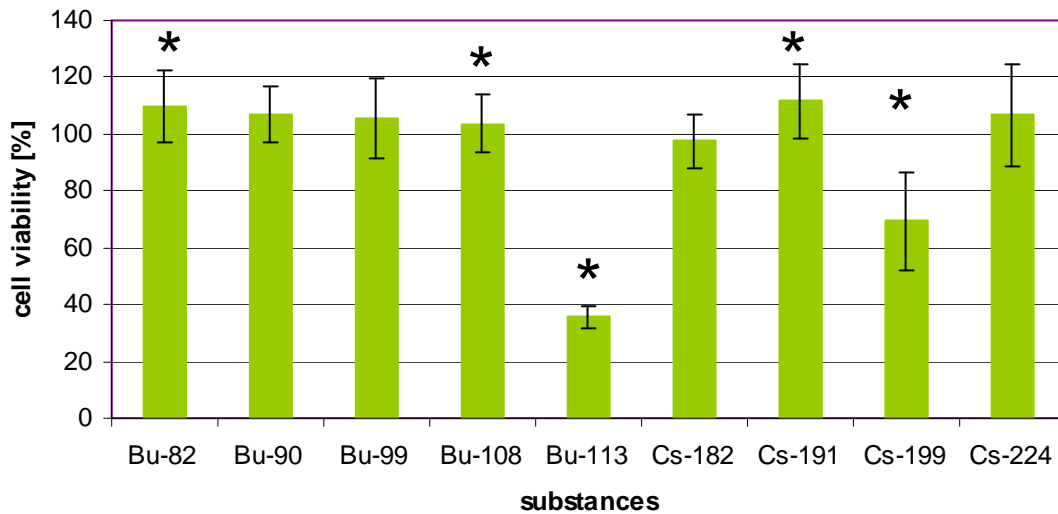
Figure 3.1.6: Absorption of the formed XTT-derivate after addition of glycine antagonists on C6 cell viability at 100µM under normoxia conditions using EZ4U-assay (4h incubation) and 30 min measuring time (A), effects of glycine antagonists on C6 cell viability at 100µM under normoxia conditions using EZ4U-assay (4h incubation) in [%] (B), data are presented as mean ± standard deviation (SD) (n=32) from 2 experiments.
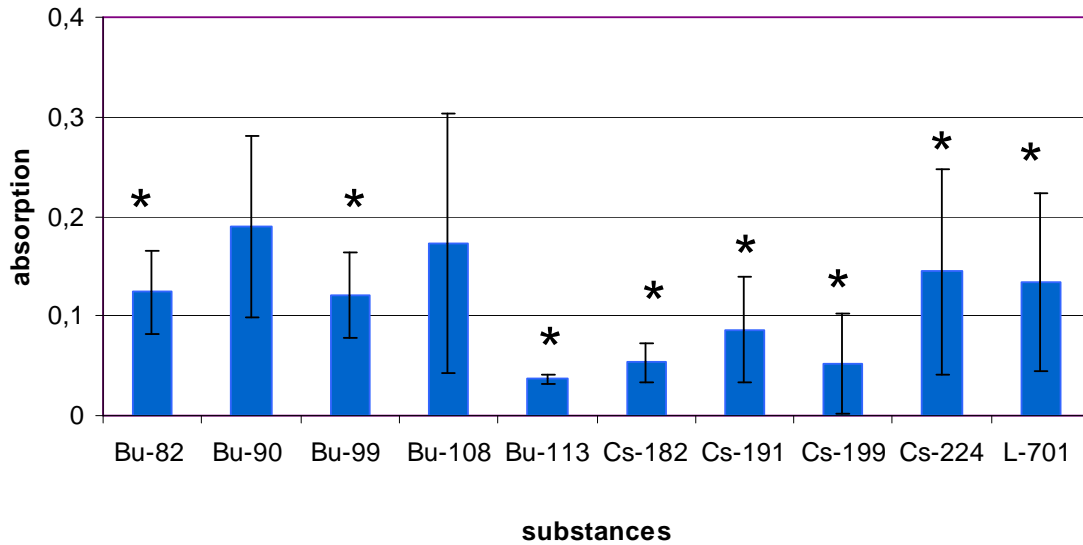
*: statistically significant vs. control, $p < 0.05$, double sided t-test with the same variance

The range of absorption values was between 0,37 and 1,14 (see figure 3.1.6A).

100µM Bu-113 (39,6 ± 4,0%) and Cs-199 (69,3 ± 17,1%) showed significant reduction of cell viability. Furthermore, Bu-82 (110,0 ±12,6%), Bu-108 (103,7 ± 10,5) and Cs-191 (111,6 ± 13,3%) could increase cell viability significantly. The residual substances didn't affect the cell viability of C6 cells under normoxic conditions at a concentration of 100µM (see figure 3.1.6B).

The next step was to find out in which concentrations Bu-99 and Cs-182 don't harm the cells any more.

A

B
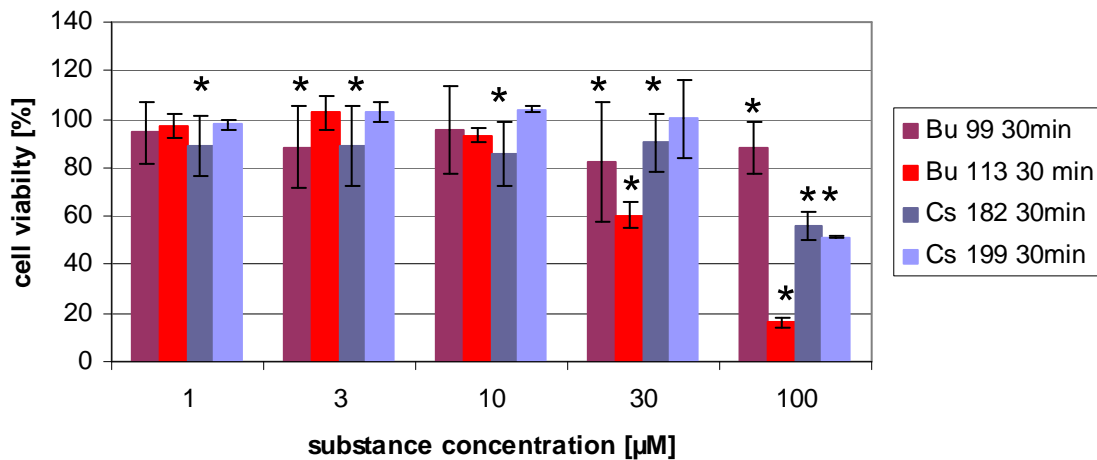
Figure 3.1.7: Absorption of the formed XTT-derivate after addition of Bu-99, Bu-113, Cs-182 and Cs-199 (1µM, 3µM, 10µM, 30µM and 100µM) to C6 cells under normoxic-conditions (4h incubation) and 30 min measuring time (A), effects of Bu-99, Bu-113, Cs-182 and Cs-199 (1µM, 3µM, 10µM, 30µM and 100µM) on C6 cells under normoxic-conditions on cell viability (4h incubation) in [%] (B), data are presented as mean ± standard deviation (SD) (n=16) from 2 experiments.
*: statistically significant vs. control, $p < 0.05$, double sided t-test with the same variance

The absorption values of this assay were in a range of 0,15 to 0,99 after 30 min exposition to test substances (see figure 3.1.7a).

Applied concentrations of Bu-99 showed weak but still significant effects on cell viability of C6 cells. Thus, it was used as a reference substance. Addition of Bu-99 led to values of 94,5% ± 11,4% (1µM), 88,5% ± 17,9% (3µM), 95,3% ± 17,3% (10M), 82,2% ± 36,6% (30µM) and 88,2% ± 12,9% (100µM).

Cs-182 showed concentration dependent effects. Cell viability of C6 cells was reduced by 100µM to 55,8 ± 6,8%. Lower concentrations showed very weak but still significant effects on C6 cells. Values of 88,8 ± 13,8% (1µM), 88,8 ± 15,5% (3µM), 86,0 ± 13,7% (10µM) and 90,3 ± 13,0% (30µM) were achieved with Cs-182.

Bu-113 treated C6 cells were also affected in concentration dependent manner. At 30µM Bu 113 cells showed a reduced viability of 60,5 ± 7,5% and 100µM further decreased the surviving cells to 16,1 ± 7,9%.

Cs-199 reduced cell viability in a concentration of 100µM to a level of 51,4 ± 10,7%. Lower concentrations didn't show a reduction of cell viability (see figure 3.1.7B).

In summary Bu-113, Cs-182 and Cs-199 showed concentration dependent effects. Bu-113 appeared as the most harmful substance, as it damaged the cells already at 30µM. Bu-99, which showed weak, ambiguous effects, turned out to be not affective under these conditions so that it was used as control-substance for later assays.

3.1.4 Glioma C6 cell line under oxygen/glucose deprivation (OGD)

Following tests examined the influence of glycine antagonists on cell viability of C6 cells under OGD conditions (1% O_2, glucose free medium).

A
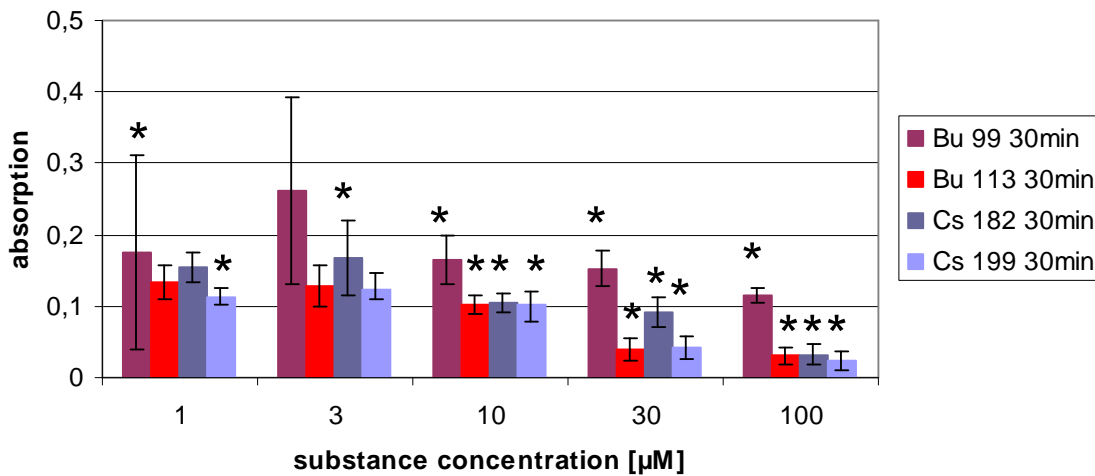
B
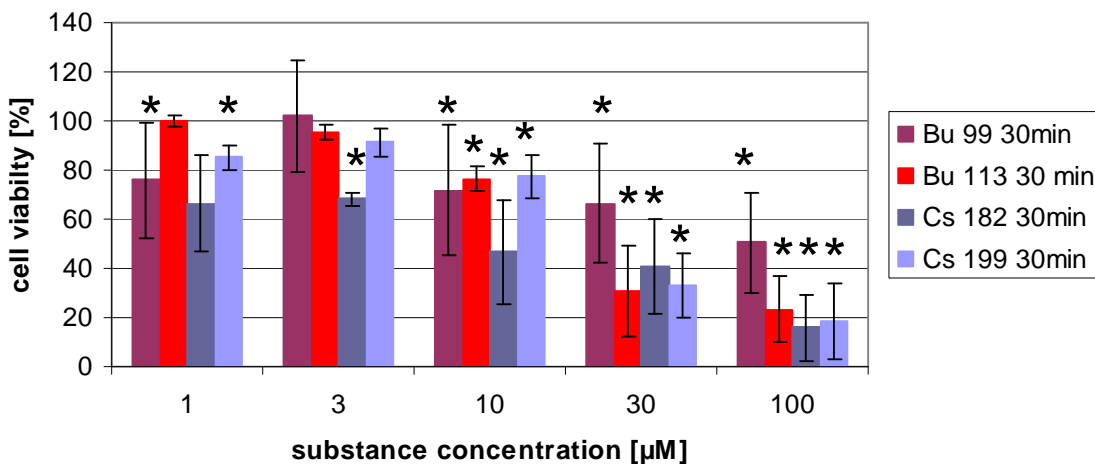
Figure 3.1.8: Absorption of the formed XTT-derivate after addition of Bu-99, Bu-113, Cs-182 and Cs-199 (1μM, 3μM, 10μM, 30μM and 100μM) to C6 cells under OGD-conditions (4h incubation) and 30 min measuring time (A), effects of Bu-99, Bu-113, Cs-182 and Cs-199 (1μM, 3μM, 10μM, 30μM and 100μM) on C6 cells under OGD-conditions on cell viability (4h incubation) in [%] (B), data are presented as mean ± standard deviation (SD) (n=16) from 2 experiments.
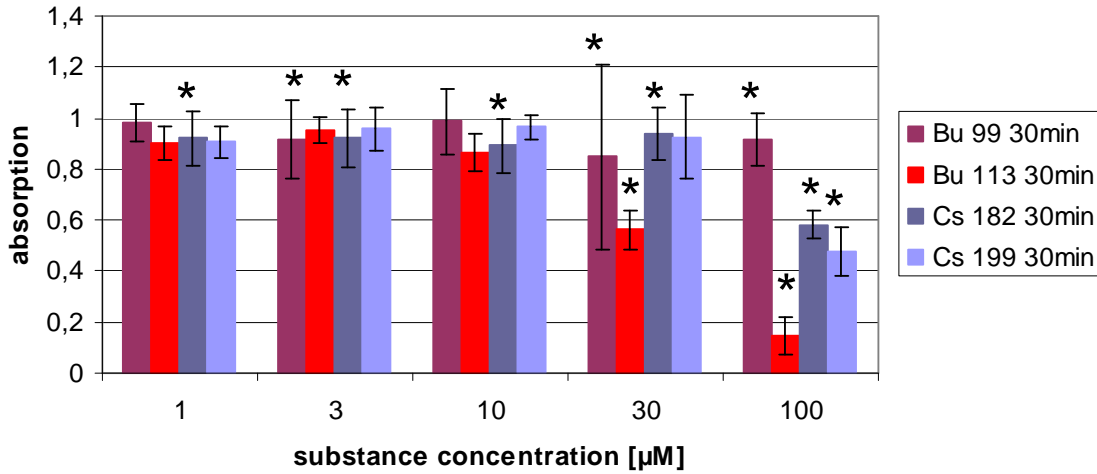*: statistically significant vs. control, p<0,05, double sided t-test with the same variance

The absorption was remarkably low (values between 0,023 and 0,176) in all OGD-assays, which accords to the decreased cell viability in general due to missing oxygen and glucose for mitochondrial activity (EZ4U test measures activity of mitochondrial dehydrogenases). (see figure 3.1.8A)

Under OGD-conditions Bu-99 demonstrated quite strong effects. It reduced cell viability to 76,0 ± 23,3% at 1µM, 71,9 ± 26,24% at 3µM, 66,5 ± 21,4% at 30µM and 50,4 ± 15,8% at 100µM concentration.

Cs-182 showed increased toxicity as the cell viability was decreased to 66,5 ± 17,5% (1µM), 68,1 ± 10,9% (3µM), 46,7 ± 15,6% (10µM), 40,9 ± 17,4% (30µM) and 15,9 ± 10,1% (100µM).

Bu-113 and Cs-199 acted in this study in a similar way, as they both developed toxicity already at low concentrations. Bu-113 decreased cell viability under OGD-conditions to 76,3 ± 10,3% (10µM), 30,5 ± 14,8% (30µM) and 23,5 ± 10,2% (100µM). Cs-199 showed decreased cell viability of 85,2 ± 8,0% (1µM), 77,3 ± 14,7% (10µM), 33,0 ± 12,6% (30µM) and 18,5 ± 11,5% (100µM) (see figure 3.1.8B).

3.1.5 Test of MK801 (channel-blocker) and L-701,324 (glycine-antagonist)

MK801 and L-701,324 are well known as NMDAR-blocking agents. For validation purposes of these substances were tested.

A
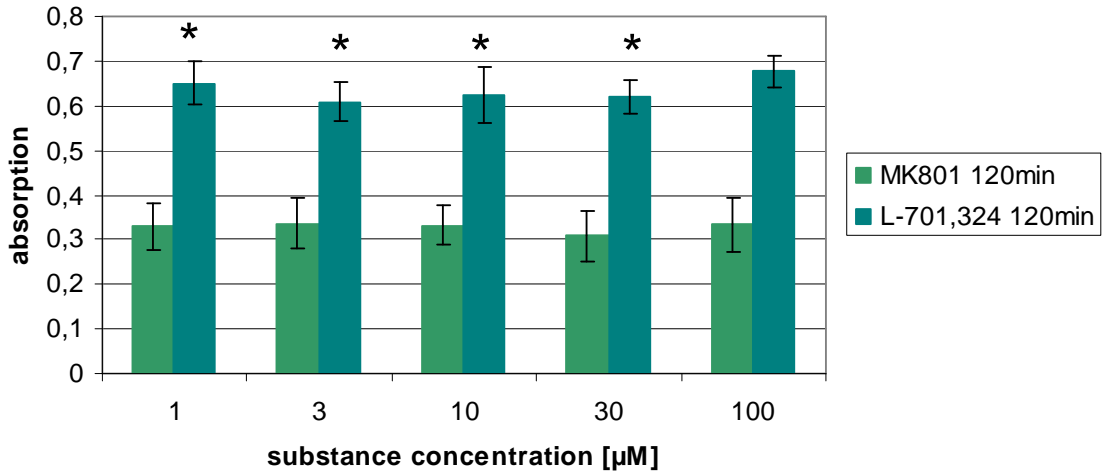
B
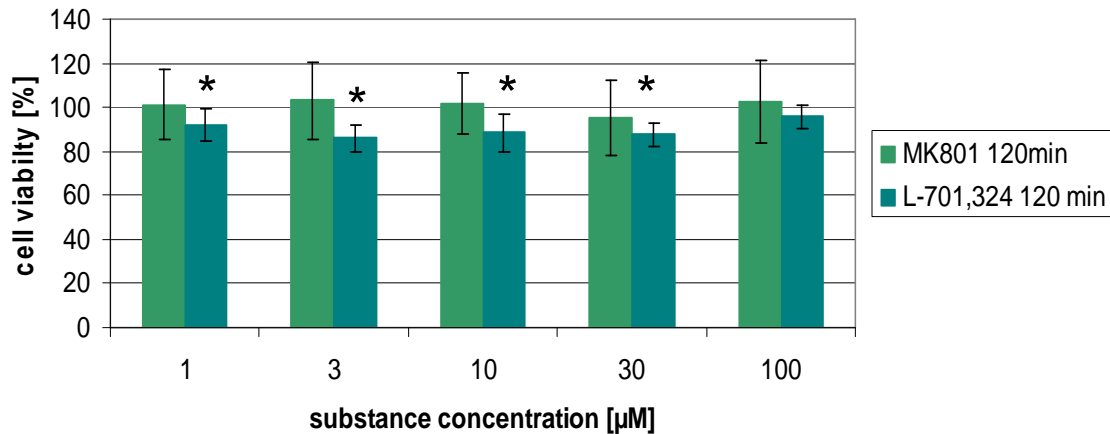
Figure 3.1.9: Absorption of the formed XTT-derivate after addition of MK801 and L-701,324 on cerebEND cell viability at 100µM under OGD conditions using EZ4U-assay (4h incubation) and 120 min measuring time (A), effects of glycine antagonists on cerebEND cell viability at 100µM under OGD conditions using EZ4U-assay (4h incubation) in [%] (B), data are presented as mean ± standard deviation (SD) (n=8) from one experiment.
*: statistically significant vs. control, p<0,05, double sided t-test with the same variance

Absorption values were between 0,31 and 0,68. (see figure 3.1.9A)

Treatment of cerebENDs with MK801 didn't show any remarkable effects. Cell viability didn't change which suggested, that the substance wasn't harmful for the cells.

Addition of L-701,324 led to significant reduction of cerebENDs cell viability to 91,9 ± 7,0% (1µM), 86,0 ± 6,2% (3µM), 88,4 ± 8,9%(10µM), 87,6 ± 5,5% (30µM) and 95,7 ± 5,0% (100µM) (see figure 3.1.9B).

Same assays were accomplished with C6 cells.

A
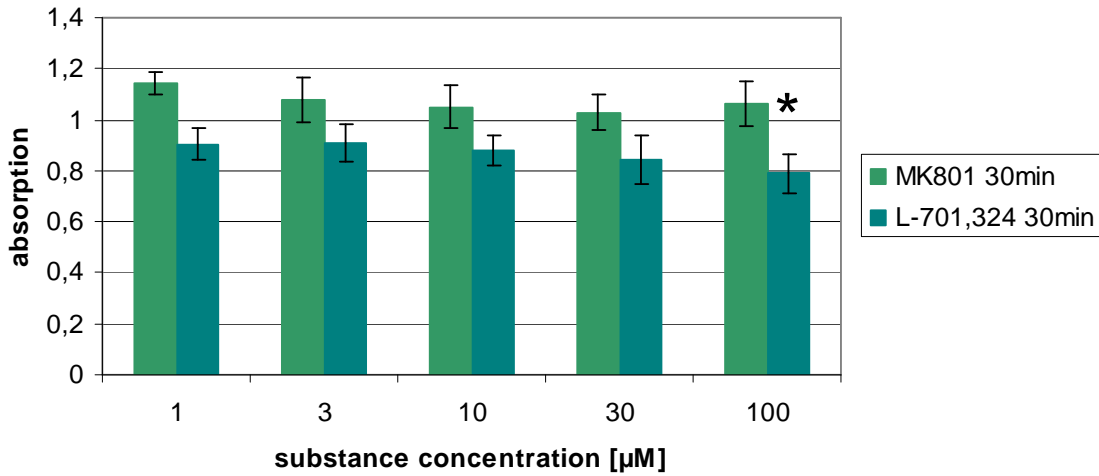
B
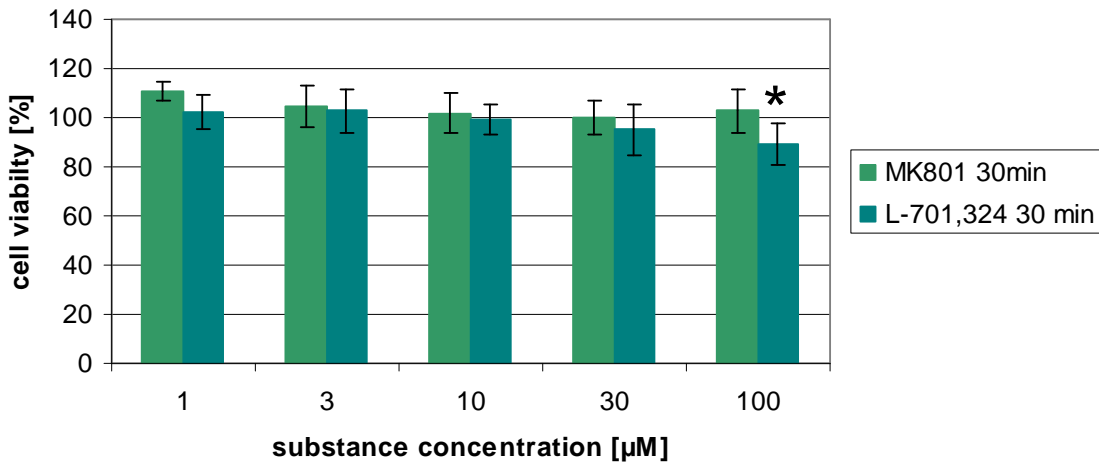
Figure 3.1.10a: Absorption of the formed XTT-derivate after addition of MK801 and L-701,324 on C6 cell viability at 100µM under OGD conditions using EZ4U-assay (4h incubation) and 30min measuring time (A), effects of glycine antagonists on C6 cell viability at 100µM under OGD conditions using EZ4U-assay (4h incubation) in [%] (B), data are presented as mean ± standard deviation (SD) (n=8) from one experiment.
*: statistically significant vs. control, p<0,05, double sided t-test with the same variance

Absorption values were between 0,87 and 1,17. (see figure 3.1.10A)

The figure shows that neither L-701,324 nor MK801 had any concentration-dependent effects on a C6 cell line. Compared to non-treated cells, cell viability values didn't change significantly, except 100µM of L-701,324 (cell viability of 96,03 ± 8,04%) (see figure 3.10B).

3.2 Transport experiments

3.2.1 Bu-82

Figure 3.2.1: Clearance curves of Bu-82 and diazepam (internal standard) across empty inserts and cerebEND cell layers.
Green lines show the clearance of Bu-82, whereas the dark line represents the blank-values and the bright line represents the cell-values. The orange line demonstrates the clearance of diazepam across blank inserts, the yellow line describes the clearance of diazepam across cerebEND cell layer.
Data are represented as mean ± SD (n=4) of 2 independent experiments.

Figure 3.2.1 shows that the clearance across blank inserts was higher than across cell layers.

Curves of clearance of Bu-82 runs much lower, compared to diazepam (see figure 3.2.1). This is probably due to differences in lipophilic properties or transport mechanisms in the membrane of the cells.

Table 3.2.1: Calculated permeability coefficients [µm/min] (PC), permeability factors normalized to diazepam (F) and recovery rates (RC) of Bu-82 and diazepam are listed.
Data are represented as mean ± SD (n=4) of 2 independent experiments.

	Time range	Bu-82	Diazepam
PC [µm/min]	10-120 min	37,98 ± 7,55	63,35 ± 5,60
PC [µm/min]	0-10 min	25,74 ± 15,37	53,42 ± 23,85
F	10-120 min	0,60 ± 0,07	1,00
F	0-10 min	0,58 ± 0,09	1,00
RC blank [%]		115,59 ± 14,74	122,59 ± 6,58
RC cells [%]		100,54 ± 12,90	106,59 ± 9,37

The recovery rates of Bu-82 confirmed that it was not absorbed by the plastic material or the cell layer.

The permeability coefficient of Bu-82 was 37,98 ± 7,55 µm/min, that was approximately half as high as the permeability coefficient of diazepam.

3.2.2 Bu-90

Figure 3.2.2: Clearance curves of Bu-90 and diazepam (internal standard) across empty inserts and cerebEND cell layers.
Green lines show the clearance of Bu-90, whereas the dark line represents the blank-values and the bright line represents the cell-values. The orange line demonstrates the clearance of diazepam across blank inserts, the yellow line describes the clearance of diazepam across cerebEND cell layer.
Data are represented as mean ± SD (n=4) of 2 independent experiments.

Figure 3.2.2 shows that the clearance of Bu-90 in cell-assays is lower than the values gained with diazepam, although there is no great difference (see figure 3.2.2). The distinct difference between the cell- and blank values of Bu-90 also implies the elevated interaction of the substance with the cell.

Table 3.2.2: Calculated permeability coefficients [µm/min] (PC), permeability factors normalized to diazepam (F) and recovery rates (RC) of Bu-90 and diazepam are listed.
Data are represented as mean ± SD (n=4) of 2 independent experiments.

	Time range	Bu-90	Diazepam
PC [µm/min]	10-120 min	21,33 ± 3,32	54,46 ± 9,61
PC [µm/min]	0-10 min	23,52 ± 20,05	29,60 ± 2,87
F	10-120 min	0,398 ± 0,07	1,00
F	0-10 min	0,46 ± 0,21	1,00
RC blank [%]		105,21 ± 24,47	120,89 ± 12,27
RC cells [%]		73,58 ± 35,71	97,56 ± 8,58

Comparison of blank and cell recovery rates suggested that Bu-90 probably got stuck partly in the cells.

Furthermore, there can be said that Bu-90 moves distinctly slow compared to diazepam. Lower PC of Bu-90 means reduced transport in comparison to diazepam.

3.2.3 Bu-99

Figure 3.2.3: Clearance curves of Bu-99 and diazepam (internal standard) across empty inserts and cerebEND cell layers.
Green lines show the clearance of Bu-99, whereas the dark line represents the blank-values and the bright line represents the cell-values. The orange line demonstrates the clearance of diazepam across blank inserts, the yellow line describes the clearance of diazepam across cerebEND cell layer.
Data are represented as mean ± SD (n=4) for 2 independent experiments.

Figure 3.2.3 shows increased clearance the longer the substance is exposed to the cells or inserts.

The transport of the substance through the blank inserts is much higher than with cells. The values of the substance and diazepam show a high difference in both setups. (see figure 3.2.3)

Table 3.2.3: Calculated permeability coefficients [µm/min] (PC), permeability factors normalized to diazepam (F) and recovery rates (RC) of Bu-99 and diazepam are listed.
Data are represented as mean ± SD (n=4) of 2 independent experiments.

	Time range	Bu-99	Diazepam
PC [µm/min]	10-120 min	22,05 ± 5,98	66,67 ± 16,70
PC [µm/min]	0-10 min	9,94 ± 0,36	28,66 ± 2,11
F	10-120 min	0,36 ± 0,15	1,00
F	0-10 min	0,35 ± 0,06	1,00
RC blank [%]		92,50 ± 17,54	108,66 ± 7,25
RC cells [%]		91,78 ± 8,78	99,98 ± 1,67

Recovery rates suggest that there is only a low amount of Bu-99 that got stuck inside the cell or in the insert.

Bu-99 is transported much slower than diazepam (22,05 ± 5,98 µm/min vs 66,67 ± 16,70 µm/min).
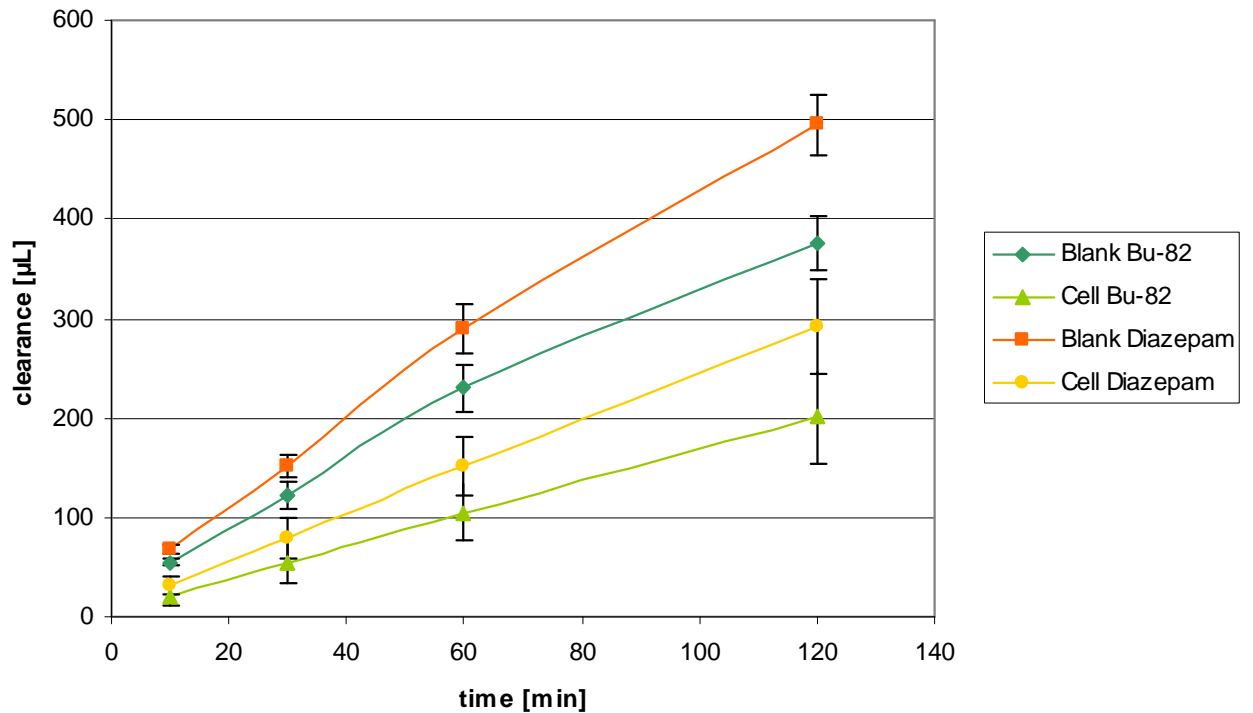
3.2.4 Bu-108

Figure 3.2.4: Clearance curves of Bu-108 and diazepam (internal standard) across empty inserts and cerebEND cell layers.
Green lines show the clearance of Bu-108, whereas the dark line represents the blank-values and the bright line represents the cell-values. The orange line demonstrates the clearance of diazepam across blank inserts, the yellow line describes the clearance of diazepam across cerebEND cell layer.
Data are represented as mean ± SD (n=4) for 2 independent experiments.

The transport-rate of Bu-108 is distinctly lower across all layers compared to diazepam (see figure 3.2.4).

Table 3.2.4: Calculated permeability coefficients [µm/min] (PC), permeability factors normalized to diazepam (F) and recovery rates (RC) of Bu-108 and diazepam are listed.
Data are represented as mean ± SD (n=4) of 2 independent experiments.

	Time range	Bu-108	Diazepam
PC [µm/min]	10-120 min	10,53 ± 2,64	55,30 ± 16,12
PC [µm/min]	0-10 min	6,72 ± 0,43	43,84 ± 0,20
F	10-120 min	0,19 ± 0,01	1,00
F	0-10 min	0,15 ± 0,01	1,00
RC blank [%]		71,28 ± 26,16	109,20 ± 3,50
RC cells [%]		60,08 ± 20,36	98,61 ± 0,72

The recovery of Bu-108 was clearly decreased in cell as well as blank experiments suggesting an interaction with the plastic material.

Low F and RC of Bu-108 supported the distinctly reduced transport of Bu-108, compared to diazepam.
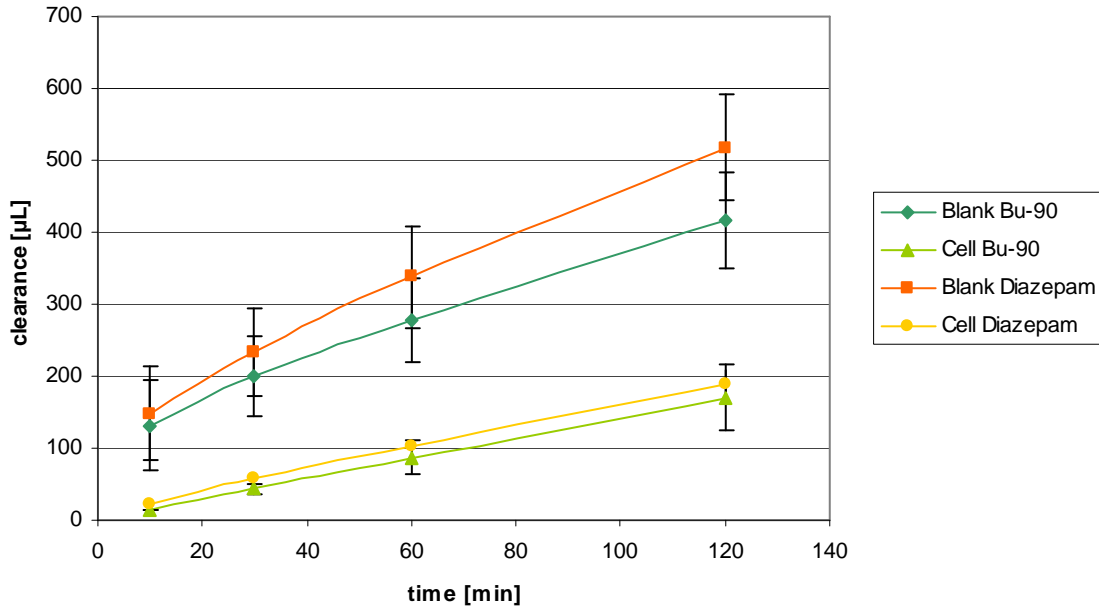
3.2.5 Bu-113

Figure 3.2.5: Clearance curves of Bu-113 and diazepam (internal standard) across empty inserts and cerebEND cell layers.
Green lines show the clearance of Bu-113, whereas the dark line represents the blank-values and the bright line represents the cell-values. The orange line demonstrates the clearance of diazepam across blank inserts, the yellow line describes the clearance of diazepam across cerebEND cell layer.
Data are represented as mean ± SD (n=4) for 2 independent experiments.

Figure 3.2.5 shows the increase of the clearance in dependence of time. The longer the cells are exposed to Bu-113 the higher is the total transport amount. Again, the clearence-curves of the blanks proceed steeper compared to curves of cell-inserts.

Bu-113 seems to be more interactive than other shown substances, as the clearance is much lower. Also the difference between diazepam and Bu-113-values is much higher (see figure 3.2.5).

Table 3.2.5: Calculated permeability coefficients [μm/min] (PC), permeability factors normalized to diazepam (F) and recovery rates (RC) of Bu-113 and diazepam are listed.
Data are represented as mean ± SD (n=4) of 2 independent experiments.

		Bu-113	Diazepam
PC [μm/min]	10-120 min	7,97 ± 1,00	30,55 ± 6,62
PC [μm/min]	0-10 min	5,90 ± 2,97	25,92 ± 1,11
F	10-120 min	0,30 ± 0,09	1,00
F	0-10 min	0,18 ± 0,06	1,00
RC blank [%]		80,45 ± 25,52	117,61 ± 8,76
RC cells [%]		52,91 ± 9,22	99,50 ± 2,00

Bu-113 shows a quite low recovery in cell experiments compared to blank experiments which suggested that part of the applied substance got stuck in the cells.

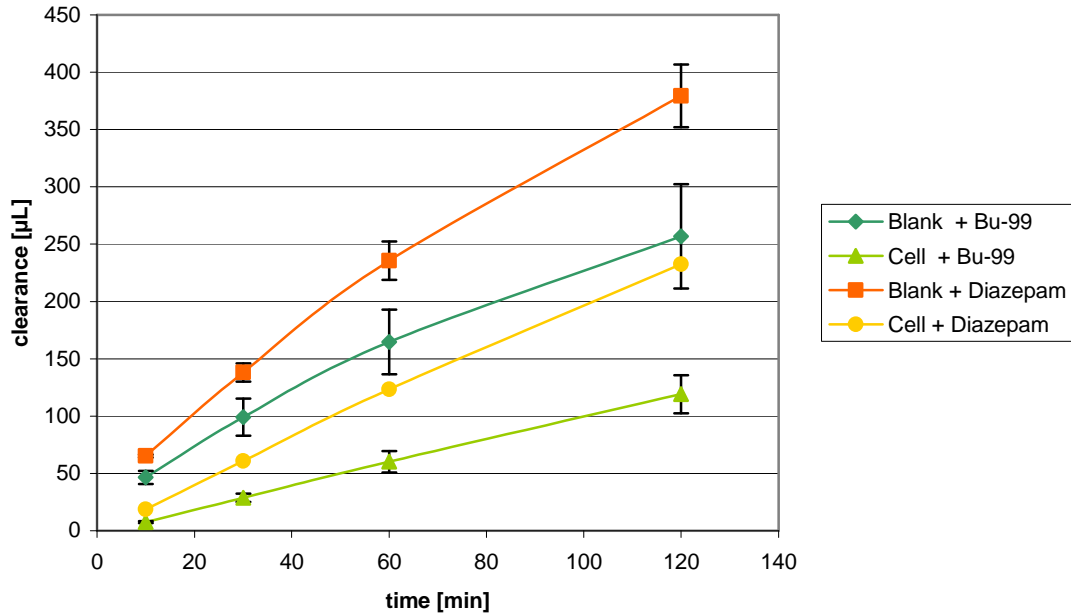Low F and PC showed that the substance permeated very slowly.

3.2.6 Cs-182

Figure 3.2.6: Clearance curves of Cs-182 and diazepam (internal standard) across empty inserts and cerebEND cell layers.
Green lines show the clearance of Cs-182, whereas the dark line represents the blank-values and the bright line represents the cell-values. The orange line demonstrates the clearance of diazepam across blank inserts, the yellow line describes the clearance of diazepam across cerebEND cell layer.
Data are represented as mean ± SD (n=4) for 2 independent experiments.

Figure 3.2.6 shows the increase of the transport-rate as the exposure-time of the cells to the substance time decreases. Blank values show higher transport-values.

As in previous assays, the clearance in blank-inserts is much higher. Cell-values are quite low, which shows the high lipophilicity of Cs-182 (see figure 3.2.6).

Table 3.2.6: Calculated permeability coefficients [μm/min] (PC), permeability factors normalized to diazepam (F) and recovery rates (RC) of Cs-182 and diazepam are listed.
Data are represented as mean ± SD (n=4) of 2 independent experiments.

	Time range	Cs-182	Diazepam
PC [μm/min]	10-120 min	39,58 ± 15,42	69,76 ± 15,44
PC [μm/min]	0-10 min	10,44 ± 0,30	31,99 ± 12,03
F	10-120 min	0,53 ± 0,08	1,00
F	0-10 min	0,32 ± 0,10	1,00
RC blank [%]		77,75 ± 13,92	112,06 ± 11,91
RC cells [%]		75,93 ± 5,96	99,18 ± 8,76

The reduced recovery of Cs-182 in blank values and cell-values are probably because of interactions with the insert itself as both RC values are reduced. The table shows furthermore, that Cs-182 is transported slowly as F and PC are quite low in comparison to diazepam.
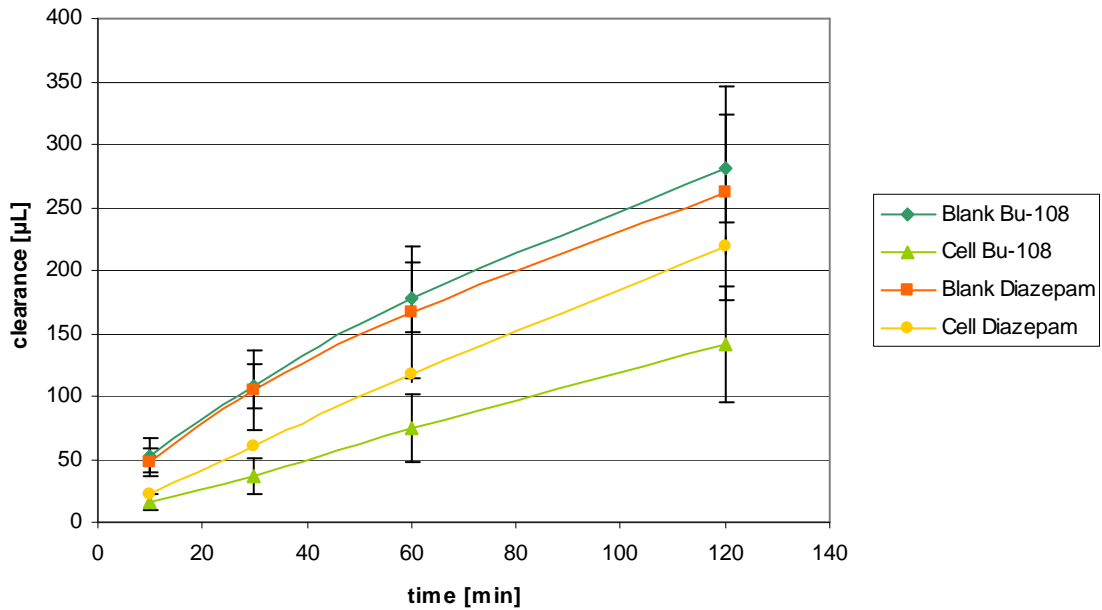
3.2.7 Cs-191

Figure 3.2.7: Clearance curves of Cs-191 and diazepam (internal standard) across empty inserts and cerebEND cell layers.
Green lines show the clearance of Cs-191, whereas the dark line represents the blank-values and the bright line represents the cell-values. The orange line demonstrates the clearance of diazepam across blank inserts, the yellow line describes the clearance of diazepam across cerebEND cell layer.
Data are represented as mean ± SD (n=4) for 2 independent experiments.

Figure 3.2.7 shows lower clearance of Cs-191 compared to diazepam. Furthermore, the curves of the blank-inserts and cell-inserts proceed in high distances (see figure 3.2.7). This suggests that the interaction is mainly referred to the cells, not to the inserts themselves.

Table 3.2.7: Calculated permeability coefficients [µm/min] (PC), permeability factors normalized to diazepam (F) and recovery rates (RC) of Cs-191 and diazepam are listed.
Data are represented as mean ± SD (n=4) of 2 independent experiments.

	Time range	Cs-191	Diazepam
PC [µm/min]	10-120 min	15,75 ± 1,86	29,96 ± 7,14
PC [µm/min]	0-10 min	7,89 ± 0,93	25,81 ± 7,89
F	10-120 min	0,54 ± 0,07	1,00
F	0-10 min	0,36 ± 0,19	1,00
RC blank [%]		103,75 ± 0,76	115,62 ± 3,87
RC cells [%]		78,05 ± 4,73	94,08 ± 10,97

The recovery of the substance in cell-setups was decreased, while the recovery of the substance in blank-setups was at about 100%. This supports the hypothesis that effects were obviously referred only to cells.

F and PC describe reduced transport rates of Cs-191, compared to diazepam.
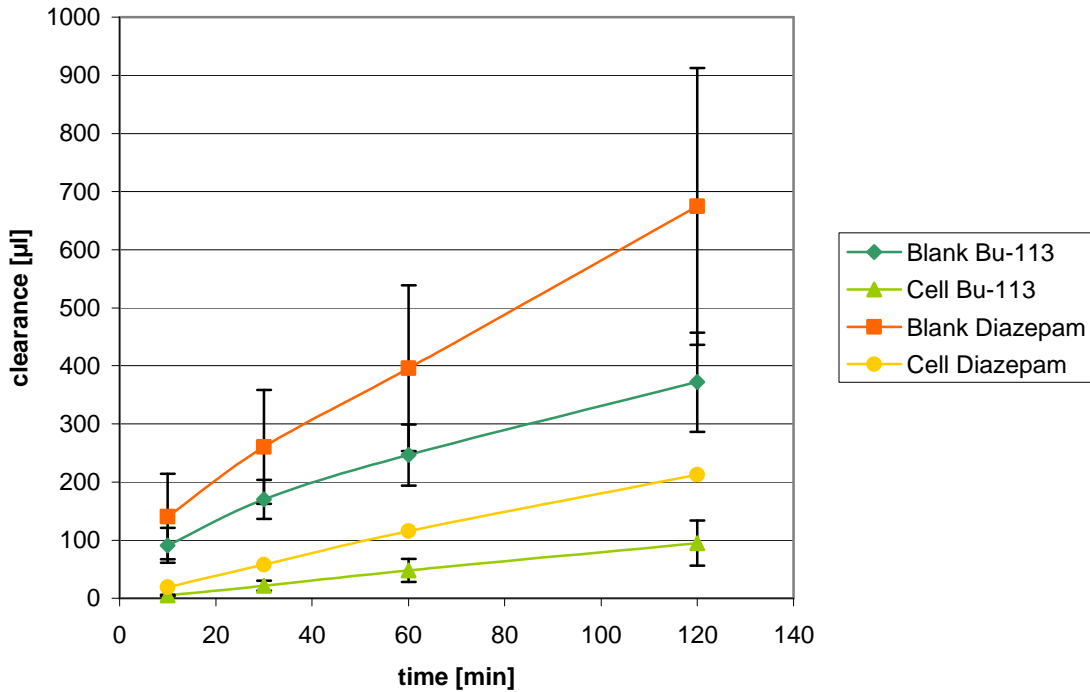
3.2.8 Cs-199
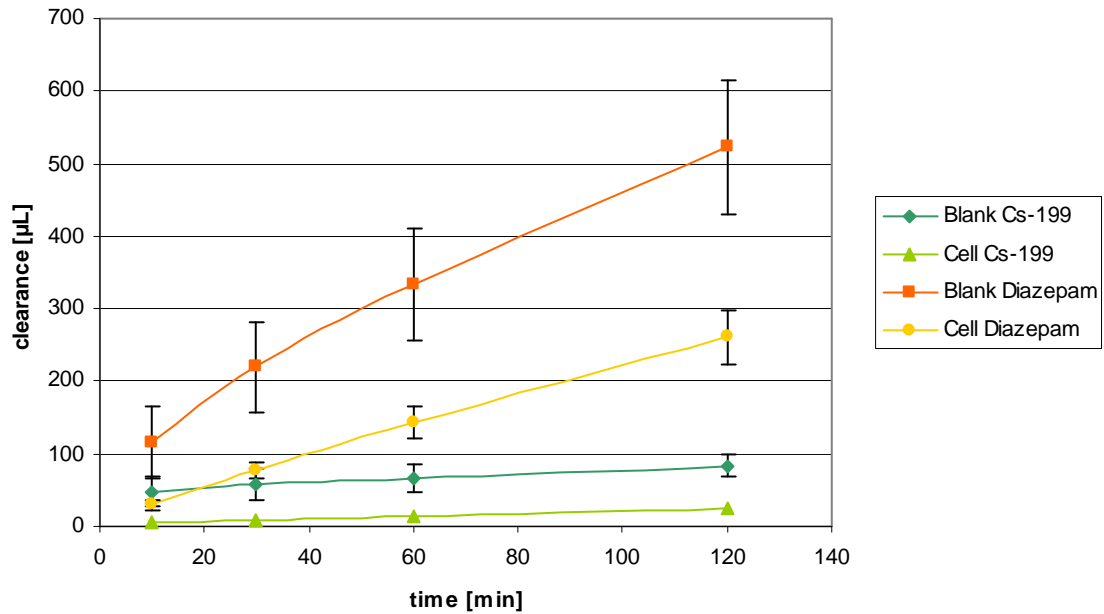
Figure 3.2.8: Clearance curves of Cs-199 and diazepam (internal standard) across empty inserts and cerebEND cell layers.
Green lines show the clearance of Cs-199, whereas the dark line represents the blank-values and the bright line represents the cell-values. The orange line demonstrates the clearance of diazepam across blank inserts, the yellow line describes the clearance of diazepam across cerebEND cell layer.
Data are represented as mean ± SD (n=4) for 2 independent experiments.

.

The clearance-values of blanks are higher than clearence of cell-values. In this setup, the cell-values of diazepam showed higher clearance than the blank-values of the substance. This suggests that Cs-199 even interacts with inserts and the cell and resulted in very low clearance-values of the substance (see figure 3.2.8).

Table 3.2.8: Calculated permeability coefficients [µm/min] (PC), permeability factors normalized to diazepam (F) and recovery rates (RC) of Cs-199 and diazepam are listed.
Data are represented as mean ± SD (n=4) of 2 independent experiments.

	Time range	Cs-199	Diazepam
PC [µm/min]	10-120 min	13,91 ± 12,76	44,45 ± 5,02
PC [µm/min]	0-10 min	6,15 ± 4,28	35,27 ± 6,68
F	10-120 min	0,11 ± 0,04	1,00
F	0-10 min	0,11 ± 0,04	1,00
RC blank [%]		29,62 ± 3,23	108,75 ± 7,51
RC cells [%]		23,95 ± 3,04	101,78 ± 6,49

Cs-199 shows a very low recovery. Due to the low values in both setups (blank- and cell-values) the interaction probably took place between the insert and the substance.

This result was confirmed by the calculated factors F and the permeability coefficient of Cs-199.
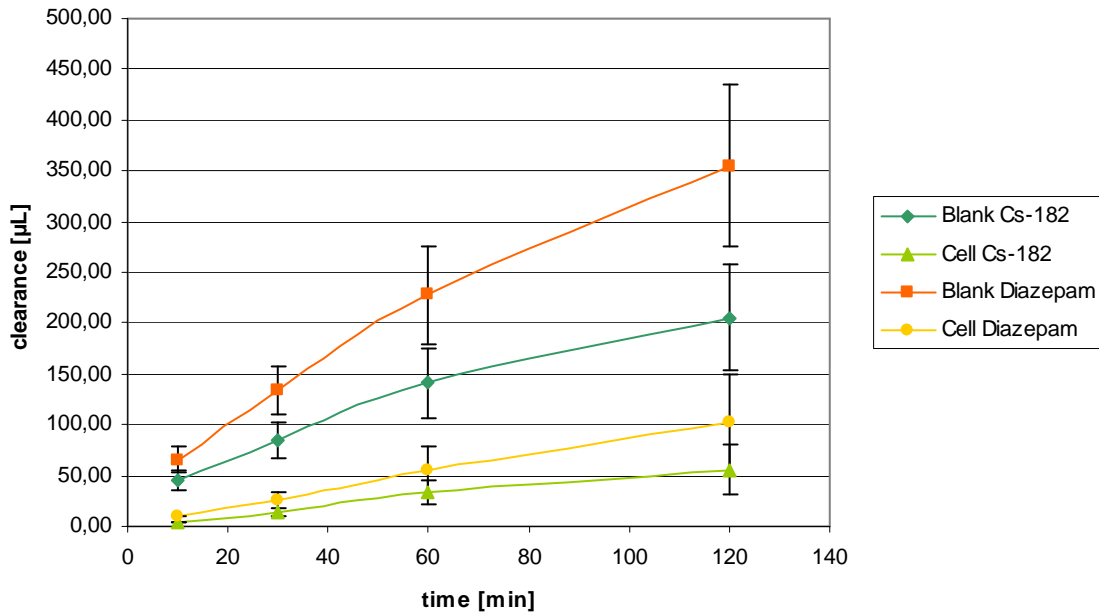
3.2.9 Cs-224
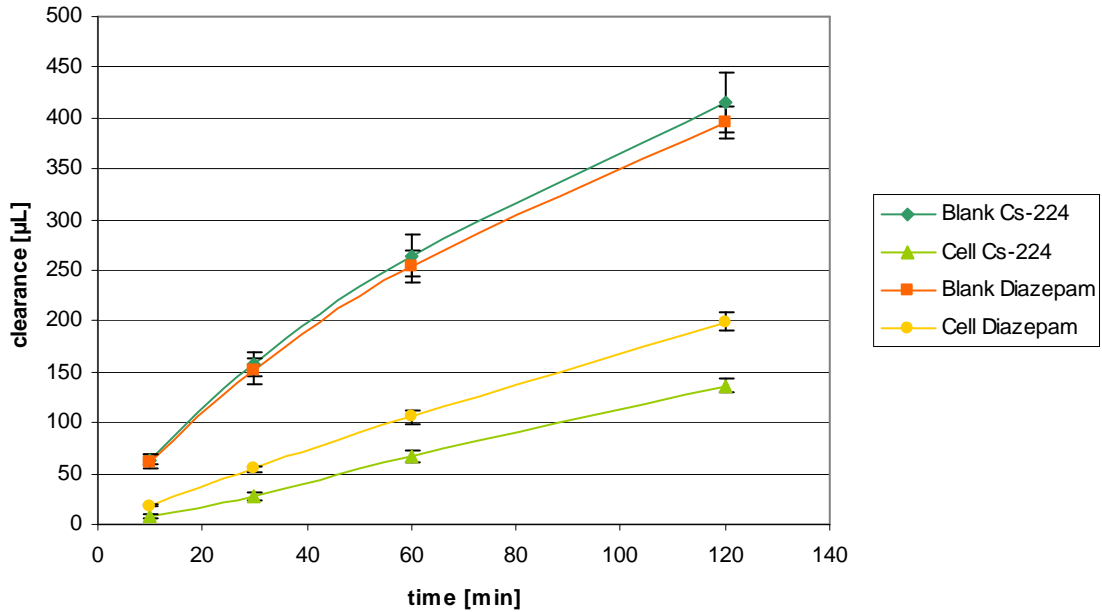
Figure 3.2.9: Clearance curves of Cs-224 and diazepam (internal standard) across empty inserts and cerebEND cell layers.
Green lines show the clearance of Cs-224, whereas the dark line represents the blank-values and the bright line represents the cell-values. The orange line demonstrates the clearance of diazepam across blank inserts, the yellow line describes the clearance of diazepam across cerebEND cell layer.
Data are represented as mean ± SD (n=4) for 2 independent experiments.

In this assay, the clearance-value of the blank insert is even higher. Nevertheless this result can be neglected as the difference is small. Still, Cs-224 shows a lower clearance as it can be discovered when cell-insert-values of the test-substance and diazepam are compared (see figure 3.2.9).

Table 3.2.9: Calculated permeability coefficients [µm/min] (PC), permeability factors normalized to diazepam (F) and recovery rates (RC) of Cs-224 and diazepam are listed.
Data are represented as mean ± SD (n=4) of 2 independent experiments.

	Time range	Cs-224	Diazepam
PC [µm/min]	10-120 min	21,36 ± 0,89	42,74 ± 10,19
PC [µm/min]	0-10 min	10,27 ± 4,02	28,58 ± 2,70
F	10-120 min	0,53 ± 0,12	1,00
F	0-10 min	0,36 ± 0,09	1,00
RC blank [%]		107,82 ± 1,45	100,97 ± 5,73
RC cells [%]		92,31 ± 3,48	92,05 ± 6,76

The recovery of Cs-224 is very similar to the recovery of diazepam. This means, that the substance didn't rest in the cells.

The factors and permeability coefficients describe reduced transport rates. The values are about half as high as diazepam-transport rates.
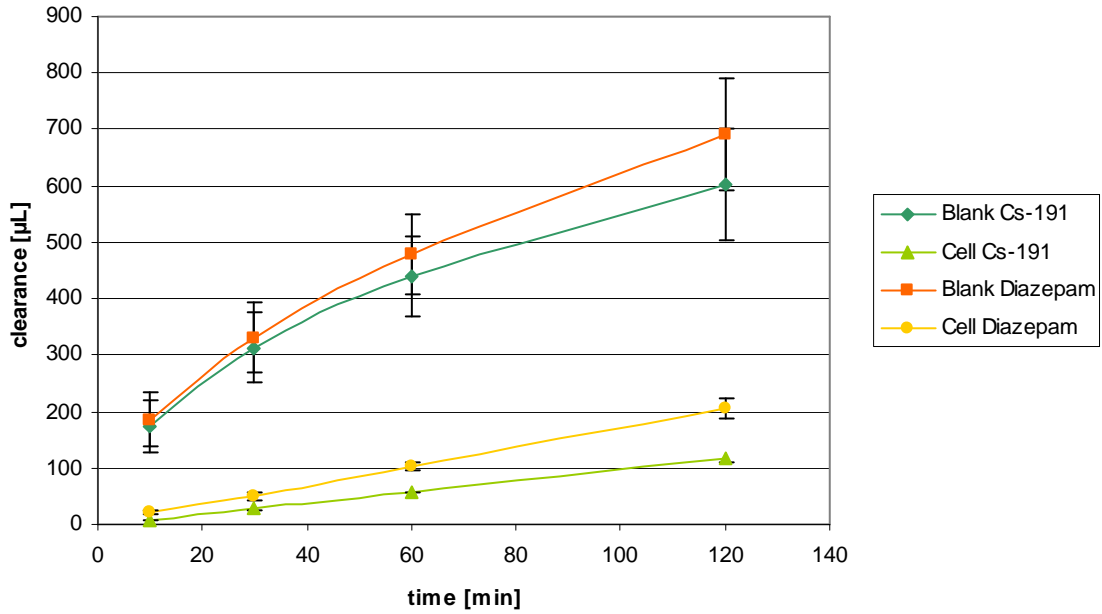
3.2.10 L-701,324
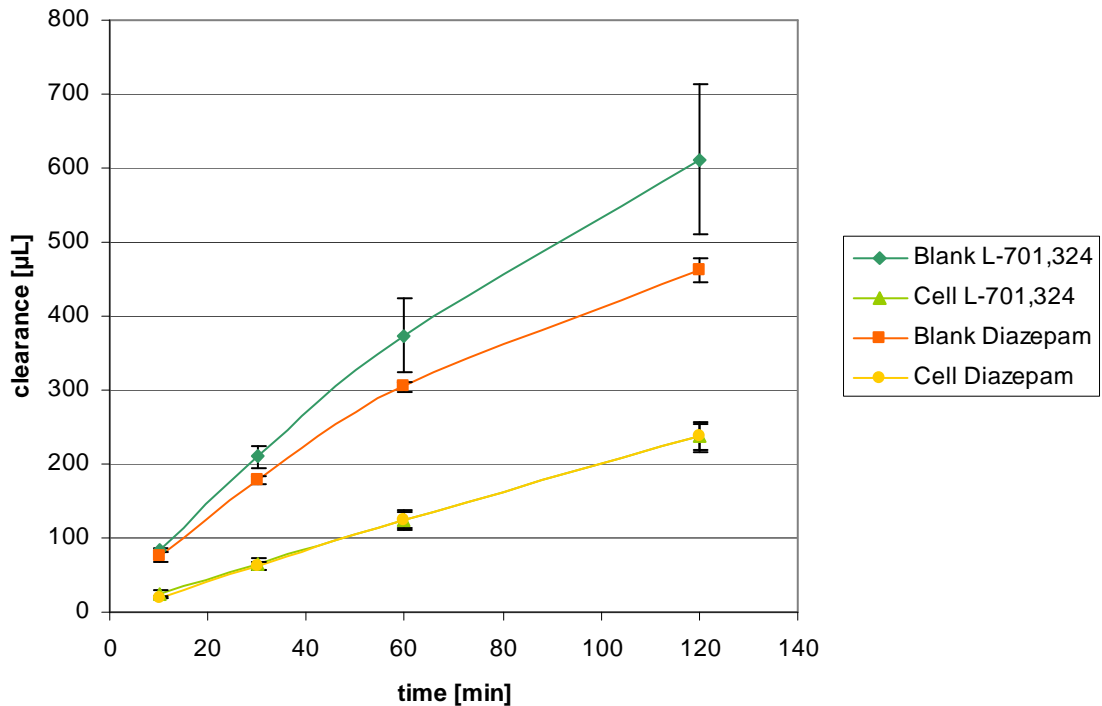
Figure 3.2.10: Clearance curves of L-701,324 and diazepam (internal standard) across empty inserts and cerebEND cell layers.
Green lines show the clearance L-701,324, whereas the dark line represents the blank-values and the bright line represents the cell-values. The orange line demonstrates the clearance of diazepam across blank inserts, the yellow line describes the clearance of diazepam across cerebEND cell layer.
Data are represented as mean ± SD (n=4) for 2 independent experiments.

In this assay, the curve of the clearance of diazepam and L-701,324 run nearly identically, which suggested that the transport properties of these two substances are very similar (see figure 3.2.10).

Table 3.2.10: Calculated permeability coefficients [µm/min] (PC), permeability factors normalized to diazepam (F) and recovery rates (RC) of L-701,324 and diazepam are listed.
Data are represented as mean ± SD (n=4) of 2 independent experiments.

	Time range	L-701,324	Diazepam
PC [µm/min]	10-120 min	46,14 ± 15,55	73,18 ± 49,52
PC [µm/min]	0-10 min	36,64 ± 26,60	33,13 ± 5,99
F	10-120 min	0,68 ± 0,44	1,00
F	0-10 min	1,59 ± 0,595	1,00
RC blank [%]		112,47 ± 12,15	125,04 ± 15,92
RC cells [%]		65,16 ± 27,40	133,60 ± 25,71

L-701,324 shows a reduced recovery in the cell value. This suggests that distinct parts of the added substance got stuck in the cells.

The calculated factors are quite variable. Nevertheless, it can be said that the transport-rate of L-701,324 was lower compared to diazepam.

3.2.11 Correlation between the normalized permeability coefficient and the clogP from literature

The correlation of these two parameters provides the information, if elevated lipophilicity leads to higher transport-rates in case of our assay.

Table 3.2.11: The table shows a list of the used substances and the parameters that were gained in context of the transport assay as well as the ranking of the test substances considering the literature clogP-values (logarithmic octanol-water partition coefficient) [47].

	RC D BI [%]	RC D C [%]	RC S BI [%]	RC S C [%]	F 10-120	F 0-10	clogP	ranking
Bu-113	117,61	99,5	80,45	52,91	0,295	0,177	7,122	1
Cs-199	108,75	101,78	29,62	23,95	0,113	0,106	6,992	2
Cs-182	112,06	99,18	77,75	75,93	0,534	0,322	6,723	3
Cs-191	115,62	94,08	103,57	78,05	0,535	0,36	6,593	4
L-701,324	125,04	133,6	112,47	65,16	0,679	1,586	5,406	5
Bu-82	122,59	106,59	115,59	100,54	0,597	0,58	5,024	6
Cs-224	100,97	92,05	107,82	92,31	0,526	0,355	4,964	7
Bu-99	108,66	99,98	92,5	91,78	0,355	0,347	4,495	8
Bu-108	109,2	98,61	71,28	60,08	0,192	0,152	4,096	9
Bu-90	120,89	97,56	105,21	73,58	0,398	0,464	3,308	10

3.2.11.1 Correlation between the normalized permeability coefficient in time of 10-120 minutes and the clogP from literature

Table 3.2.12: Correlation of the clogP and the coefficient, calculated from the values that were obtained after a time of 10 to 120 min.

F 10-120		clogP		difference	D²
Substance	Rank	Substance	Rank		
Cs-199	10	Cs-199	2	8	64
Bu-108	9	Bu-108	9	0	0
Bu-113	8	Bu-113	1	7	49
Bu-99	7	Bu-99	8	-1	1
Bu-90	6	Bu-90	10	-4	16
Cs-224	5	Cs-224	7	-2	4
Cs-182	4	Cs-182	3	1	1
Cs-191	3	Cs-191	4	-1	1
Bu-82	2	Bu-82	6	-4	16
L-701,324	1	L-701,324	5	-4	16
rs=	0,01818	df=8	n=10	sum:	168

The assumption was the more lipophilic the compound is, the better it diffuses across the barrier. This means, the higher the clogP, the higher the coefficient. Pairs were ranked to show a postitive correlation.

As r_s amounts only 0,01818, it could be said, that the parameters do not correlate with a probability of 95% to 99% (p<0,05 and <0,01).

The low recovery of some substances, may lead to lower permeability values, as less substance is left to diffuse across the cell layer. So additional correlation excluding substances with low recovery such as Bu-108. Bu-113 and Cs-199 (RC< 70%) was calculated.

Table 3.2.13: Correlation of the clogP and the coefficient, calculated from values that were obtained after a time of 10-120 min with high recovery values.

F 10-120		clogP		difference	D²
Substance	Rank	Substance	Rank		
Bu-99	**6**	**Bu-99**	**5**	1	1
Bu-90	**5**	**Bu-90**	**6**	-1	1
Cs-224	**4**	**Cs-224**	**4**	0	0
Cs-182	**3**	**Cs-182**	**1**	2	4
Cs-191	**2**	**Cs-191**	**2**	0	0
Bu-82	**1**	**Bu-82**	**3**	-2	4
rs=	**0,714286**	df=4	n=6	sum:	10

The assumption was the higher the lipophilicity, the faster the transport takes place across the barrier.

The r_s of 0,714286 shows no correlation between clogP and the calculated $F_{10-120min}$ at a probability of 95-99%.

3.2.11.2 Correlation between the normalized permeability coefficient in time of 0-10 minutes and the clogP from literature

Table 3.2.14: Correlation between clogP and the coefficient, calculated from the values that were obtained after a time of 0 to 10 min.

F 0-10		clogP		difference	D²
Substance	Rank	Substance	Rank		
Cs-199	10	Cs-199	2	8	64
Bu-108	9	Bu-108	9	0	0
Bu-113	8	Bu-113	1	7	49
Cs-182	7	Cs-182	3	4	16
Bu-99	6	Bu-99	8	-2	4
Cs-224	5	Cs-224	7	-2	4
Cs-191	4	Cs-191	4	0	0
Bu-90	3	Bu-90	10	-7	49
Bu-82	2	Bu-82	6	-4	16
L-701,324	1	L-701,324	5	-4	16
rs=	**0,006061**		n=10	sum:	164

The assumption was that higher lipophilicity leads to better transport through the cells. This means, the higher the clogP, the higher the coefficient. Pairs were ranked to show a positive correlation.

The r_s of 0,0061 suggests, that the parameters do not correlate with a probability of 95-99% ($p < 0,05$ and $p < 0,01$).

Same calculations were accomplished without substances that showed low RC-values.

Table 3.2.15: Correlation between clogP and the coefficient, calculated from the values that were obtained after a time of 0 to 10 min for substances with high recovery values.

F 0-10		clogP		difference	D²
Substance	Rank	Substance	Rank		
Cs-182	6	Cs-182	1	5	25
Bu-99	5	Bu-99	5	0	0
Cs-224	4	Cs-224	4	0	0
Cs-191	3	Cs-191	2	1	1
Bu-90	2	Bu-90	6	-4	16
Bu-82	1	Bu-82	3	-2	4
rs=	-0,31429		n=6	sum:	46

The assumption was the higher the lipophilicity, the faster the transport takes place across the barrier.

The r_s of -0,31429 shows no correlation between the values with a probability of 95-99% ($p < 0,05$ and $p < 0,01$).

These results indicated that the time window between 0-10 minutes is maybe not representative for transport studies across cell layers.

3.3 Oxygen/glucose deprivation barrier experiments

Changes of barrier functionality of the blood-brain barrier in-vitro model consisting of a co-culture of cerebENDs and C6 cells was assessed by measurement of transendothelial electrical resistance (TEER) and permeability of paracellular marker carboxyfluorescein after 4h OGD treatment.

3.3.1 Bu-82

Figure 3.3.1.1: Change of TEER [%] in dependence on the applied condition and substance concentrations of Bu-82.
Data are presented as mean ± standard error of mean (SEM) [%] (n= 8), from 2 experiments.

Figure 3.3.1.1 visualizes the strong damage caused by OGD-conditions, as it lowers TEER [%] to 46,51 ± 8,05%. The addition of Bu-82 showed no beneficial effects on TEER decrease. (see figure 3.3.1.1)

Figure 3.3.1.2: Bu-82 was applied in concentrations of 3µM, 5µM, 10µM and 30µM. The figure shows the permeability of the cell layer, measured by the transport of 10µM carboxyfluorescein, referred to cells that were exposed to OGD-conditions before. The values are compared to blank-values, single-cultured cerebEND cells under normoxia conditions (Norm Cere) and to cerebEND cells that were co-cultured with C6 cell line under normoxia conditions (Norm CC).
Data are presented as mean ± SEM (n=8) from 2 independent experiments.

Addition of Bu-82 led to an elevation of carboxyfluorescein transport between the cells. PS-values were decreased to 94,61 ± 3,71% (3µM), 89,07 ± 2,00% (5µM), 91,15 ± 2,26% (10µM) and 87,07 ± 6,60% (30µM) compared to 100% of OGD-treated cells without exposition to any additional substances (see figure 3.3.1.2).

Figure 3.3.1.3: Bu-82 was applied in concentrations of 3µM, 5µM, 10µM and 30µM. The figure shows the permeability of the cell layer, measured by the penetration of carboxyfluorescein, referred to cells that were exposed to OGD-conditions before. The values are compared to single-cultured cerebEND cells under normoxia conditions (Norm Cere) and to cerebEND cells that were co-cultured with C6 cell line under normoxia conditions (Norm CC). The represented values consider additionally the surface of the insert as well as the blanks.
Data are presented as mean ± SEM (n=8) from 2 independent experiments

Calculation of permeability coefficients for carboxyfluorescein revealed no significant difference (for 5 µM p=0.054) in comparison to the OGD-treated control (see figure 3.3.1.3).

In these experiments blank values were quite low complicating the calculation of permeability coefficients. Therefore, only TEER values should be considered for data analysis.

3.3.2 Bu-90

Figure 3.3.2.1: Change of TEER [%] in dependence on the applied condition and substance concentrations of Bu-90.
Data are presented as mean ± SEM [%] (n= 12) from 3 experiments.

Figure 3.3.2.1 proves the damage caused by OGD-conditions, because TEER [%] was significantly reduced to 39,05 ± 5,29%. 1µM and 3µM of Bu-90 showed weak effects, as TEER was increased to 41,93 ± 3,53% and 41,96 ± 7,61% (not significant). Other concentrations reduced the resistance compared to co-cultured cerebEND cells under OGD-conditions indicating a possible additional toxic effect (see figure 3.3.2.1).

Figure 3.3.2.2: Bu-90 was applied in concentrations of 1µM, 3µM, 5µM and 10µM. The figure shows the permeability of the cell layer, measured by the transport of 10µM carboxyfluorescein, referred to cells that were exposed to OGD-conditions before. The values are compared to blanks, single-cultured cerebEND cells under normoxia conditions (Norm Cere) and to cerebEND cells that were co-cultured with C6 cell line under normoxia conditions (Norm CC).
Data are presented as mean ± SEM (n=12) from 3 independent experiments.
*: statistically significant vs. control (OGD-CC), p<0,05, double sided t-test with the same variance

As it is shown clearly in figure 3.3.2.2, OGD-conditions led to damage of the cells as the PS-value is much higher than of normoxia controls. Addition of Bu-90 led to a reduction of carboxyfluorescein permeability concomitant with an increase of tightness of the barrier. Values of 92,03 ± 2,54% (1µM), 93,33 ± 2,68% (3µM), 98,90 ± 4,08% (5µM) and 79,75 ± 7,56% (10µM, significant) were achieved (see figure 3.3.2.2).

Figure 3.3.2.3: Bu-90 was applied in concentrations of 1µM, 3µM, 5µM and 10µM. The figure shows the permeability of the cell layer, measured by the penetration of carboxyfluorescein, referred to cells that were exposed to OGD-conditions before. The values are compared to single-cultured cerebEND cells under normoxia conditions (Norm Cere) and to cerebEND cells that were co-cultured with C6 cell line under normoxia conditions (Norm CC). The represented values consider additionally the surface of the insert as well as the blanks.
Data are presented as mean ± SEM (n=12) from 3 independent experiments.
*: statistically significant vs. control (OGD-CC), p<0,05, double sided t-test with the same variance

Calculated coefficient of CF [%] was significantly decreased to 54,91 ± 8,01% with 1µM, 67,49 ± 26,54% with 3µM, and 29,91 ± 28,42% with 10µM of Bu-90 (see figure 3.3.2.3).
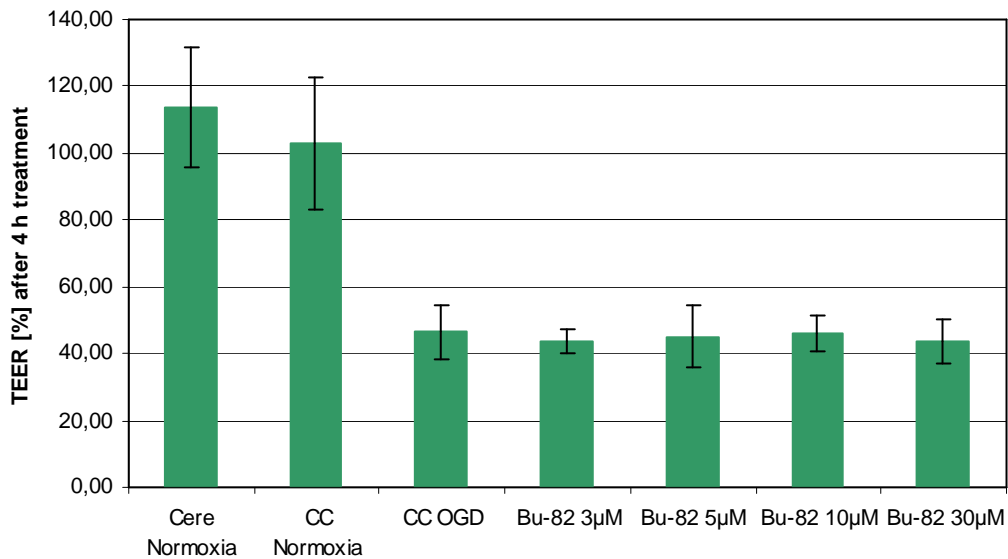
3.3.3 Bu-99

Figure 3.3.3.1: Change of TEER [%] in dependence on the applied condition and substance concentrations of Bu-99.
Data are presented as mean ± SEM [%] (n= 8) from 2 experiments.

Figure 3.3.3.1 shows the difference between OGD- and normoxia conditions on co-cultured cells. The TEER was reduced significantly to 50,0 ± 8,67%. Addition of 1µM of Bu-99 didn't change the TEER much as it was elevated only to 51,38 ± 5,80%. The concentrations of 3µM and 5µM reduced the values to 36,05 ± 3,44% and 46,80 ± 6,32%. Only 10µM of Bu-99 led to an increase of TEER to 64,91 ± 12,97% (not significant), which suggests, that the substance was able to reduce the damage in this concentration (see figure 3.3.3.1).
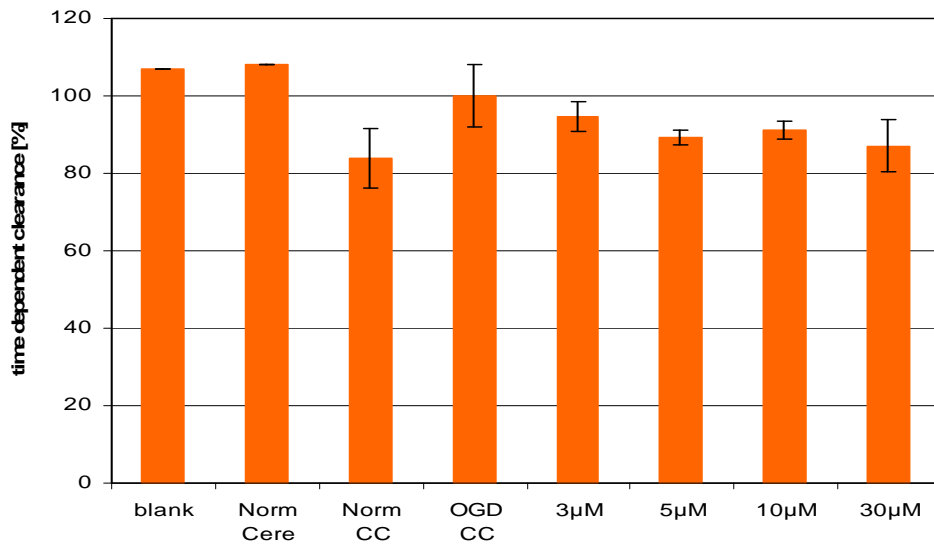
Figure 3.3.3.2: Bu-99 was applied in concentrations of 1µM, 3µM, 5µM and 10µM. The figure shows the permeability of the cell layer, measured by the transport of 10µM carboxyfluorescein, referred to cells that were exposed to OGD-conditions before. The values are compared to blanks, single-cultured cerebEND cells under normoxia conditions (Norm Cere) and to cerebEND cells that were co-cultured with C6 cell line under normoxia conditions (Norm CC).
Data are presented as mean ± SEM (n=8) from 2 independent experiments.

Addition of Bu-99 led to different effects. Cells that were exposed to 1µM, 3µM and 10µM showed elevation of the PS-value for carboxyfluorescein to 104,33 ± 3,61%, 101,22 ± 2,94% and 107,71 ± 3,07%. Concentrations of 5µM showed reduction of the permeability to 94,22 ± 2,23% (see figure 3.3.3.2).
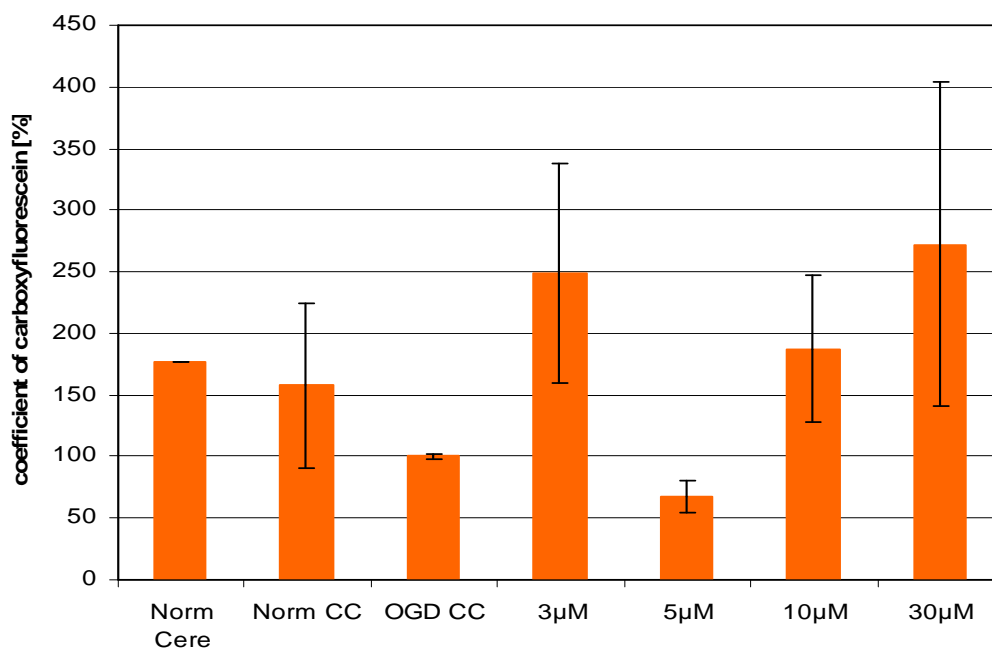
Figure 3.3.3.3: Bu-99 was applied in concentrations of 1µM, 3µM, 5µM and 10µM. The figure shows the permeability of the cell layer, measured by the penetration of carboxyfluorescein, referred to cells that were exposed to OGD-conditions before. The values are compared to single-cultured cerebEND cells under normoxia conditions (Norm Cere) and to cerebEND cells that were co-cultured with C6 cell line under normoxia conditions (Norm CC). The represented values consider additionally the surface of the insert as well as the blanks.
Data are presented as mean ± SEM (n=8) from 2 independent experiments.

Considering the calculated permeability coefficient of CF, a concentration of 1µM led to a value of 167,32 ± 54,10%, a concentration of 3µM showed values of 119,88± 54,09%, which means, that these concentrations lead to a higher damage. Higher concentrations of the substance led to better results. Addition of 5µM showed a value of 78,50 ± 8,09% and 10µM reduced the coefficient to 76,28 ± 19,03% (see figure 3.3.3.3).
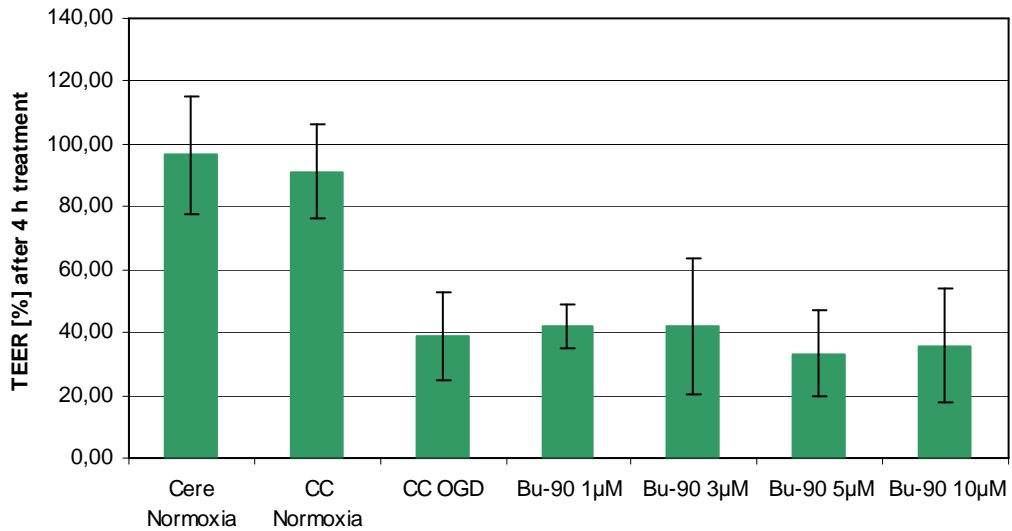
3.3.4 Bu-108

Figure 3.3.4.1: Change of TEER [%] in dependence on the applied condition and substance concentrations of Bu-108.
Data are presented as mean ± SEM [%] (n= 16) from 4 experiments.

The difference between the normal and the co-cultured cell line proves the influence of different conditions and composition of the cell line on the tightness of the barrier. OGD-conditions led to a clear decrease of TEER [%], related to co-cultured endothelial cells under normoxia to 47,11 ± 5,07% .

The figure visualizes the elevation of the resistance when co-cultured cells were exposed to 10µM of Bu-108. The TEER was increased to 55,12 ± 7,10%. The remaining concentrations didn't show a positive effect (see figure 3.3.4.1).
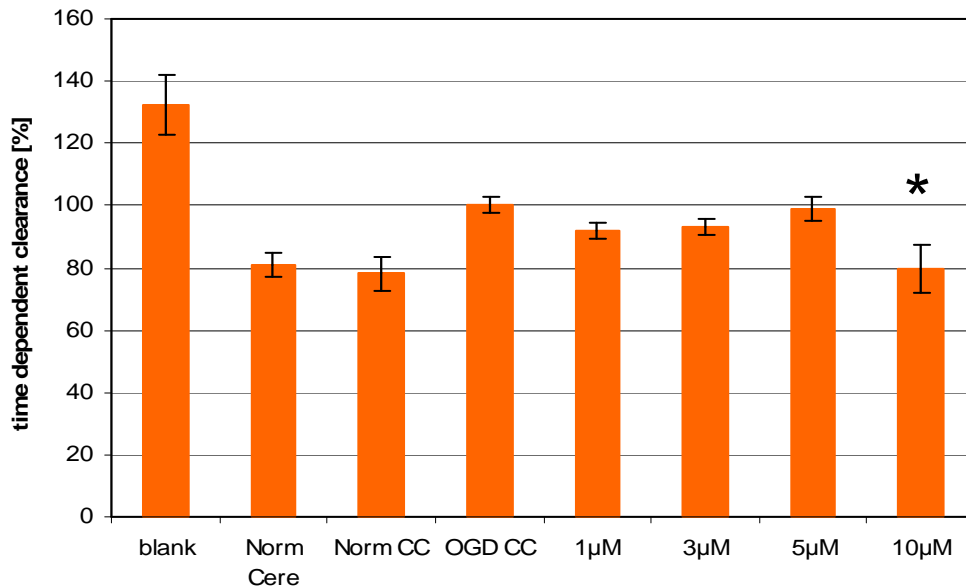
Figure 3.3.4.2: Bu-108 was applied in concentrations of 3µM, 10µM and 30µM. The figure shows the permeability of the cell layer, measured by the transport of 10µM carboxyfluorescein, referred to cells that were exposed to OGD-conditions before. The values are compared to blank-values, single-cultured cerebEND cells under normoxia conditions (Norm Cere) and to cerebEND cells that were co-cultured with C6 cell line under normoxia conditions (Norm CC).
Data are presented as mean ± SEM (n=16) from 4 independent experiments.
*: statistically significant vs. control (OGD-CC), p<0,05, double sided t-test with the same variance

Low concentrations of Bu-108 didn't show an effect as the clearance of CF rested at about 100% of the OGD-treated cells without substance application. Higher concentrations of 30µM led to an increase of the clearance (125,16 ± 8,40%), which is probably due to toxicity that elevates the damage (see figure 3.3.4.2).
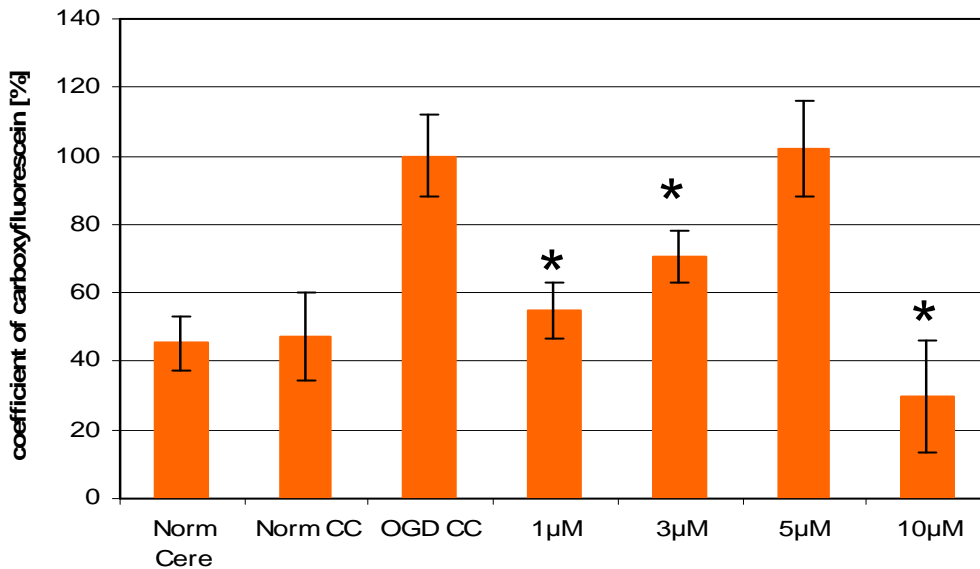
Figure 3.3.4.3: Bu-108 was applied in concentrations of 3µM, 10µM and 30µM. The figure shows the permeability of the cell layer, measured by the penetration of carboxyfluorescein, referred to cells that were exposed to OGD-conditions before. The values are compared to single-cultured cerebEND cells under normoxia conditions (Norm Cere) and to cerebEND cells that were co-cultured with C6 cell line under normoxia conditions (Norm CC). The represented values consider additionally the surface of the insert as well as the blanks.
Data are presented as mean ± SEM (n=16) from 4 independent experiments.

The addition of low concentrations (3µM, 10µM) didn't show changes of the coefficient of CF. When a concentration of 30µM was applied to the cells the value was even increased (138,21 ± 41,15), which is probably due to toxicity (see figure 3.3.4.3).

3.3.5 Bu-113
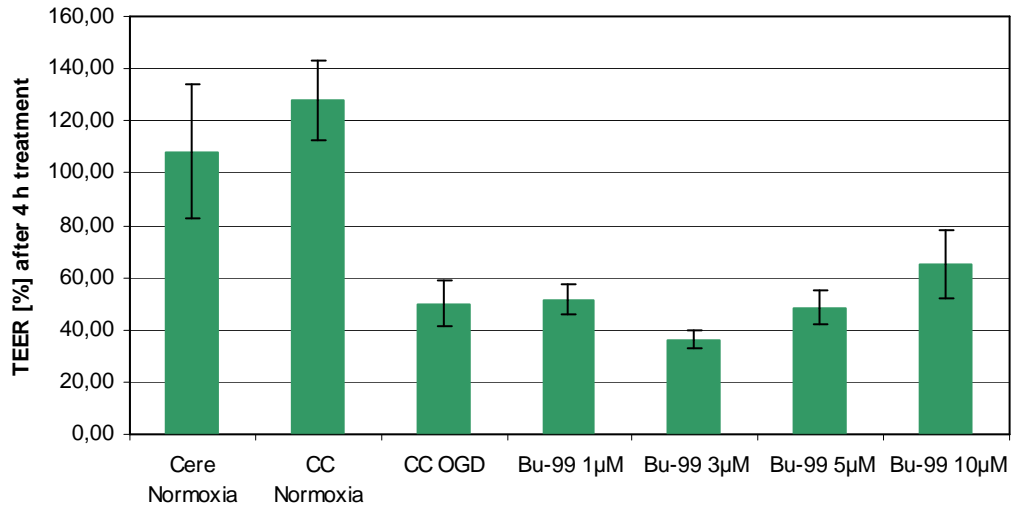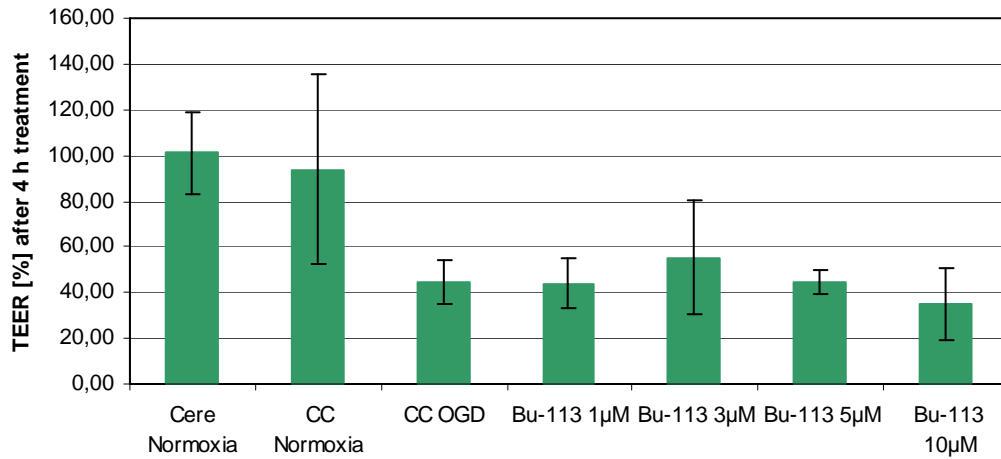

Figure 3.3.5.1: Change of TEER [%] in dependence on the applied condition and substance concentrations of Bu-113.
Data are presented as mean ± SEM [%] (n=)] from 2 experiments.

Figure 3.3.5.1 shows the clear difference between OGD and normoxia-conditions. Only a concentration of 3µM was able to reduce the damage (55,36 ± 10,16%) in cells, that were treated with Bu-113, whereas higher concentrations probably harmed the cells. Lower concentrations didn't influence the cells (see figure 3.3.5.1).

Figure 3.3.5.2: Bu-113 was applied in concentrations of 1µM, 3µM, 5µM and 10µM. The figure shows the permeability of the cell layer, measured by the transport of 10µM carboxyfluorescein, referred to cells that were exposed to OGD-conditions before. The values are compared to blank-values, single-cultured cerebEND cells under normoxia conditions (Norm Cere) and to cerebEND cells that were co-cultured with C6 cell line under normoxia conditions (Norm CC).
Data are presented as mean ± SEM (n=8) from 2 independent experiments.
*: statistically significant vs. control (OGD-CC), p<0,05, double sided t-test with the same variance

Low concentrations of Bu-113 led to a decrease of the time dependent clearance, which suggests, that the damage could be reduced. Permeability-values could be reduced to 85,39 ± 2,55% (1µM) and 86,36 ± 2,84% (3µM). 5µM of the substance didn't show an effect, whereas high concentrations of 10µM for example showed a significant value (194,13 ± 8,72%) due to damage of the cell-barrier (see figure 3.3.5.2).

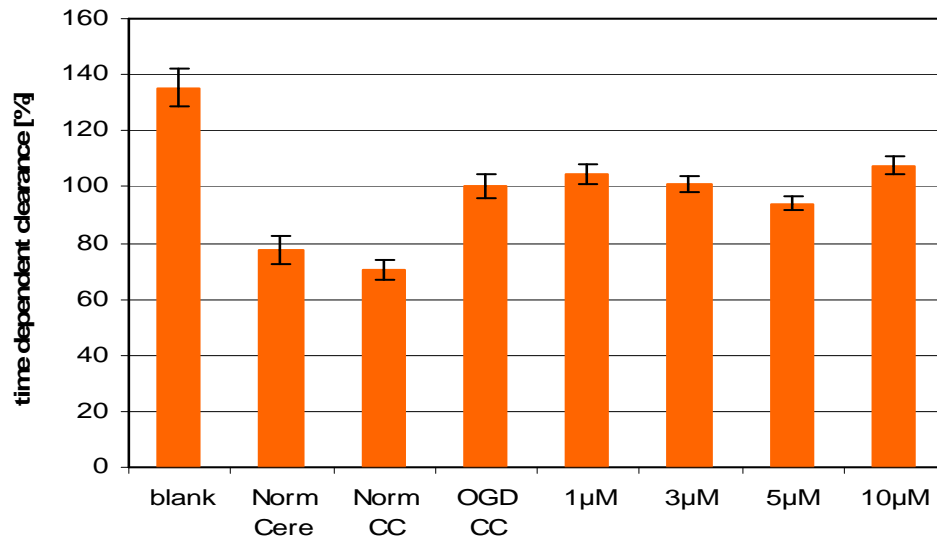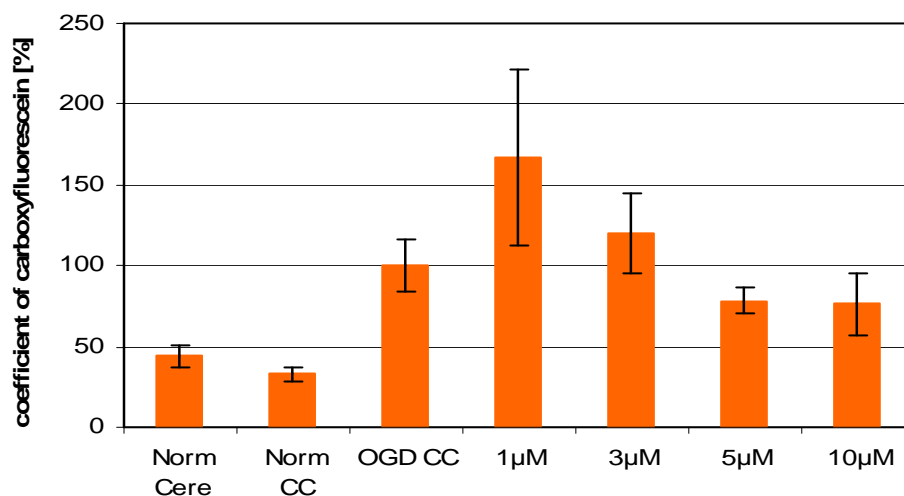Figure 3.3.5.3: Bu-113 was applied in concentrations of 1µM, 3µM and 5µM. The figure shows the permeability of the cell layer, measured by the penetration of carboxyfluorescein, referred to cells that were exposed to OGD-conditions before. The values are compared to single-cultured cerebEND cells under normoxia conditions (Norm Cere) and to cerebEND cells that were co-cultured with C6 cell line under normoxia conditions (Norm CC). The represented values consider additionally the surface of the insert as well as the blanks.
Data are presented as mean ± SEM (n=8) from 2 independent experiments.
*: statistically significant vs. control (OGD-CC), p<0,05, double sided t-test with the same variance

Concentrations of 1µM and 3µM showed significant reduction of the permeability coefficient of CF. It was decreased to 58,45 ± 4,61% (1µM) and 54,22 ± 11,17% (3µM). Although the permeability was lower at 5µM, this concentration showed already less effects than lower concentrations (72,78 ± 6,53%), which is probably due to the toxicity that was confirmed in previous assays (see figure 3.3.5.3). Data of 10µM Bu113 are not shown, due to high toxicity, which led to incomparable values.

3.3.6 Cs-182
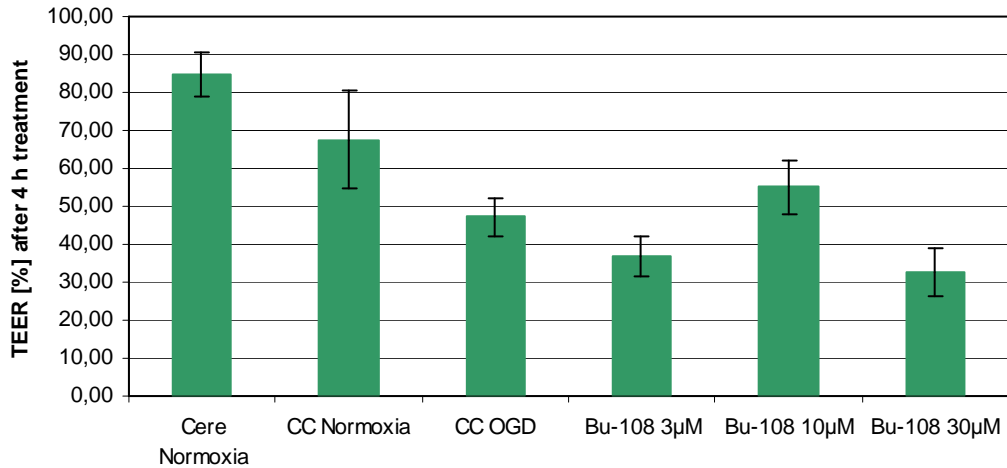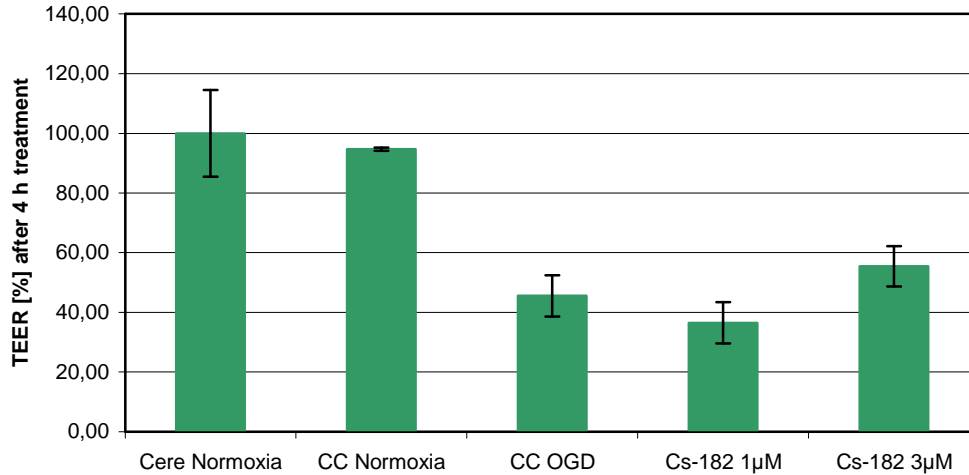

Figure 3.3.6.1: Change of TEER [%] in dependence on the applied condition and substance concentrations of Cs-182.
Data are presented as mean ± SEM [%] (n= 4) from 1 experiment.

Figure 3.3.6.1 visualizes the difference between the TEER of co-cultured cells under OGD- and normoxia-conditions. Addition of 1µM of the substance showed a decrease of the tightness of the barrier, whereas 3µM increased TEER of the cells from 45,57 ± 6,88% to 55,46 ± 6,93% (see figure 3.3.6.1).

Figure 3.3.6.2: Cs-182 was applied in concentrations of 1µM and 3µM. The figure shows the permeability of the cell layer, measured by the transport of 10µM carboxyfluorescein, referred to cells that were exposed to OGD-conditions before. The values are compared to blank-values, single-cultured cerebEND cells under normoxia conditions (Norm Cere) and to cerebEND cells that were co-cultured with C6 cell line under normoxia conditions (Norm CC).
Data are presented as mean ± SEM (n=4) from 1 experiments.
*: statistically significant vs. control (OGD-CC), p<0,05, double sided t-test with the same variance

Addition of the substance Cs-182 led to a decrease of time dependent clearance to 90,25 ± 3,20% in a concentration of 1µM and 68,46 ± 6,85% (significant) in a concentration of 3µM. Thus, the substance was able to reduce the damage caused by glucose and oxygen deprivation (see figure 3.3.6.2).
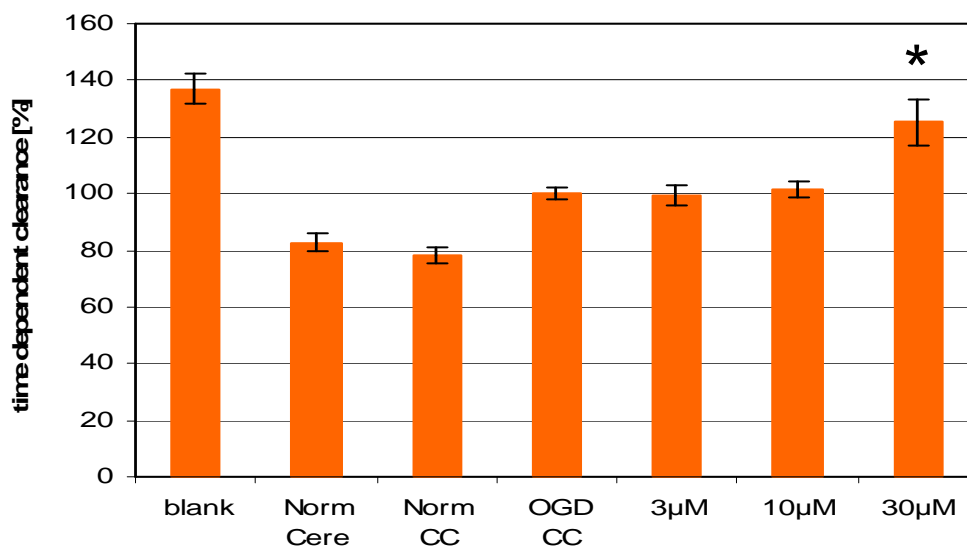
Figure 3.3.6.3: Cs-182 was applied in concentrations of 1µM and 3µM. The figure shows the permeability of the cell layer, measured by the penetration of carboxyfluorescein, referred to cells that were exposed to OGD-conditions before. The values are compared to single-cultured cerebEND cells under normoxia conditions (Norm Cere) and to cerebEND cells that were co-cultured with C6 cell line under normoxia conditions (Norm CC). The represented values consider additionally the surface of the insert as well as the blanks.
Data are presented as mean ± SEM (n=2-4) from 1 experiments.

Addition of 1µM and 3µM of Cs-182 reduced the coefficient to 49,87± 9,50% and 19,95 ± 5,96% (not significant, for 3 µM p=0.069). (see figure 3.3.6.3).

3.3.7 Cs-191
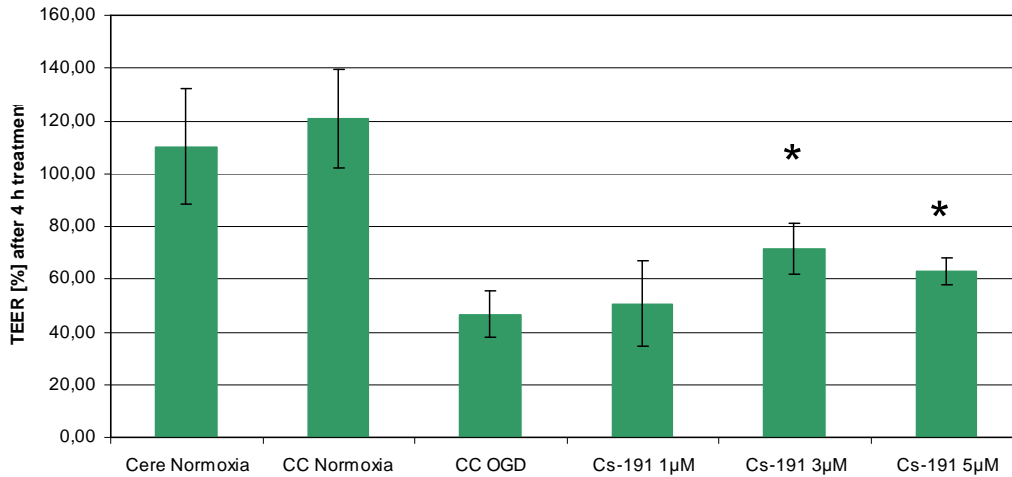
Figure 3.3.7.1: Change of TEER [%] in dependence on the applied condition and substance concentrations of Cs-191.
Data are presented as mean ± SEM [%] (n= 8) from 2 experiments.
*: statistically significant vs. control, p<0,05, double sided t-test with the same variance

Figure 3.3.7.1 shows that Cs-191 was able to reduce the damage that was caused due to OGD-conditions. Cells that were exposed to 3µM of Cs-191 showed a significant increase of TEER to 71,44 ± 3,70%. Addition of 5 µM also elevated TEER significantly to 62,94 ± 2,61% (see figure 3.3.7.1).
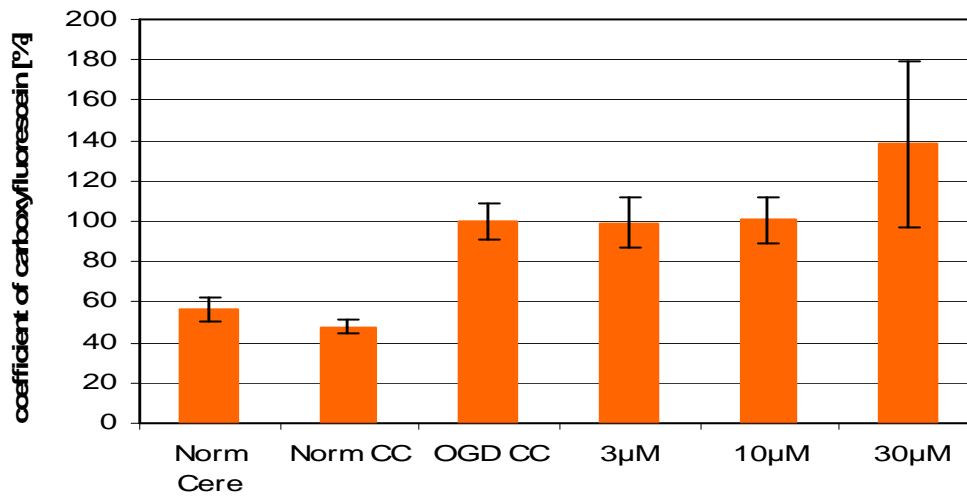
Figure 3.3.7.2: Cs-191 was applied in concentrations of 1µM, 3µM and 5µM. The figure shows the permeability of the cell layer, measured by the transport of 10µM carboxyfluorescein, referred to cells that were exposed to OGD-conditions before. The values are compared to blank-values, single-cultured cerebEND cells under normoxia conditions (Norm Cere) and to cerebEND cells that were co-cultured with C6 cell line under normoxia conditions (Norm CC).
Data are presented as mean ± SEM (n=8) from 2 independent experiments.
*: statistically significant vs. control (OGD-CC), p<0,05, double sided t-test with the same variance

Cells that were treated with Cs-191 showed less damage, compared to untreated cells exposed to OGD-conditions alone. Addition of 1µM of the substance led to a clear reduction of the clearance to 77,22 ± 8,73%. The decrease of the substance concentration showed similar, but weaker effects. 3µM of the substance reduced the clearance to 91,60 ± 1,73% and a concentration of 5µM led to a value of 98,68 ± 1,15% (see figure 3.3.7.2).
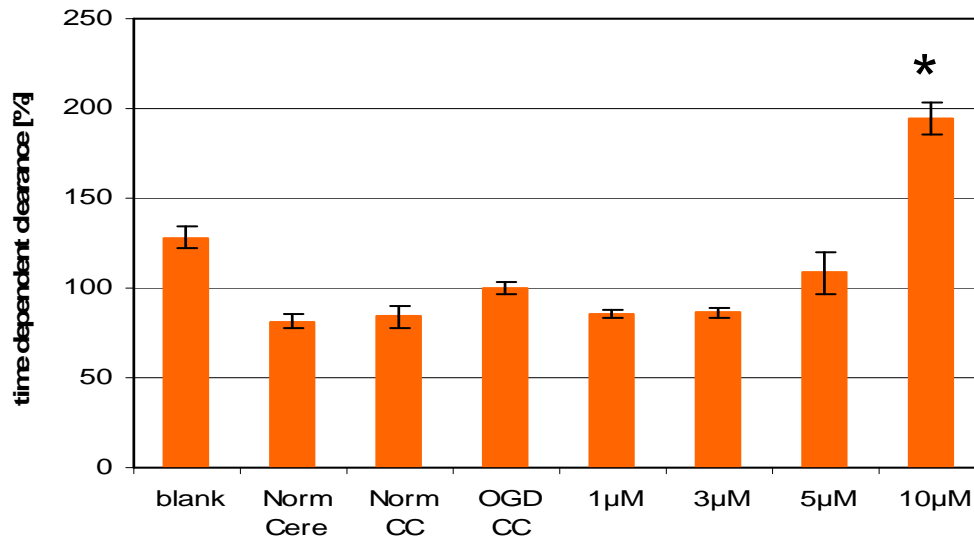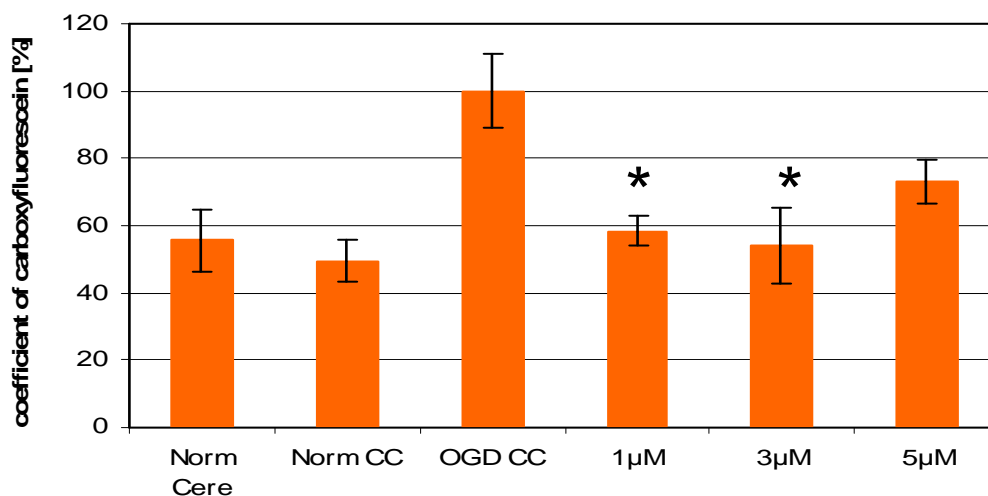
Figure 3.3.7.3: Cs-191 was applied in concentrations of 1µM, 3µM and 5µM. The figure shows the permeability of the cell layer, measured by the penetration of carboxyfluorescein, referred to cells that were exposed to OGD-conditions before. The values are compared to single-cultured cerebEND cells under normoxia conditions (Norm Cere) and to cerebEND cells that were co-cultured with C6 cell line under normoxia conditions (Norm CC). The represented values consider additionally the surface of the insert as well as the blanks.
Data are presented as mean ± SEM (n=8) from 2 independent experiments.
*: statistically significant vs. control (OGD-CC), $p < 0,05$, double sided t-test with the same variance

Figure 3.3.7.3 shows that Cs-191 had a clear positive effect on cells, as already low concentrations reduced the calculated permeability coefficient of carboxyfluorescein. Considering the surface of the cell-layer the value was decreased to 49,57 ± 9,70% after apical aplication of 1µM carboxyfluorescein. Addition of 3µM led to values of 64,03 ± 4,69% whereas the addition of 5µM of Cs-191 showed a reduction of the coefficient to 81,79 ± 6,61% (see figure 3.3.7.3).

3.3.8 Cs-199
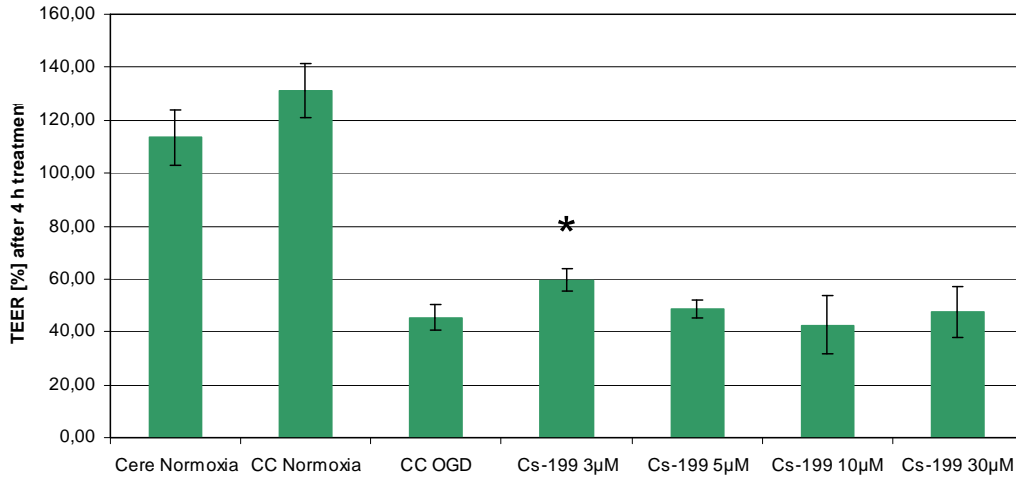
Figure 3.3.8.1: Change of TEER [%] in dependence on the applied condition and substance concentrations of Cs-199.
Data are presented as mean ± SEM [%] (n= 8) from 2 experiments.
*: statistically significant vs. control, p<0,05, double sided t-test with the same variance

The difference between the co-cultured and the normal cerebEND cells is quite high, which shows the clear influence of the added C6 cell line in building the barrier. Furthermore, the OGD-effect was quite strong, as the values were reduced to 45,5 ± 4,95%. Only a concentration of 3µM led to a significant increase of the TEER in % as the values were at 59,55 ± 4,13%, whereas other tested concentrations didn't have an effect (see figure 3.3.8.1).
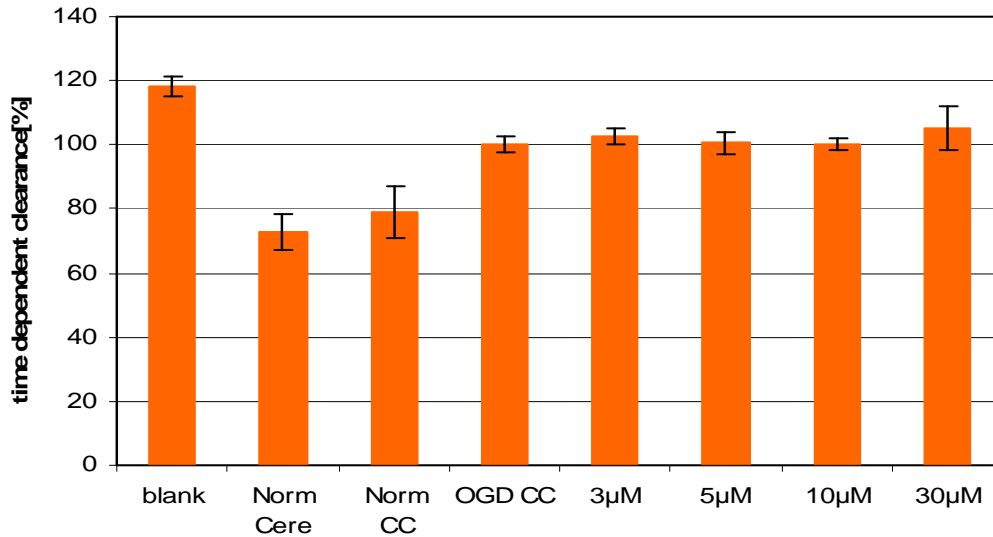
Figure 3.3.8.2: Cs-199 was applied in concentrations of 3µM, 5µM, 10µM and 30µM. The figure shows the permeability of the cell layer, measured by the transport of 10µM carboxyfluorescein, referred to cells that were exposed to OGD-conditions before. The values are compared to blank-values, single-cultured cerebEND cells under normoxia conditions (Norm Cere) and to cerebEND cells that were co-cultured with C6 cell line under normoxia conditions (Norm CC).
Data are presented as mean ± SEM (n=8) from 2 independent experiments.

As figure 3.3.8.2 visualizes, the addition of Cs-199 didn't show any (significant) changes of the time dependent clearance of carboxyfluorescein as all values rested at about 100%. This probably means that the substance doesn't influence the paracellular transport (see figure 3.3.8.2).
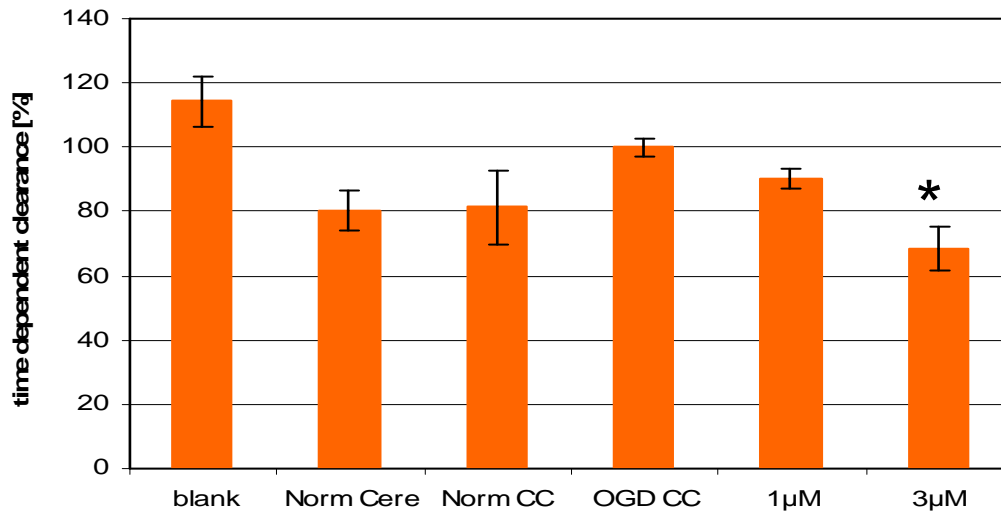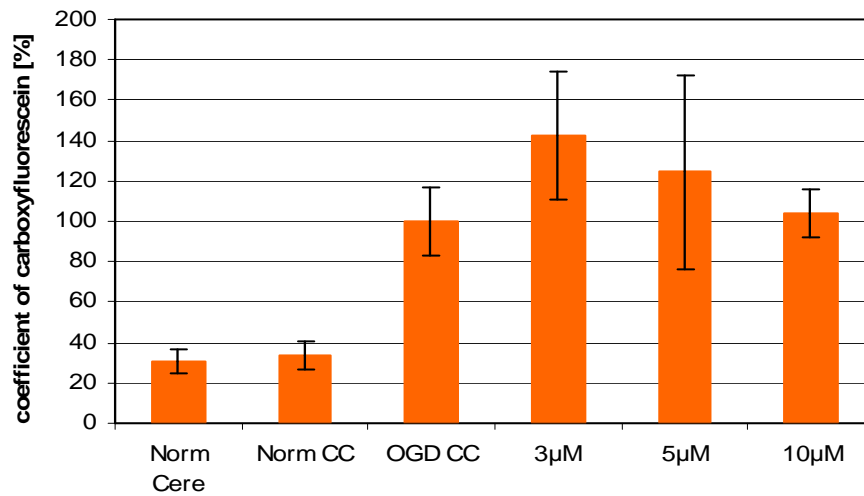
Figure 3.3.8.3: Cs-199 was applied in concentrations of 3µM. 5µM, 10µM and 30µM. The figure shows the permeability of the cell layer, measured by the penetration of carboxyfluorescein, referred to cells that were exposed to OGD-conditions before. The values are compared to single-cultured cerebEND cells under normoxia conditions (Norm Cere) and to cerebEND cells that were co-cultured with C6 cell line under normoxia conditions (Norm CC). The represented values consider additionally the surface of the insert as well as the blanks.
Data are presented as mean ± SEM (n=8) from 2 independent experiments.

The addition of 3µM and 5µM elevated the coefficient to 142,43 ± 31,80% and 124,56 ± 47,92%. A concentration of 10µM didn't show a change of the value. (see figure 3.3.8.3). Data of 30µM Cs-199 are not shown, as the results exceeded values of 400% and were not comparable due to high toxicity.

3.3.9 Cs-224
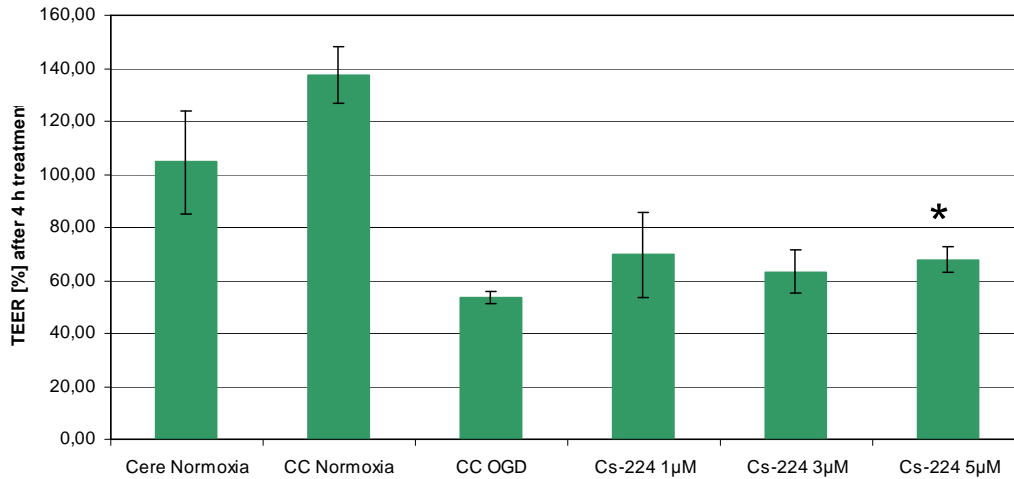
Figure 3.3.9.1: Change of TEER [%] in dependence on the applied condition and substance concentrations of Cs-224.
Data are presented as mean ± SEM [%] (n= 12) from 3 experiments.
*: statistically significant vs. control, p<0,05, double sided t-test with the same variance

All tested concentrations showed a strong effect. Addition of 1μM showed an increase of TEER to 69,70 ± 16,08%. Elevating the concentration to 3μM led to a value of 63,36 ± 8,20% and a concentration of 5μM showed change of TEER to 67,88 ± 4,76% (significant) (see figure 3.3.9.1).
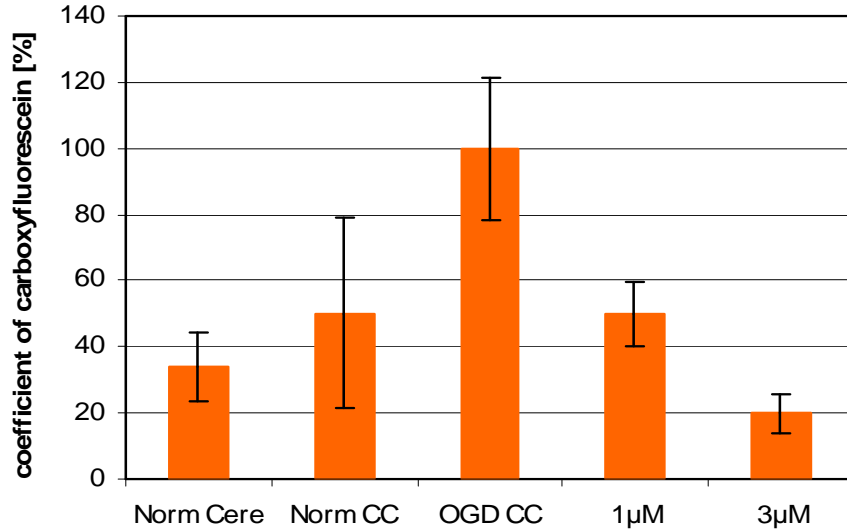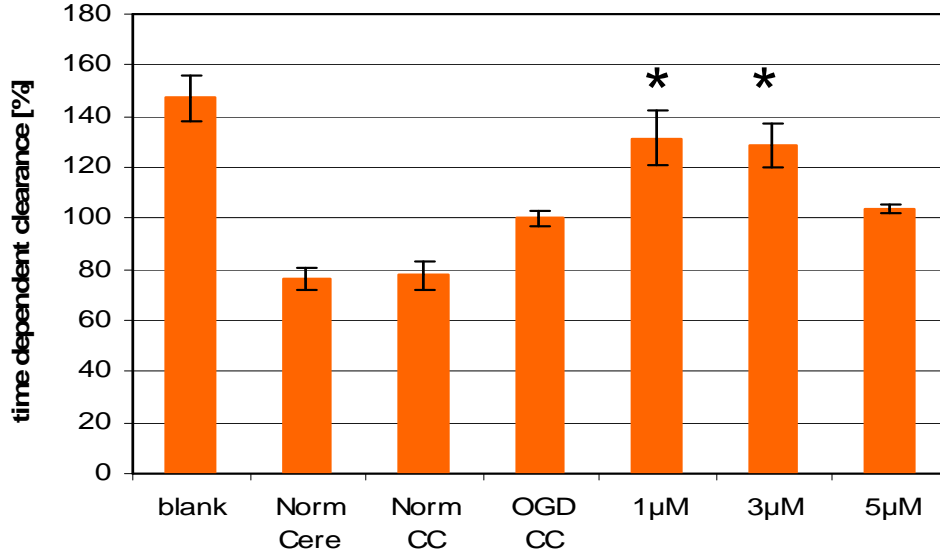
Figure 3.3.9.2: Cs-224 was applied in concentrations of 1μM, 3μM and 5μM. The figure shows the permeability of the cell layer, measured by the transport of 10μM carboxyfluorescein, referred to cells that were exposed to OGD-conditions before. The values are compared to blank-values, single-cultured cerebEND cells under normoxia conditions (Norm Cere) and to cerebEND cells that were co-cultured with C6 cell line under normoxia conditions (Norm CC).
Data are presented as mean ± SEM (n=12) from 3 independent experiments.
*: statistically significant vs. control (OGD-CC), p<0,05, double sided t-test with the same variance

Addition of Cs-224 showed elevated time dependent clearance. It was increased significantly to 131,33 ± 10,65% (1μM) and 128,47 ± 8,29% (3μM). Addition of 5μM didn't lead to a significant change (103,73 ± 1,32%) (see figure 3.3.9.2).
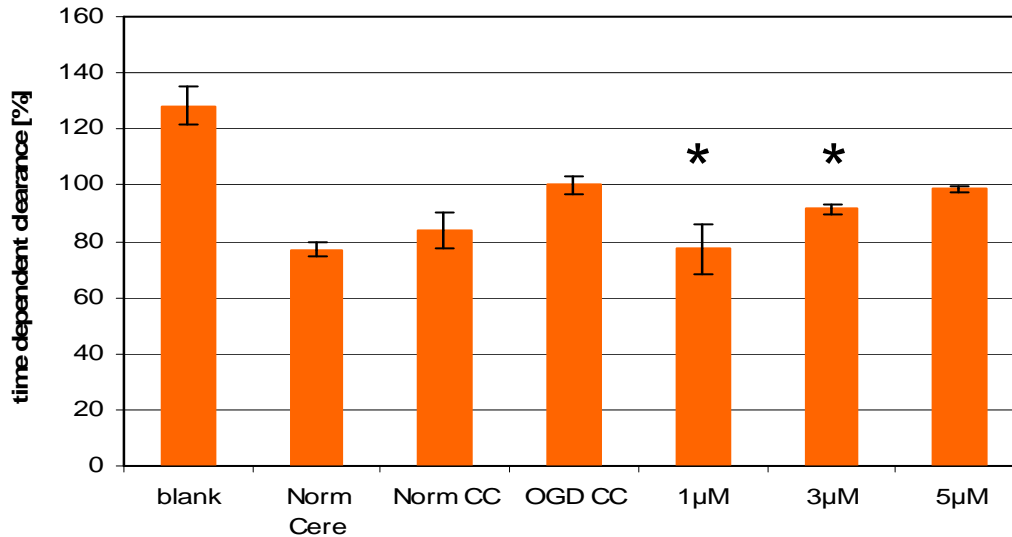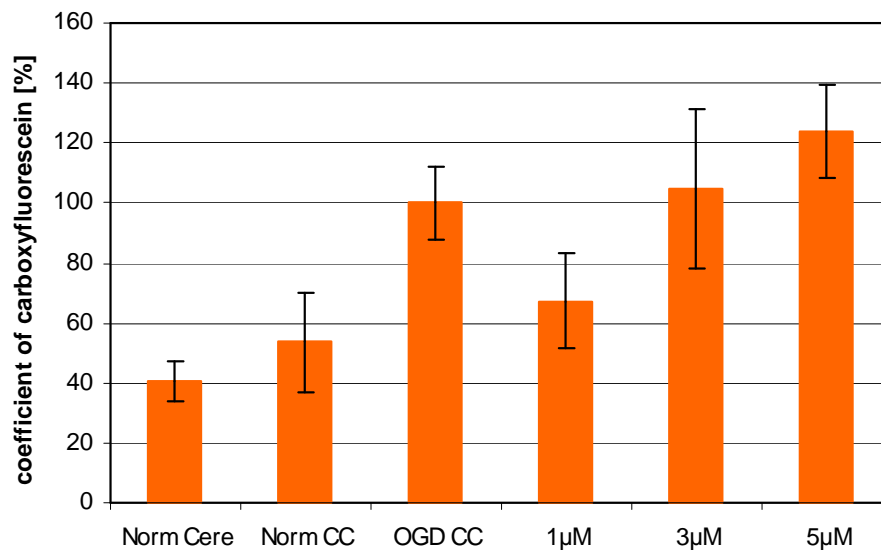
Figure 3.3.9.3: Cs-224 was applied in concentrations of 1µM, 3µM and 5µM. The figure shows the permeability of the cell layer, measured by the penetration of carboxyfluorescein, referred to cells that were exposed to OGD-conditions before. The values are compared to single-cultured cerebEND cells under normoxia conditions (Norm Cere) and to cerebEND cells that were co-cultured with C6 cell line under normoxia conditions (Norm CC). The represented values consider additionally the surface of the insert as well as the blanks.
Data are presented as mean ± SEM (n=12) from 3 independent experiments.

1µM of the substance reduced the calculated permeability coefficient of CF to 67,40 ± 15,92%. 3µM of Cs-224 showed no positive effect, as the value was elevated to 104,64 ± 26,61%. Also the addition of 5µM of the substance elevated the coefficient to 123,79 ± 15,66% (see figure 3.3.9.3).

3.3.10 L-701,324
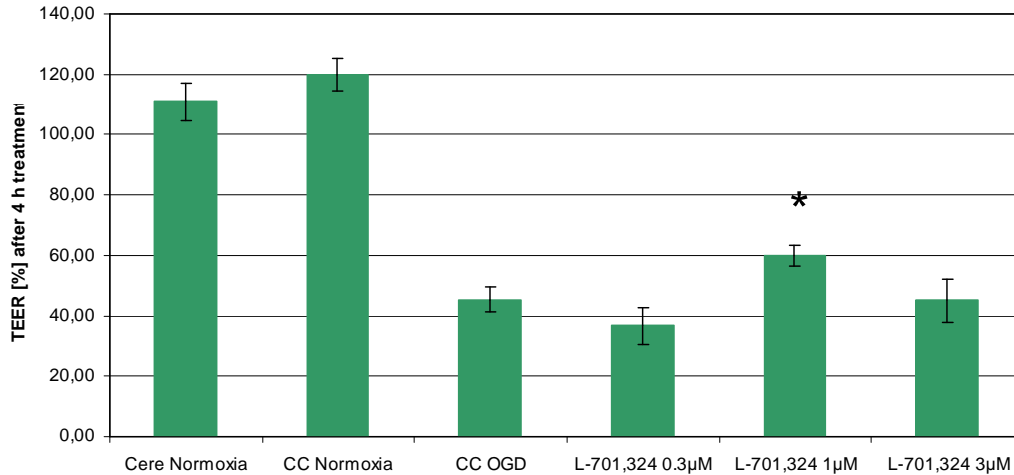
Figure 3.3.10.1: Change of TEER [%] in dependence on the applied condition and substance concentrations of L-701,324.
Data are presented as mean ± SEM [%, n= 12], from 3 experiments.
*: statistically significant vs. control, p<0,05, double sided t-test with the same variance

Figure 3.3.10.1 visualizes the strong effect of oxygen and glucose deprivation. When cells were exposed to OGD-conditions TEER changed to 45,13 ± 4,24% compared to 119,66 ± 5,42% in normoxia conditions. A concentration of 1μM of L-701,324 showed strong effects, as the TEER was significantly increased to 59,94 ± 3,59%.The other tested concentrations didn't show a change of the resistance (see figure 3.3.10.1).
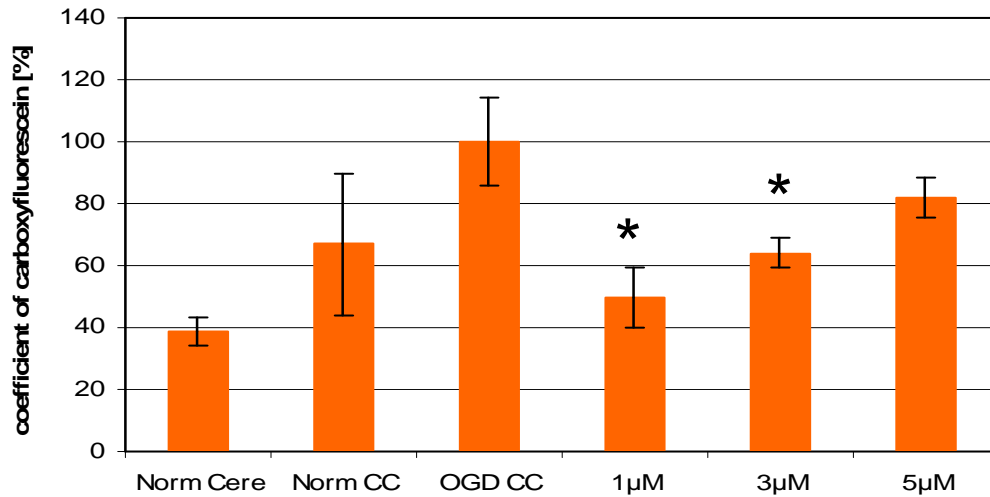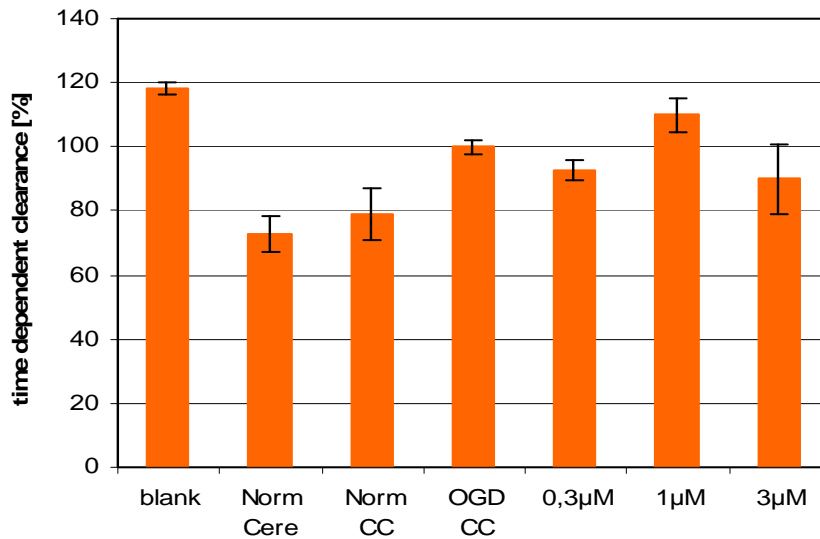
Figure 3.3.10.2: L-701,324 was applied in concentrations of 0,3µM, 1µM and 3µM. The figure shows the permeability of the cell layer, measured by the transport of 10µM carboxyfluorescein, referred to cells that were exposed to OGD-conditions before. The values are compared to blank-values, single-cultured cerebEND cells under normoxia conditions (Norm Cere) and to cerebEND cells that were co-cultured with C6 cell line under normoxia conditions (Norm CC).
Data are presented as mean ± SEM (n=12) from 3 independent experiments.

Figure 3.3.10.2 shows that the addition of 0,3 µM and 3µM led to an improvement of the clearance. It could be reduced to 92,56 ± 3,05% (0,3µM) and 89,91 ± 11,02% (3µM). A concentration of 1µM increased the permeability to 109,99 ± 5,16% (see figure 3.3.10.2).
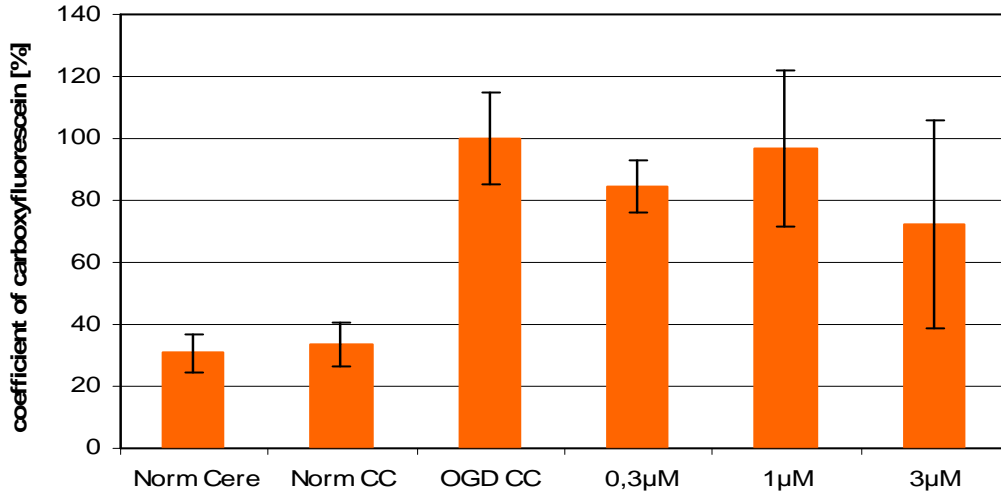
Figure 3.3.10.3: L-701,324 was applied in concentrations of 0,3µM, 1µM and 3µM. The figure shows the permeability of the cell layer, measured by the penetration of carboxyfluorescein, referred to cells that were exposed to OGD-conditions before. The values are compared to single-cultured cerebEND cells under normoxia conditions (Norm Cere) and to cerebEND cells that were co-cultured with C6 cell line under normoxia conditions (Norm CC). The represented values consider additionally the surface of the insert as well as the blanks.
Data are presented as mean ± SEM (n=12) from 3 independent experiments.

As it can be shown in figure 3.3.10.3, L-701,324 can prevent the cell from the damage that is caused by OGD-conditions. It reduces the calculated permeability coefficient of CF to 69,61 ± 9,76% (0,3µM), 97,00 ± 29,87% (1µM) and 72,45 ± 33,58% (3µM) (see figure 3.3.10.3).

4. Discussion

4.1 Potential NR-1 antagonists and their role in stroke therapy

4.1.1 Modulating the glycine binding-site of NMDAR

The aim of the work was to find substances, which act as NMDAR-glycine-binding-site (NR-1 subunit) antagonists. As this receptor plays an essential role in many physiological as well as pathological processes especially in the central nervous system, targeting of this structure may lead to desired but also undesired effects. The present work focuses on utilisation of the substance in case of ischemia, whose progress is mainly influenced by NMDAR-activation. The blockade of these receptors may lead to reduction of the Ca^{2+} influx [18]. Thus, NR1-blocking substances may lead to a reduction of cell death and so decrease the damage that is caused by ischemia [32].

Previous studies describe the test of glycine-binding site antagonist in several test-systems.

HA-966 (1-Amino-2-Hydroxypyrolid -2-one) is a substance which was known to modulate the NMDAR long before the NR1-subunit was explored. The substance was tested by inhibition of binding of ^{3}H-glycine from its binding-site on the NR1-subunit in rat cerebral cortex synaptic plasma membranes. Inhibitory maximum was achieved at 250µM, higher concentrations didn't achieve an improvement of inhibition [63].

Further NR1-antagonists like MDL-105,519 or MDL-100,748 were tested by Baron et al. Both showed inhibitory effects in radioligand-binding assays accomplished with ^{3}H-glycine. IC50 values of 10,9±1,4nM for MDL 105,519 and 70±20nM for MDL 100,748 were achieved [64].

Priestley et al. proved the effect of L-701,324 and L-695,902, whereas the first compound showed higher potency. Inhibitory effects were already achieved at

concentrations of 0,1-1µM of the substance, which complys to the results of the current work (significant TEER-elevation at 1µM, See figure 3.3.10.1) [65].

4.1.2 Influence of tissue-plasminogen activator on NMDAR-neurotoxicity and its dependence on NR-1

Tissue-plasminogen (t-PA) activator is a widely expressed protein, with the endothelial cells as their main source. Still, it is also expressed within neurons and astrocytes of the hippocampus and hypothalamus and there it seems to have a deciding role in physiological and pathological processes as it binds to lipoprotein related receptor protein (LRP), 5–8 annexin-II9 or NMDAR [43, 66].

Tissue-plamsinogen activator is well known as modulator of thrombus-formation, as it activates plasminogen which finally leads to thrombolysis. Its utilisation in therapy of stroke within three hours after the event has led to beneficial effects for the patients [43, 44].

Nevertheless, the therapy became questionable as it was discovered by Tsirka et al (1995) that this protein also influences the process of neurotoxicity during ischemia [69].

Depolarisation leads to Ca^{2+} dependent release of t-PA from neurons to the extracellular space. The protein binds at the amino terminal domain of the NR1 subunit of NMDAR, which finally leads to enhanced activation of the receptor and the progress of excitotoxic effects [43, 44].

By adding rPAI-1, a molecule which inhibits the catalytic side of t-PA, the damage can be prevented [42].

A recent study indicated that the neurotoxic effect is modulated via MAPK (mitogen activated protein-kinase) and ERK1/2 (see 1.4.2.1) as the number of phosphorylated ERK1/2-proteins was elevated [66].

Furthermore there could be proved that the t-PA modulated NMDAR over-activation is dependent on the constitution of the receptor, as the process shows

selectivity on NR2-D-subunit containing NMDARs. Addition of NR2-D antagonist (2S*, 3R*)-1-(phenanthrene-2-carbonyl) piperazine-2,3-dicarboxylic acid (PPDA) could show the expected inhibition of t-PA modulated NMDAR-stimulation at 0,2µM [66].

Again binding of the glycine binding site appears as an opportunity to prevent the cell from neurotoxic damage after ischemia. This could be proved by Vivien et al. (2011), who was able to achieve a beneficial effect in-vitro and in-vivo via t-PA binding site antagonizing antibodies that prevent the cleavage with the amino terminal domain of the NR1-subunit in-vitro at a concentration of 0,1mg/ml (complete blockade of recombinant t-PA induced neurotoxicity) and in-vivo via bolus injektion of 160µg in mice (reduction of brain lesion size of 47%) [46].

4.2 Structure-activity relationships

The gained results of the several assays were necessary, as the huge amount of data allows the prediction of structure-activity relationships. It could be explored, whether the activity depends on lipophilicity alone, or on the presence of certain substructures or if there is no correlation at all. This information is necessary to predict several effects with the help of the chemical structure alone and to enable directed research to find potential targets for modulation of the test-system.

With the several assays that were accomplished, it is possible to make some statements that describe the properties and the behaviour of the substances in context of the in-vitro test-system much better than simple values.

As the glycine antagonists may also harm the cells themselves in certain concentrations, instead of preventing them from damage, it was necessary to prove their cell toxicity at first. This was accomplished with EZ4U-assays. Thus, it could be discovered, in which concentrations the substances harm the cell. With these results it was possible to adapt substance's concentrations for following assays like the test of transport-properties or the change of TEER after oxygen and glucose deprivation.

Taking into account that substances that diffuse unhindered through the blood-brain barrier and are present in high concentration in the CNS are more likely to harm the tissue, than compounds that rest inside the cells due to affection of diffusion the aim would be to find substances that accord with the latter. When substances, with these properties were found, they could be offered for further explorations, such as in-vivo assays.

The chemical structure of the test-substances consists of an annealed basement-ring-system with heteroaromates.

The used substances differed mainly from the ring-structure, whether there was a thiophene (figure 4.1) or benzene-ring (figure 4.2) annealed to the pyridine-ring.
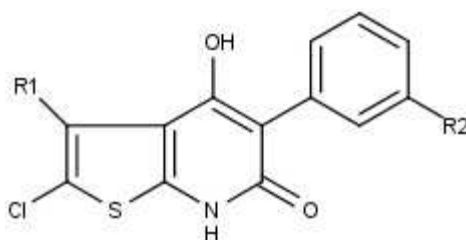
Figure 4.1: One basement structure of the used compounds consisting of a thiophen-ring, that is annealed with a pyridine [2,3-b].

Residues that compounds with this basement structure had in common were the Cl-residue in position 2, a hydroxy-group in position 4, a phenyl-residue in position 5 and an oxo-group in position 6. The residues differed in postion 3 and 3' (according R1 and R2).
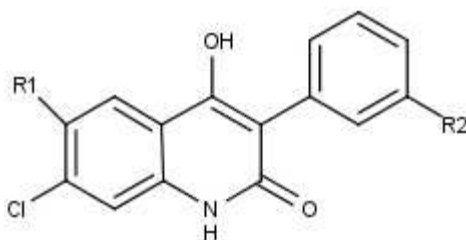
Figure 4.2: The other basement structure consists of a pyridine ring annealed with a benzene [2,3 –a]. Constant residues were the oxo-group in position 2, the phenyle-ring in position 3, the hydroxy-group in position 4 and the chloride-atom in position 7. Differing residues were in position 3' of the phenyl-rest (R2).

4.2.1 Relationship between cell-toxicity and the substance's structures

Table 4.1: The table shows the differences in the structure of the substances and the concentration, in which they act toxic under the apparent conditions.
The values were gained from cell viability assays (EZ4U) (see 3.1)

Basic structures:

Substance	Ring-structure	R1	R2	Normoxia Tox conc C6	Normoxia Tox conc cere	OGD Tox conc C6	OGD Tox conc cere
Bu-82	Thiophene	1-Methyl-propyl	-	-	-	-	10µM
Bu-90	Benzene	-	-	-	-	-	-
Bu-99	Thiophene	Isopropyl	-	-	-	-	-
Bu-108	Thiophene	Ethyl	-	-	-	-	-
Bu-113	Thiophene	Cyclopropyl	Phenoxy	30µM	10µM	30µM	10µM
Cs-182	Thiophene	Propyl	Phenoxy	100µM	10µM	100µM	10µM
Cs-191	Thiophene	Isopropyl	Phenoxy	-	-	-	10µM
Cs-199	Thiophene	Tert. butyl	Phenoxy	30µM	10µM	30µM	10µM
Cs-224	Thiophene	Methoxy-methyl	Phenoxy	-	-	-	-
L-701,324	Benzene	-	Phenoxy	-	-	-	-

The table shows that it doesn't play an important role for inducing toxicity whether the structure contains a thienopyridine- or a benzopyridine-ring, as both structures can lead to cell damage. Nevertheless, compounds with an annealed thiophene-ring tend to harm the cells more likely, because they show toxicity

already in the quite resistant C6 cell lines as well as under mild condition when glucose- and oxygen-supply is sufficient.

R1 substituting residues don't make a great difference in toxicity of the compound.

However, the residue in position R2 seems to be the deciding structure, whether a substance acts toxic or not. A main part of the substances that have a phenyl-residue in position R2 acts toxic in high and low concentration, independent of the used cell line. This can be proven by the substances Bu-113, Cs-182, Cs-191 and Cs-199.

The toxicity of the substances has several consequences. One example is the adaption of the concentration for later assays. Furthermore, toxic substances have to be handled with care for in-vivo assays. To reach the possible effective concentration in the desired compartiment in an in-vivo-model, a dose has to be determined, that doesn't exceed the toxic concentration.

In general, the absorption was remarkably low in all OGD-assays (compared to absorption values at normoxic conditions). This is because of missing oxygen and glucose for mitochondiral activity. EZ4U tests are dependent of the activity of mitochondrial dehydrogenases, as they are part of the reduction of applied XTT-derivates. (see methods 2.2.2.1)

In the context of this work, IC50-values, gained from Mayrhofer 2015 [47] could be included and compared to the gained cell-toxity concentrations.

Table 4.2: IC50 and toxic concentration-values of Mayrhofer, compared to results of the present work.

Substance	IC50 Mayrhofer [µM]	Toxic conc Mayrhofer [µM]	Normoxia		OGD	
			Tox conc C6	Tox conc cere	Tox conc C6	Tox conc cere
Bu-82	56,38	100	-	-	-	10µM
Bu-90	89,65	100	-	-	-	-
Bu-99	32,74	60	-	-	-	-
Bu-108	71,37	100	-	-	-	-
Bu-113	27,41	30	30µM	10µM	30µM	10µM
Cs-182	179,80	100	100µM	10µM	100µM	10µM
Cs-191	39,76	100	-	-	-	10µM
Cs-199	66,70	100	30µM	10µM	30µM	10µM
Cs-224	25,66	30	-	-	-	-
L-701,324	14,22	50	-	-	-	-

The table shows, that some toxic effects that Mayrhofer gained in case of his work, were confirmed in case of the present work (Bu-113, Cs-182 and Cs-199, see table 4.2), despite the utilisation of different cell cultures. Whereas assays of this work were accomplished with cerebellar endothelial (cerebEND) cell line and glioma (C6) cell line, Mayrhofer used human embryonic kidney (HEK) 293 cell line. Furthermore, assays with HEK-cells were only carried out under normoxic conditions [47].

NMDAR-subunit-expression was induced by addition of tetracycline in context of Mayrhofers work, leading to cell death due to Ca^{2+} overload. By adding of NR-1 antagonists it was sought to find substances that prevent the cell from the damage by antagonising this receptor [47].

The most toxic substances in the current work, Bu-113, Cs-182 and Cs-199, also showed harming effects on HEK-293 cells (See table 4.2).

Both Cs-224 and L-701,324, showed preventive effects (IC50 of 16,63 µM and 14,22) and didn't lead to further cell-damage in cell-toxicity assays.
Interestingly, some substances such as Bu-99, Cs-224 and L-701,324 were toxic for the HEK-cells, but nor for cerebENDs or C6 cells.

As the IC50-values of some substances exceed the concentration, that acts toxic under oxygen/glucose deprivation, the utilisation of these substances is questionable (see table 4.2), as it is probably not possible to achieve the effective concentration of the substance without harming the cell additionally. Still, there has to be mentioned that the different conditions (normoxic instead of OGD) and utilisation of a different cell line may lead to different results, which probably requires further tests to explore IC50 values in cerebEND-cell line and under OGD-conditions.

4.2.2 Relationship between the transport across the blood—brain barrier and the substance's structures

Table 4.3: The table shows the transport-properties in dependence of the structure of the substances, including recovery (RC) and the factor (F). The recovery describes how much of the substance was found after application in context of the assay outside of the cells.

The factor F is calculated by dividing the transport rate of the test-substance by the transport rate of diazepam.

Basic structure:

Substance	Ring-structure	R1	R2	RC S Bl [%]	RC S C [%]	F 10-120	F 0-10	clogP
Bu-82	Thiophene	1-Methyl-propyl	-	115,59	100,54	0,597	0,580	5,024
Bu-90	Benzene	-	-	105,21	73,58	0,398	0,464	3,308
Bu-99	Thiophene	Isopropyl	-	92,50	91,78	0,355	0,347	4,495
Bu-108	Thiophene	Ethyl	-	71,28	60,08	0,192	0,152	4,096
Bu-113	Thiophene	Cyclopropyl	Phenoxy	80,45	52,91	0,295	0,177	7,122
Cs-182	Thiophene	Propyl	Phenoxy	77,75	75,93	0,534	0,322	6,723
Cs-191	Thiophene	Isopropyl	Phenoxy	103,57	78,05	0,535	0,360	6,593
Cs-199	Thiophene	Tert. buthyl	Phenoxy	29,62	23,95	0,113	0,106	6,992
Cs-224	Thiophene	Methoxy-methyl	Phenoxy	107,82	92,31	0,526	0,355	4,964
L-701,324	Benzene	-	Phenoxy	112,47	65,16	0,679	1,586	5,406
Diazepam	Benzodiazepin	-	-	112,93	98,81	1,000	1,000	2,961

As it was shown in 3.2.12, there was no correlation found between elevated lipophilicity (represented by the clogP-value) and the transport-properties of the compound.

Thus, the question remains, if there are several substructures that influence the transport more than others.

The additional phenoxy-residue may suggest an elevated transport, due to its increased lipophilicity. The results show that this is the case for the substances Cs-182, Cs-191, Cs-224 and L-701,324. These substances diffuse at least approximately half as fast as diazepam (see table 4.3).

Other compounds that contain the phenoxy ring like Cs-191 and Bu-113 didn't show the expected effect as they were transported slowly. Bu-108, a compound without phenoxy rest, was transported slowly too, whereas the remaining substances with this substructure were transported faster (see table 4.3).

The residue in position R1 could be important too for the interpretation of the transport rates. Bu-113 with a cyclopropyl-residue and Cs-199 with a tertiary butyl residue, both groups are expected to have an elevated lipophilicity, showed a reduced transport. Nevertheless, other substances with lipohphilic residues show again good transport properties, as they diffuse half as fast as diazepam.

Bu-108, with a less lipophilic ethyl-group showed reduced transport accross the in-vitro barrier.

Bu-82 and Cs-224 revealed high recovery rates in cell- values and blank values (only inserts), which suggested that these substances tend to diffuse across the barrier better than others.

Residual substances tended to remain in the cell, as the recovery rate is clearly under 100% of diazepam for example.

Bu-90, Cs-191, Cs-224 and L-701,324 show normal RC values accross blanks, and lower RC values across the in-vitro cell barrier. This means, that these substances was probably uptaken or bound to the cell.

In contrary, Bu-99, Bu-108, Bu-113, Cs-182 and Cs-199 showed reduced RC values in both setups, which suggested that the diffusion of these substances was mainly hindered by absorption by the plastic material of the blank inserts.

Actually, Cs-199 tended to interact with the inserts most likely, as the RC-values amount were 29,62% (blanks) and 23,95% (cell value) (see table 4.3).

The more substance remains in the cells, the lower the concentration will be in the ISF (interstitial fluid). The high diffusion rate of NMDA-receptor-antagonists in previous assays probably was one of the reasons, why many of those failed in clinical due to high toxicity [42].
Thus, high uptake in brein endothelial cells would lead to less damage in neurons or glia cells and so facilitate the utilisation of the compounds in further tests.

4.2.3 Relationship between used substances and change of TEER under OGD conditions

Table 4.4: Change of TEER in % referred to 100% OGD-co-cultured conditions considering the structural differences between the substances
CerebEND co-culture (CC) values of the table represent the average of the TEER of co-cultured cells under OGD conditions of the assays that were accomplished with each substance. Significant values are marked bold.

Basic structures:

Substance	Ring-structure	R1	R2	CC OGD	0,3µM	1µM	3µM	5µM	10µM	30µM
Bu-82	Thiophene	1-Methyl-propyl	-	46,51		43,60	45,08	46,02	43,79	
Bu-90	Benzene	-	-	39,05		41,93	41,96	33,36	35,86	
Bu-99	Thiophene	Isopropyl	-	50,00		51,38	36,05	48,60	64,91	
Bu-108	Thiophene	Ethyl	-	47,11			36,84		55,12	32,45
Bu-113	Thiophene	Cyclopropyl	Phenoxy	44,73		43,92	55,36	44,57	34,93	
Cs-182	Thiophene	Propyl	Phenoxy	45,57		36,50	55,46			
Cs-191	Thiophene	Isopropyl	Phenoxy	46,79		50,77	**71,44**	**62,94**		
Cs-199	Thiophene	Tert. buthyl	Phenoxy	45,40			**59,55**	48,55	42,68	47,47
Cs-224	Thiophene	Methoxy-methyl	Phenoxy	53,70		69,70	63,36	**67,88**		
L-701,324	Benzene	-	Phenoxy	45,31	36,67	**59,94**	45,13			

The aim of this assay was to investigate the potential of the test compounds to reduce barrier breakdown measured by TEER.

Nearly every substance showed the expected effect. Only Bu-82, a thieno-pyridine with a methyl-1-propyl residue and Bu-90, a benzo-pyridin without

residues in positions 6 and 3' showed no elevation of the TEER after OGD-treatment.

Bu-99 and Bu-108 showed weak effects at relative high concentrations of 10µM. Both substances have a thiophene-ring and similar residues in position 3 (isopropyl- and ethylresidues).

Bu-113 and Cs-182 showed stronger effects. The two thieno-pyridines have a phenoxy-phenyl group in position 3 and similar residues in position 5 (propyl- and cyclopropyl-residue). Even low concentrations of 3µM achieved a remarkable, but not significant increase of the resistance. Nevertheless, higher concentrations of Bu-113 showed lower resistance of the cells. This is probably due to its toxicity, which was proved in previous assays at 10µM under OGD conditions. Thus, the substance shows potential, but only in low concentrations.

Cs-191, Cs-199 and Cs-224 consist all of a thieno-pyridine structure. The residue in position 3 is identical (phenoxy-phenyl-group) but the residue in position 5 is quite variable. Cs-191 has an isopropyl-residue, Cs-199 has a very lipophilic tertiary butyl residue and Cs-224, with a methoxy-methyl, shows a quite hydrophilic structure in position 5 of the thieno-pyrdine ring. Nevertheless, these substances showed the strongest effects of all test-compounds. The addition of these substances in low concentrations led to prevention of the OGD induced barrier breakdown. The potency to antagonize the glycine-binding-site of the NMDA-receptor seems to be higher in these molecules, than in other substances, because the elevation of the resistance of the co-cultured endothelial cells is achieved with relative low concentrations (1µM, 3µM, 5µM) which was according to their low IC50 values in the HEK-293 model (table 4.2).

L-701,324, a standard glycine antagonist [31, 67, 68] showed, as expected, strong effects. This impact was already achieved in low concentrations of 1µM and 5µM. L-701,324 consists of benzo-pyridine ring, with a phenoxy-phenyl residue in position 3 and no residue in position 6.

In conclusion, mainly the phenoxy residue in position 3' seems to play a deciding role in developing protective effects. Compounds that contain this structure tend

to be more efficient in preventing the damage as they act in lower concentrations and show a higher difference between treated and untreated cells.

The residue in position R1 seems to be less deciding for the effect, as similar residues don't always show the general expected similar effect, whereas different structures in this position act similar strong.

Applying OGD-conditions to the cells leads to several effects as published by Neuhaus et al. 2014, including changes in tight junctions or in activity of tissue plasminogen activator (t-PA) and matrixmetalloproteinase (MMP) [7]. These effects are represented by the co-culture OGD-value, which tends to be clearly lower, compared to non-affected cells in or without co-culture. Furthermore, cells were incubated with concentrations of substances that turned out to be non-toxic in previous assays. It was expected that these substances would reduce OGD-induced damage and stabilize the barrier.

Compared to Neuhaus et al (2014) [7], the OGD-damage in the current study was stronger in context of the present work was stronger, which means that the TEER was quite low (average of 46%), whereas in the work of Neuhaus et al. TEER reduction to approximately 60% was achieved. This higher damage may lead to weaker protective effects that are caused by potent substances.

4.3 Comparison of the results

4.3.1 Correlation of the recovery rate during transport studies and the change of TEER

Substances that remain in the cell due to weak diffusion can't block the glycine-binding site which is localised at the outside of the cell (see figure 1.2). This property can be represented by the determined recovery rate. Bu-108, Bu-113, Cs-199 and L-701,324 are substances that show low recovery-rates and probably would show higher effects in elevating TEER in transport independent assays.

This hypothesis is proved by the calculation of spearman's correlation coefficient.

Table 4.4 Correlation between recovery and TEER elevation

Recovery		TEER elevation		difference	D²
Substance	Rank	Substance	Rank		
Bu-82	**1**	**Bu-82**	**10**	-9	81
Cs-224	**2**	**Cs-224**	**3**	-1	1
Bu-99	**3**	**Bu-99**	**5**	-2	4
Cs-191	**4**	**Cs-191**	**1**	3	9
Cs-182	**5**	**Cs-182**	**7**	-2	4
Bu-90	**6**	**Bu-90**	**9**	-3	9
L-701,324	**7**	**L-701,324**	**2**	5	25
Bu-108	**8**	**Bu-108**	**8**	0	0
Bu-113	**9**	**Bu-113**	**6**	3	9
Cs-199	**10**	**Cs-199**	**4**	6	36
$r_s =$ **0,418182**	df=8	n=10		sum:	96

The assumption was, the higher the recovery-rate, the better the substance binds to the extracellular glycine-binding site and so leads to prevention of cell-death and elevation of TEER.

The calculated coefficient r_s amounts 0,418182, which accords to no correlation between RC and TEER-elevation with a probability of 95-99% ($p<0,05$ and $p<0,01$).

4.3.2 Correlation of IC50 values (literature) and TEER elevation

Substances with high potential for inhibiting the barrier breakdown in case of stroke should show high TEER values as well as low IC50-values, which were gained from Mayrhofer [47].

Table 4.5: Correlation between IC50 values from Mayrhofer [47] and the TEER- values that were gained in context of the OGD assays.

IC50		TEER elevation		difference	D²
Substance	Rank	Substance	Rank		
L-701,324	**1**	**L-701,324**	**2**	-1	1
Cs-224	**2**	**Cs-224**	**3**	-1	1
Bu-113	**3**	**Bu-113**	**6**	-3	9
Bu-99	**4**	**Bu-99**	**5**	-1	1
Cs-191	**5**	**Cs-191**	**1**	4	16
Bu-82	**6**	**Bu-90**	**9**	-3	9
Cs-199	**7**	**Cs-199**	**4**	3	9
Bu-108	**8**	**Bu-108**	**8**	0	0
Bu-90	**9**	**Bu-90**	**9**	0	0
Cs-182	**10**	**Cs-182**	**7**	3	9
rs=	**0,666667**	**df=8**	n=10	sum:	55

The assumption was, the lower the IC50, the higher the TEER-values get after exposition to OGD-condition.

The calculated coefficient rs of 0,67 means that there is a correlation between the IC50-values from Mayrhofer and the TEER-elevation in context of the OGD-assays. Differences of single rankpairs could be due to toxicity or low recovery-rates of the substances.

4.3.3 Relationship between recovery, TEER and IC50-values

Table 4.5: Comparison of IC50 (values gained from Mayrhofer, 2014) changes of TEER (in %, related to OGD-treated cells, without substance exposition) and recovery rate.
Significant values are marked bold.

Substance	IC50 Mayrhofer [µM]	RC S Bl [%]	RC S C [%]	Change of TEER					
				0,3µM	1µM	3µM	5µM	10µM	30µM
Bu-82	56,38	115,59	100,54			93,74	96,93	98,95	94,15
Bu-90	89,65	105,21	73,58		107,36	107,45	85,43	91,82	
Bu-99	32,74	92,50	91,78		102,76	72,10	97,19	129,80	
Bu-108	71,37	71,28	60,08			78,21		117,02	68,88
Bu-113	27,41	80,45	52,91		98,18	123,76	99,64	78,10	
Cs-182	179,8	77,75	75,93		80,10	121,70			
Cs-191	39,76	103,57	78,05		108,50	**152,69**	**134,52**		
Cs-199	66,7	29,62	23,95			**131,16**	106,93	94,01	104,55
Cs-224	25,66	107,82	92,31		129,80	117,99	**126,41**		
L-701,324	14,22	112,47	65,16	80,94	**132,29**	99,59			

The table visualizes the relationship between recovery-rates and the effect on TEER of glycine antagonists, including the IC50-values of Mayrhofer [31] to see possible differences of the results that probably can be related to dependence of the diffusion through the barrier of endothelial cells.

Bu-82 and Bu-90 didn't show an effect in the applied concentrations.

Addition of Bu-99 led to quite strong preventive effects, represented by an elevated TEER-value at 10µM. The concentration, where 50% of the cells could be protected from cell-death discovered by Mayrhofer (32,74 µM), was not tested.

Bu-108 showed effects only at a concentration of 10µM. Higher concentrations showed no effects or were not tested. The recovery-rate of Bu-108 is quite low, which means that the substance might have better effects as soon as it would be independent of the diffusion through the barrier.

Bu-113 led to elevation of TEER only at a concentration of 3µM. Also the results from Mayrhofer showed high potency, as the IC50-value was quite low. Higher concentrations showed no effects or were not tested due to toxicity that could be proved in cell-viability assays. The diffusion might also play a role for this substance as the RC-value was quite low. Higher recovery might lead to elevated TEER on the one hand or increased toxicity on the other hand.

Cs-182 showed weak positive effects at 3µM. Higher concentrations were not tested due to low potency and IC50, referring to the results gained by Mayrhofer [47]. Furthermore, Cs-182 showed lower RC-values, which might be one reason for the weaker effect.

The low IC50 (39,76 µM) of Cs-191 referring to Mayrhofer's results could be confirmed by these assays, as the TEER was elevated at quite low concentrations of 3µM and 5µM. Higher concentrations were not tested. A part of Cs-191 remained with the cells and could not act as glycine-binding site antagonist, which means that the effect was even reduced due to its diffusion properties.

Cs-199 showed very low recovery rates. Nevertheless, the substance showed weak effects in elevating TEER values. These weak changes of TEER are probably due to the slow diffusion accross the cell barrier, which leads to less presence of the substance in the extracellular space, where the substance would have its binding site. This probably led to decreased effects.

Cs-224 showed strong elevation of TEER in all tested concentrations which confirms the low IC50 gained by Mayrhofer. The diffusion didn't affect the effect of Cs-224.

L-701,324 showed strong elevation of TEER only at a concentration of 1µM. There has to be mentioned, that this substance had low recovery rates in cell experiments indicating strong interaction with the cells. (see table 4.5)

4.4 Effects of the test substances on the permeability of a paracellular-transport marker after OGD-treatment

Table 4.6a: Time dependent clearance of carboxyfluorescein in % referred to the transport across OGD treated, co-cultured cerebEND cells.
Signifcant values are marked bold.

	time dependent clearence [%]					
Substance	0,3µM	1µM	3µM	5µM	10µM	30µM
Bu-82			94,61	89,07	91,15	87,07
Bu-90		92,03	93,33	98,90	**79,75**	
Bu-99		104,33	101,21	94,22	107,71	
Bu-108			99,23		101,20	**125,16**
Bu-113		85,39	86,36	108,60	**194,13**	
Cs-182		90,25	**68,46**			
Cs-191		**77,22**	**91,60**	98,68		
Cs-199			102,59	100,53	100,25	105,33
Cs-224		**139,10**	**120,29**	103,73		
L-701,324	92,56	109,99	89,91			

Table 4.6b: Calculated permeability coefficient of carboxyfluorescein, considering the surface and with subtracted blanks

	Permeability coefficient of carboxyfluorescein [%]					
Substance	0,3µM	1µM	3µM	5µM	10µM	30µM
Bu-82			248,81	97,23	187,54	272,42
Bu-90		**54,91**	**70,56**	102,00	**29,91**	
Bu-99		167,32	119,88	78,50	76,28	
Bu-108			99,30		100,50	138,21
Bu-113		**58,45**	**54,22**	72,78		
Cs-182		**49,87**	19,95			
Cs-191		**49,57**	**64,03**	81,79		
Cs-199			142,43	124,56	104,00	
Cs-224		51,92	93,46	123,79		
L-701,324	69,61	97,00	72,45			

Additional transport assays were accomplished by addition of the paracellular marker carboxyfluorescein after the exposition to OGD-conditions for 4h. As the

transport of carboxyfluorescein is mainly accomplished through the intercellular space, its permeation is strong dependent on the tightness of the present tight-junctions. Thus, this assay is a second method to describe OGD induced barrier damage [7, 54].

Additionally, the simulation of the reoxygenisation-phase, as the cells are supplied with oxygen again, may also lead to additional damage, caused by ROS that is formed in context of the over-supplementation with oxygen [58, 59].

The results of 3.3 generally show that the carboxyfluorescein-transport was elevated by OGD-conditions. Normoxia-treated cells showed lower permeability values, which suggested, that the cell-barrier was tighter.

Addition of Bu-82 showed a clear reduction of the clearance of carboxyfluorescein. Substance-concentrations of 3µM, 5µM, 10µM and 30µM led to a lower diffusion of carboxyfluorescein. Thus the substance was able to reduce OGD induced barrier breakdown. Considering the permeability coefficient of carboxyfluorescein, Bu-82 even elevated the permeability in concentrations of 3µM, 10µM and 30µM. This is probably due to ROS damage in context of the reoxygenation-phase or the previous exposition to OGD-conditions [58, 59].

Bu-90 also showed reduced time dependent clearance. Concentrations of 1µM, 3µM and 10µM were able to elevate the tightness of the barrier. The permeability coefficient of carboxyfluorescein showed similar effects. 1µM, 3µM and 10µM reduced the permeability coefficient significantly whereas 5µM showed no effect.

Cells that were treated with Bu-99, showed reduced barrier breakdown at a concentration of 5µM. Calculation of the permeability coefficient of carboxyfluorescein led to results, which confirmed protective effects in higher concentrations of 5µM and 10µM, whereas concentrations of 1µM and 3µM showed an increase of the permeability.

Bu-108 didn't show an influence on the cell barrier. Only high concentrations (30µM) led to additional cell-damage as the paracellular permeability of the cell-

layer was increased to 125,16% and the coefficient of carboxyfluorescein augmented to 138,21%.

When Bu-113 was added, a reduction of the clearance could be observed in low concentrations of 1μM and 3μM. A concentration of 10μM led to clear toxic effects. This was shown by a strong increase of the permeability and was already proved in previous cell viability tests (3.1). Due to the high toxicity, data of the permeability coefficient of carboxyfluorescein at 10μM are not shown as they were too high. Lower concentrations of 1μM, 3μM and 5μM showed again protective effects.

Cs-182 showed protective effects. Clearance could be reduced to a value of 90,25% with 1μM and 68,48% with 3μM of the substance. The permeability coefficient of carboxyfluorescein confirmed these results.

Cs-191 was one of the most effective substances in reducing the permeability. All tested concentrations led to a clear effect considering the coefficient of carboxyfluorescein as well as the clearance. The permeability could even be reduced to levels of normoxia-cells.

Addition of Cs-199 didn't show positive effects considering the permeability coefficient of carboxyfluorescein or the clearance.

Treatment with Cs-224 didn't show a positive effect in reducing the clearance of carboxyfluorescein. The permeability coefficient of carboxyfluorescein showed that the addition of these substances could elevate the tightness of the cell-barrier in concentrations of 1μM and 3μM.

L-701,324 was a very active substance in this assay too. Thus, the addition of 0,3μM and 3μM led to a reduction of the clearance of carboxyfluorescein. A concentration of 1μM didn't show a change of the permeability. Also the permeability coefficient was clearly decreased at concentrations of 0,3μM and 3μM.

As the cells were exposed to some damaging factors (addition of possibly toxic compounds, OGD-conditions, ROS in context of reoxygenation phase) the gained values were not always as representative as it was possibly expected in

the context of this work. The results were partly inexplicably high or low (negative values), which arise when the cell barrier is destroyed near to a level of uncoated inserts, which usually served as blank values.

5. Summary and conclusion

Table 5.1: Summary of the observed results. First columns describe the toxicity (tox) of cerebEND- (cere) and C6 cells under oxygen and gludose deprivation (OGD) and normoxia conditions. Further columns show the transport properties including the recovery (RC) of each substance (S) in the cell (C) after addition. The factor F describes the transport-rate normalized to diazepam. ClogP-values describe the lipophilicity of each substance and were gained from [47]. The protective effects against the damage caused by OGD-conditions, are shown by the elevation of the barrier tightness represented by TEER-values and the paracellular permeability measured by carboxyfluorescein (CF) transport.
Significant results are marked bold.

Substance	cytotoxicity normoxia		cytotoxicity OGD		transport-properties				OGD-protective effect	
	Tox C6	Tox cere	Tox C6	Tox cere	RC S C [%]	F 10-120	F 0-10	clogP	TEER-elevation	CF-permeability reduction
Bu-82	-	-	-	**10µM**	100,54	0,597	0,580	5,024	-	5-30µM
Bu-90	-	**-**	-	-	73,58	0,398	0,464	3,308	1- 3M	**1-10µM**
Bu-99	-	-	-	-	91,78	0,355	0,347	4,495	10µM	3-5µM
Bu-108	-	-	-	-	60,08	0,192	0,152	4,096	10µM	-
Bu-113	30µM	10µM	30µM	10µM	52,91	0,295	0,177	7,122	3µM	**1-5µM**
Cs-182	100µM	10µM	100µM	10µM	75,93	0,534	0,322	6,723	3µM	**1- 3µM**
Cs-191	-	-	-	**10µM**	78,05	0,535	0,360	6,593	**1-3µM**	**1-5µM**
Cs-199	30µM	10µM	30µM	10µM	23,95	0,113	0,106	6,992	**3-5µM**	(10µM)
Cs-224	-	-	-	-	92,31	0,526	0,355	4,964	**1-5µM**	1µM
L-701,324	-	-	-	-	65,16	0,679	1,586	5,406	**1µM**	**0,3µM, 3µM**

As already mentioned, the aim of the present work was to find substances that show optimal properties to prevent the brain tissue from damage that is caused in case of stroke or ischemia in general. These properties provide potent, antagonizing interactions with the glycine-binding site of the NMDA-receptor. Due to the elevated impairment of the blood-brain barrier in context of ischemia, another aim of this work was to sort out those substances that diffuse easily through the barrier, which was imitated by in-vitro transport assays. By using

substances that stay inside the cell or diffuse very weak into the ISF, the undesired side effects could probably be prevented or at least reduced. Considering the toxicity of the substances themselves, allowed an individualized utilisation of the structures, by adaptation of the applied concentration.

The cell-viabilty assays showed which substances were toxic at which concentrations. Under normoxia- conditions Bu-113, Cs-182 and Cs-199 showed clear damaging effects. OGD-conditions lead to enforcement of the toxic effects, many substances showed toxicity already in low concentrations such as 10µM. In transport assays, substances were searched, which comply with the desired properties. Thus, Bu-108, Bu-113 and Cs-199 showed the best results, as they were transported hardly across the barrier. The change of TEER in dependence of the added substances and the applied conditions showed, in how far they could prevent the cells from the damage that is caused by lack of oxygen and glucose. Cs-191, Cs-199, Cs-224 and L-701-324 showed the most effective prevention of the damage.

Bu-82 was able to reduce the paracellular transport slightly and was not toxic. The substance showed good transport accross the barrier, which suggested, that the substance could bind at a proposed abluminal site at the ATD of NR-1 to a large extent but also may lead to more side effects on glial and neuronal cells than others due to its higher concentration inside the ISF. There was no protective effect on TEER after OGD-exposition.

Bu-90 was only protective with regard to CF-permeability, but did not improve TEER values. Furthermore, it was transported well across the barrier which suggested that the substance probably leads to more side effects.

Bu-99 showed effects in prevention of the OGD-caused damage and was transported well across the barrier as the clearance and the recovery-rate were high. The substance didn't harm the cells additionally and showed good results in OGD-assays, as the damage could be reduced in concentrations of 3µM and 5µM.

Bu-108 and Bu-113 diffused across the barrier quite slow and showed weak protective effects under OGD-conditions. Bu-113 showed toxicity in cell viability assays and transport-assays already in low concentrations, but was able to reduce the damage of OGD-conditions as the paracellular transport of CF was reduced. Bu-108 showed better results in elevating TEER, although the reduction of the permeability after OGD-exposition was missing. Both substances could be considered as quite promising. Low protective effects and cytotoxicity could be due to decreased permeation of the substances.

Cs-182 was able to reduce the damage caused by OGD (elevated TEER, reduced paracellular permeability) but acted toxic in cell viability assays in higher concentrations. Transport studies showed high permeation across the barrier.

Although Cs-191 diffuses well across the barrier and leads to more damage than other substances, it probably prevents the cell from ischemia-damage very effectively. Furthermore, Cs-191 acted less toxic at endothelial-cells as Cs-199 for example and showed strong reduction of the paracellular permeability of CF.

As Cs-199 showed strong reduction of the damage in concentrations of 3µM and 5µM and was transported slowly across the in-vitro blood-brain barrier model (as it was probably adsorbed by the plastic material) it is handled as one of the most potent compounds for prevention of the damage caused by ischemia and stroke. Nevertheless, it has to be used carefully, as it showed toxic effects under normmoxic as well as OGD conditions. Although the substance didn't show an effect on permeability of CF and the low recovery-rates indicated a high loss in the plastic, it has promising results in remaining assays and is so a candidate for further tests.

Similar to Cs-191, Cs-224 showed good effects in elevating the TEER (1µM) and was transported across the barrier to a large extent. Additionally, it seemed to act toxic to the cerebEND cell line which was proved by the elevation of the permeability of CF after OGD-treatment and the cell viability assay.

L-701,324 was tested in several other studies, as mentioned above. It showed clear reduction of the damage caused by OGD, although it didn't show optimal transport properties. The lower recovery rate indicated interaction with the cell. L-

701,324 also showed good results in reducing the transport of CF through the paracellular space after OGD-exposition.

Summarizing these results, most of the test substances could be used for following assays. Especially substances, that showed clear reduction of the damage in the OGD-assays, can be considered as quite promising. Low transport across the barrier would probably mean fewer side effects. Cs-191 and Cs-199 comply with most of the properties and thus can be seen as the most potent compounds.

In future, further assays could be accomplished using the tested compounds, such as in-vivo models to obtain additional information about their influence on stroke induced brain damage. In-vivo assays would allow more precise statements about the possible effects of these substances extrapolated to the human brain. In-vivo data have been generated with L-701,324 and MK801 [70, 71]. Still, there is lack of success of NMDAR-antagonists in clinical trials [42].

6. References

1. Hawkins RA, O'Kane RL, Simpson IA, Viña JR (2006) Structure of the Blood–Brain Barrier and its role in the transport of amino acids. J Nutr, 136 (1 Suppl):218S-26S

2. John Laterra, Richard Keep, Lorris A Betz, and Gary W Goldstein (1999) Basic Neurochemistry: Molecular, Cellular and Medical Aspects. University of Michigan, Departments of Pediatrics, Surgery and Neurology

3. Giles E, Bading H (2010) Synaptic versus extrasynaptic NMDA receptor signalling: implications for neurodegenerative disorders. Nat Rev Neurosci. (11)10: 682-696 doi:10,1038/nrn2911.

4. Ohtsuki S, Terasaki T (2007) Contribution of carrier-mediated transport systems to the blood-brain barrier as a supporting and protecting interface for the brain; importance for CNS drug discovery and development. Springer, Pharm Res. 24(9):1745-58.

5. Tamai I, Tsuji A (2000) Transporter-mediated permeation of drugs across the blood–brain barrier. Journal of pharmaceutical sciences, 89(11):1371-88

6. Jia M, Njapo SA, Rastogi V, Hedna VS (2015) Taming glutamate excitotoxicity: Strategic pathway imodulation for neuroprotection. CNS Drugs. 29(2):153-62. doi: 10.1007/s40263-015-0225-3

7. Neuhaus W, Gaiser F, Mahringer A, Franz J, Riethmüller C, Förster C . (2014) The pivotal role of astrocytes in an in-vitro stroke model of the blood-brain barrier. University hospital Würzburg, Front Cell Neurosci. 28(8):352. doi: 10.3389/fncel.2014.00352.

8. Bellamy WT (1996) P-glycoproteins and multidrug resistance. Annu Rev Pharmacol Toxicol. 36:161-83.

9. Yousif S, Chaves C, Potin S, Margaill I, Scherrmann JM, Decleves X (2012) Induction of P-glycoprotein and Bcrp at the rat blood-brain barrier following a subchronic morphine treatment is mediated through NMDA/COX-2 activation. J Neurochem. 123(4):491-503. doi: 10.1111/j.1471-4159.2012.07890.

10. Helms HC, Hersom M, Kuhlmann LB, Badolo L, Nielsen CU, Brodin B (2014) An electrically tight in-vitro blood-brain barrier model displays net brain-to-blood efflux of substrates for the ABC transporters, P-gp, Bcrp and Mrp-1. AAPS J.16(5):1046-55. doi: 10.1208/s12248-014-9628-1.

11. Wolburg H., Lippoldt A. (2002) Tight junctions of the blood–brain barrier: Development, composition and regulation. Vascular Pharmacology 38(6), 323– 337

12. Neuhaus W, Freidl M, Szkokan P Berger M, Wirth M, Winkler J, Gabor F, Pifl C, Noe CR (2011) Effects of NMDA receptor modulators on a blood–brain barrier in-vitro model. Brain Res. 1394:49-61. doi: 10.1016/j.brainres.2011.04.003

13. Cummins PM (2012) Occludin: one protein, many forms. Mol Cell Biol. 32(2):242-50. doi: 10.1128/MCB.06029-11.

14. Lau A, Tymianski M (2010) Glutamate receptors, neurotoxicity and neurodegeneration. Pflugers Arch. 460(2):525-42. doi: 10.1007/s00424-010-0809-1.

15. Van Dongen, A. M. (Ed.). (2009). Biology of the NMDA Receptor. North Carolina: Duke University Medical Center

16. Zhang SJ, Steijaert MN, Lau D, Schütz G, Delucinge-Vivier C, Descombes P, Bading H (2007) Decoding NMDA receptor signaling: identification of genomic programs specifying neuronal survival and death. Neuron. 53(4):549-62.

17. Ferreira IL, Ferreiro E, Schmidt J, Cardoso JM, Pereira CM, Carvalho AL, Oliveira CR, Rego AC (2014) Aβ and NMDAR activation cause mitochondrial dysfunction involving ER calcium release. Neurobiol Aging. 36(2):680-92. doi: 10.1016/j.neurobiolaging.2014.09.006.

18. Vizi ES, Kisfali M, Lorincz T (2013) Role of nonsynaptic GluN2B-containing NMDA receptors in excitotoxicity: Evidence that fluoxetine selectively inhibits these receptors and may have neuroprotective effects   Brain Res Bull. 93:32-8. doi: 10.1016/j.brainresbull.2012.10.005.

19. Bromfield EB, Cavazos JE, Sirven JI (2006) An Introduction to Epilepsy. West Hartford (CT): American Epilepsy Society

20. Paoletti P, Neyton J (2006) NMDA receptor subunits: function and pharmacology. Curr Opin Pharmacol. 7(1):39-47

21. Hardingham GE, Bading H (2010) Synaptic versus extrasynaptic NMDA receptor signalling: implications for neurodegenerative disorders. Nat Rev Neurosci. (10):682-96. doi: 10.1038/nrn2911

22. Kaufman AM, Milnerwood AJ, Sepers MD, Coquinco A, She K, Wang L, Lee H, Craig AM, Cynader M, Raymond LA (2012) Opposing roles of synaptic and extrasynaptic NMDA receptor signaling in cocultured striatal and cortical neurons. J Neurosci. 32(12):3992-4003. doi: 10.1523/JNEUROSCI.4129-11.2012.
.
23. Chen S, Evans HG, Evans DR (2012) FLASH knockdown sensitizes cells to Fas-mediated apoptosis via down-regulation of the anti-apoptotic proteins, MCL-1 and Cflip short. PLoS One. doi: 10.1371/journal.pone.0032971.

24. Chen HS, Lipton SA (2006) The chemical biology of clinically tolerated NMDA receptor antagonists. Wiley online library, J Neurochem. 97(6):1611-26.

25. Raymond LA, André VM, Cepeda C, Gladding CM, Milnerwood AJ, Levine MS (2011) Pathophysiology of Huntington's disease: time-dependent alterations in synaptic and receptor function. Neuroscience, 198:252-73. doi: 10.1016/j.neuroscience.2011.08.052

26. Lason W, Chlebicka M, Rejdak K (2013) Research advances in basic mechanisms of seizures and antiepileptic drug action. Pharmaco Rep. 65(4), 787.801.

27. Bordji K, Becerril-Ortega J, Nicole O, Buisson A (2010) Activation of extrasynaptic, but not synaptic, NMDA receptors modifies amyloid precursor protein expression pattern and increases amyloid-ß production. J Neurosci. 30(47):15927-42. doi: 10.1523/JNEUROSCI.3021-10.2010.

28. Wu YN, Johnson SW (2015) Memantine selectively blocks extrasynaptic NMDA receptors in rat substantia nigra dopamine neurons. Brain Res.1603:1-7. doi: 10.1016

29. Kew JN. John A. Kemp JA (2005) Ionotropic and metabotropic glutamate receptor structure and pharmacology. Psychopharmacology 179: 4–29, doi: 10.1007/s00213-005-2200-z

30. Nahum-Levy R, Fossom LH, Skolnick P, Benveniste M (1999) Putative partial agonist 1-aminocyclopropanecarboxylic acid acts concurrently as a glycine-site agonist and a glutamate-site antagonist at N-methyl-D-aspartate receptors. Mol Pharmacol. 56(6):1207-1218.

31. Zellinger C, Salvamoser JD, Soerensen J (2014) Pre-treatment with the NMDA receptor glycine-binding site antagonist L-701,324 improves pharmacosensitivity in a mouse kindling model. Epilepsy Res. 108(4):634-643. doi: 10.1016

32. Williams K (1993) Ifenprodil discriminates subtypes of the N-methyl-D-aspartate receptor: selectivity and mechanisms at recombinant heteromeric receptors. Mol Pharmacol. 44(4):851-859.

33. Anis NA, Berry SC, Burton NR, Lodge D (1983) The dissociative anaesthetics, ketamine and phencyclidine, selectively reduce excitation of central mammalian neurones by N-methyl-aspartate. Br J Pharmacol. 79(2):565-75.

34. Parsons CG, Danysz W, Quack G (1999) Memantine is a clinically well tolerated N-methyl-D-aspartate (NMDA) receptor antagonist-a review of preclinical data. Neuropharmacology, 38(6):735-67.

35. Lipton SA (2004) Failures and successes of NMDA receptor antagonists: molecular basis for the use of open-channel blockers like memantine in the treatment of acute and chronic neurologic insults. NeuroRx.1(1):101-10.

36. Paul Morley, Daniel L Small, Christine L Murray, Geoffrey A Mealing, Michael O Poulter, Jon P Durkin and Danica B Stanimirovic (1998) Evidence that functional glutamate receptors are not expressed on rat or human cerebromicrovascular endothelial cells. J Cereb Blood Flow Metab. 18, 396–406; doi:10.1097/00004647-199804000-00008.

37. Giese H, Mertsch K, Blasig IE (1995) Effect of MK-801 and U83836E on a porcine brain capillary endothelial cell barrier during hypoxia. Neurosci Lett. 191(3):169-72.

38. Koenig H, Trot JJ, Goldstone AD, Lu CY. (1992) Capillary NMDA receptors regulate blood-brain barrier function and breakdown. Brain Res 588: 297–303.

39. Krizbai IA, Deli MA, Pestenacz A, Siklos L, Szabo CA, Andras I, Joo F (1998) Expression of Glutamate Receptors on Cultured Cerebral Endothelial Cells, Journ Neurosc Res. 54(6):814–819

40. Olney J, Price M, Salles KS, Labruyere J, Frierdich G (1987). MK-801 powerfully protects against N-methyl aspartate neurotoxicity. Eur J Pharmacol. 141(3):357-61.

41. Clineschmidt BV (1982) Effect of the benzodiazepine receptor antagonist Ro 15-1788 on the anticonvulsant and anticonflict actions of MK-801. Eur J Pharmacol. 84(1-2):119-21.

42. Ikonomidou C, Turski L (2002) Why did NMDA receptor antagonists fail clinical trials for stroke and traumatic brain injury? Lancet Neurol. 1(6): 383–863.

43. Nicole O, Docagne F, Ali C, Margaill I, Carmeliet P, MacKenzie ET, Vivien D, Buisson A (2001) The proteolytic activity of tissue-plasminogen activator enhances NMDA receptor-mediated signaling. Nat Med. 7(1):59-64.

44. Gaberel T, Macrez R, Gauberti M, Montagne A, Hebert M, Petersen KU, Touze E, Agin V, Emery E, Ali C, Vivien D (2013) Immunotherapy blocking the tissue plasminogen activator-dependent activation of N-methyl-D-aspartate glutamate receptors improves hemorrhagic stroke outcome. Neuropharmacology, 67:267-71. doi: 10.1016/j.neuropharm.2012.11.023.

45. Macrez R, Bezin L, Le Mauff B, Ali C, Vivien D (2010) Functional occurrence of the interaction of tissue plasminogen activator with the NR1 Subunit of N-methyl-D-aspartate receptors during stroke. Stroke. 41(12):2950-5. doi: 10.1161/STROKEAHA.110.592360.

46. Macrez R, Obiang P, Gauberti M, Roussel B, Baron A, Parcq J, Cassé F, Hommet Y, Orset C, Agin V, Bezin L, Berrocoso TG, Petersen KU, Montaner J, Maubert E, Vivien D, Ali C (2011) Antibodies preventing the interaction of tissue-type plasminogen activator with N-methyl-D-aspartate receptors reduce stroke damages and extend the therapeutic window of thrombolysis. Stroke. 42(8):2315-22. doi:0.1161/STROKEAHA.110.606293.

47. Mayrhofer JF (2015) Establishment of a cell culture assay to measure NMDA-receptor-inhibtors. Diploma thesis, Department of Pharmceutical Chemistry in Vienna

48. Buchstaller HP, Siebert CD, Steinmetz R, Frank I, Berger ML, Gottschlich R, Leibrock J, Krug M, Steinhilber D, Noe CR (2006) Synthesis of Thieno[2,3-b]Pyridinones acting as cytoprotectants and as inhibitors of [3H]glycine binding to the N-Methyl-D-aspartate (NMDA) receptor. J Med Chem. 49(3):864-71

49. Owens J, Tebbutt AA, McGregor AL, Kodama K, Magar SS, Perlman ME, Robins DJ, Durant

GJ, McCulloch J (2000) Synthesis and Binding Characteristics of N-(1-Naphthyl)-N9-(3-[125I]-iodophenyl)-N9-methylguanidine ([125I]-CNS 1261):A Potential SPECT Agent for Imaging NMDA Receptor Activation. Nucl Med Biol. 27(6), 557–564.

50. Barth RF , Kaur B (2009) Rat brain tumor models in experimental neuro-oncology: the C6, 9L, T9, RG2, F98, BT4C, RT-2 and CNS-1 gliomas. J Neurooncol. 94(3):299-312. doi: 10.1007/s11060-009-9875-7.

51. Applichem. AppliCations Nr.12. Cell proliferation assay XTT. Retrieved from the applichem website: https://www.applichem.com

52. Berridge, M. V., Herst, P. M., & Tan, A. S. (2005). Tetrazolium dyes as tools in cell biology: New insights into their cellular reduction. Biotechnology Annu Rev. 11, 127-152.

53. Burek M, Salvador E, Foerster CY (2012) Generation of an immortalized murine brain microvascular endothelial cell line as an in-vitro blood-brain barrier model. J Vis Exp. 29(66):e4022. doi: 10.3791/4022

54. Novakova I, Subileau EA, Toegel S, Gruber D, Lachmann B, Urban E, Chesne C, Noe CR, Neuhaus W (2014) Transport rankings of non-steroidal antiinflammatory drugs across blood-brain barrier in-vitro models. PLoS One, 9(1):e86806. doi: 10.1371.

55. Zagrobelny J, Chavez C, Constanzer M, Matuszewski BK (1995) Determination of a glycine/NMDA receptor antagonist in human plasma and urine using column-switching high-performance liquid chromatography with ultraviolet, fluorescence and tandem mass spectrometric detection. J Pharm Biomed Anal. 13(10):1215-23.

56. Bujak R, Struck-Lewicka W, Kaliszan M, Kaliszan R, Markuszewski MJ (2015) Blood-brain barrier permeability mechanisms in view of quantitative structure-activity relationships (QSAR). J Pharm Biomed Anal.108:29-37. doi: 10.1016/j.jpba.2015.01.046.

57. Ueno Y, Jiao G, Burgess K (2004) Preparation of 5- and 6-carboxyfluorescein. Synthesis, 15:2591-2593. doi:10.1055/s-2004-829194.

58. Ryu S, Park H, Seol GH, Choi IY (2014) 1,8-Cineole ameliorates oxygen-glucose deprivation/reoxygenation-induced ischaemic injury by reducing oxidative stress in rat cortical neuron/glia. J Pharm Pharmacol. 66(12):1818-26. doi: 10.1111/jphp.12295.

59. Gao XY, Huang JO, Hu YF, Gu Y, Zhu SZ (2014) Combination of mild hypothermia with neuroprotectants has greater neuroprotective effects during oxygen-glucose deprivation and reoxygenation-mediated neuronal injury. Sci Rep.18;4:7091. doi: 10.1038/srep07091.

60. Kainz J (2004) Comparison of different methods for the prediction of membrane permeation, diploma thesis, Department of Pharmaceutical Chemistry Vienna

61. http: www.york.ac.uk/depts/maths/tables/spearman.pdf.

62.http://psychology.ucdavis.edu/faculty_sites/sommerb/sommerdemo/correlation/hand/critvalues _rs.htm

63. Foster AC, Kemp JA (1989) HA-966 antagonizes N-methyl-D-aspartate receptors through a selective interaction with the glycine modulatory site. J Neurosci. 9(6):2191-6.

64. Baron BM, Harrison BL, Kehne JH, Schmidt CJ, van Giersbergen PL, White HS, Siegel BW, Senyah Y, McCloskey TC, Fadayel GM, Taylor VL, Murawsky MK, Nyce P, Salituro FG (1997) Pharmacological characterization of MDL 105,519, an NMDA receptor glycine site antagonist. Eur J Pharmacol. 323(2-3):181-92.

65. Priestley T, Laughton P, Macaulay AJ, Hill RG, Kemp JA (1996) Electrophysiological characterisation of the antagonist properties of two novel NMDA receptor glycine site antagonists, L-695,902 and L-701,324. Neuropharmacology. 35(11):1573-81.

66. Baron A, Montagne A, Cassé F, Launay S, Maubert E, Ali C, Vivien D (2010) NR2D-containing NMDA receptors mediate tissue plasminogen activator-promoted neuronal excitotoxicity. Cell Death Differ. 17(5):860-71. doi: 10.1038/cdd.2009.172.

67. Bristow LJ, Hutson PH, Kulagowski JJ, Leeson PD (1996) Anticonvulsant and behavioral profile of L-701,324, a potent, orally active antagonist at the glycine modulatory site on the N-methyl-D-aspartate receptor complex. J Pharmacol Exp Ther. 279(2):492-501.

68. Kotlińska J (2001) NMDA antagonists inhibit the development of ethanol dependence in rats. Pol J Pharmacol. 53(1):47-50.

69. Tsirka SE, Gualandris A, Amaral DG, Strickland S (1995) Excitotoxin-induced neuronal degeneration and seizure are mediated by tissue plasminogen activator.
Nature, 377(6547):340-4.

70. Kanahara N, Shimizu E, Ohgake S, Fujita Y (2008) Glycine and D: -serine, but not D: -cycloserine, attenuate prepulse inhibition deficits induced by NMDA receptor antagonist MK801. Psychopharmacology 198(3):363-74. doi: 10.1007/s00213-008-1151-6.

71. Obrenovitch TP, Hardy AM, Zilkha E (1997) Effects of L-701,324, a high-affinity antagonist at the N-methyl-D-aspartate (NMDA) receptor glycine site, on the rat electroencephalogram. Naunyn Schmiedebergs Arch Pharmacol. 355(6):779-86.

7. Appendix

7.1 Summary (german)

Die Blut-Hirn-Schranke spielt eine zentrale Rolle in der Regulation des Stofftransports zwischen dem Blut und dem zerebralen Gewebe und regelt dadurch die Homöostase von Elektrolyten, Aminosäuren etc. Die Funktion dieser physiologischen Barriere ist aber auch entscheidend für die Entstehung und die Entwicklung von pathologischen Prozessen und Krankheiten wie Morbus Alzheimer, Morbus Huntington, Epilepsie oder Schlaganfall.

Die vorliegende Arbeit beschäftigt sich überwiegend mit der Veränderung der Funktionalität der Blut-Hirn-Schranke im Rahmen von zerebraler Ischämie. Die damit verbundenen pathologischen Vorgänge sind abhängig von einem extrazellulär entstehenden Glutamat-Überschuss, der zu einer vermehrten Aktivierung von exzitatorischen Glutamat-abhängigen Rezeptoren und schlussendlich zum Zelltod führt. Einer dieser Rezeptoren ist der in dieser Arbeit behandelte N-methyl-D-Aspartat-Rezeptor (NMDAR).

Studien der letzten Jahre insbesondere von Vivien et al. (2011-2015) bestätigten die bedeutende Rolle der Glycin-Bindungsstelle NR1 des NMDAR in der Entstehung des Zellschadens im zentralen Nervensystem (ZNS), unter anderem auch an dem Blut-Hirn Schranken Endothel. Als weiterer zentraler Regulator dieses Prozesses wurde der tissue-Plasminogen activator (t-PA) identifiziert. Dieser Faktor bindet ebenfalls an die NR1 Untereinheit des NMDAR und aktiviert diesen wiederum. Dieser Mechanismus unterstreicht die Bedeutsamkeit der Glycin-Bindungsstelle an der Entstehung und Entwicklung des zellulären Schadens im Rahmen der zerebralen Ischämie. Dementsprechend sind Glycin-Antagonisten gesucht, die den Schaden durch die Blockade des Rezeptors verhindern können.

Im Rahmen der vorliegenden Arbeit wurden mehrere, am Department für Pharmazeutische Chemie in Wien vorhandene Glycin-Antagonisten getestet. Die

optimale Substanz blockiert den durch OGD (oxygen/glucose deprivation) induzierten Schaden der Barriere des Blut-Hirn Schranken in-vitro Schlaganfallmodells. Zudem sollte sie in den angewandten Konzentrationen nicht toxisch sein und geringe Permeabilität durch das Blut-Hirn Schranken in-vitro Modell aufweisen. Dies ist besonders wichtig, um die unerwünschten Nebeneffekte der Glycinantagonisten auf Gliazellen und Neuronen im ZNS zu minimieren. Für die Blut-Hirn Schranken Modelle wurden die Zelllinien cerebEND (immortalisierte, murine Hirnkapillarendothelzellen) und C6 (Rattenglioma) eingesetzt. Die untersuchten Glycinantagonisten konnten die Zellviabilität (EZ4U assay) unter Normoxie als auch OGD-Bedingungen konzentrationsabhängig reduzieren. Dementsprechend wurden nicht-toxische Konzentrationen der Substanzen für die nachfolgenden Transportversuche im Blut-Hirn Schranken Modell verwendet und mittels HPLC analysiert. Die Resultate (Clearance, Wiederfindung, Transportrate) wurden auf den internen Standard Diazepam normalisiert und mit physiko-chemischen Parametern wie ClogP korreliert.

Die Fähigkeit der Glycinantagonisten den durch die OGD-Behandlung verursachten Barriereschaden zu blockieren, wurde in einem Transwell Ko-Kulturmodell bestehend aus cerebEND und C6 Zellen untersucht und anhand der Änderungen des transendothelialer elektrischer Widerstandsmessung und der Permeabilität des parazellularen Markers Carboxyfluoreszein bestimmt.

Zusammenfassend waren beinahe alle ausgewählten Glycinantagonisten im Blut-Hirn Schranken in-vitro Schlaganfallsmodell wirksam. Mit Hilfe der zusätzlich ermittelten Toxizitäts- und Transportdaten könnten die Substanzen mit dem höchsten Potenzial für in-vivo Studien ausgewählt werden.

7.2 Curriculum vitae (english)

personal dates:

last name:	Membier
first name:	Sebastian
date of birth:	27th of August 1991
place of birth:	Neunkirchen, Austria
nationality:	Austria
address:	Lindenplatz 7, 2731 St. Egyden, Austria

field of studies:

dato	Diploma-thesis: "Studies with selected antagonists of the N-methyl-D-aspartate receptor in an in-vitro blood-brain barrier model of ischemia", Department of Pharmaceutical Chemistry, University of Vienna, under the supervision of Ao. Univ.-Prof. Mag. Dr. Ernst Urban;
since 2010/11	Study of Pharmacy, University of Vienna;

summer jobs:

2011-2015	"Alte Kronen Apotheke", 2700 Wr.Neustadt, Austria
2011-2015	"Heiland Apotheke", 2700 Wr.Neustadt, Austria

community service:

09/2009 – 04/2010	supporting service in "Stadtheim Wr.Neustadt" (Nö)
04/2010-05/2010	service in hospital (Wr. Neustadt)

schoolcareer:

2005-2009	BORG, Wr. Neustadt (Nö)
2001-2005	secondary school, with main focus on informatics, Winzendorf (Nö);
1997-2001	primary school, St.Egyden (Nö);

7.3 Curriculum vitae (german)

<u>Persönliche Daten:</u>

Nachname: Membier

Vorname: Sebastian

Geburtsdatum: 27. August 1991

Geburtsort: Neunkirchen, Österreich

Nationalität: Österreich

Adresse: Lindenplatz 7, 2731 St. Egyden, Nö

<u>Studienrichtung:</u>

Dato   Diplomarbeit: „Untersuchungen mit ausgewählten Antagonisten des N-methyl-D-aspartat-Rezeptors an einem in-vitro Blut-Hirn-Schranken Modell für Ischämie", Department für Pharmazeutische Chemie, Universität Wien, unter der Aufsicht von Ao. Univ.-Prof. Mag. Dr. Ernst Urban;

Seit 2010/11   Studium Pharmazie, Universität Wien;

<u>Ferialpraktika:</u>

2011-2015   „Alte Kronen Apotheke", 2700 Wr.Neustadt, Austria

2011-2015   "Heiland Apotheke", 2700 Wr.Neustadt, Austria

Zivildienst:

09/2009 – 04/2010   Zivildienst als Ünterstützungskraft im

                           "Stadtheim Wr.Neustadt" (Nö)

04/2010-05/2010   Zivildienst im Krankenhaus (Wr. Neustadt)

Schullaufbahn:

2005-2009   BORG, Wr. Neustadt (Nö)

2001-2005   Informatik-Hauptschule, Winzendorf (Nö);

1997-2001   Volksschule, St.Egyden (Nö);

Unterschrift: